ผลและกลไกการรักษาภาวะกระดูกพรุนของกวาวเครือขาว *Pueraria mirifica* Airy Shaw et Suvatabandhu ในลิงแสมวัยแก่: การศึกษาในหลอดทดลองและในสัตว์ทดลอง

นางสาวดลพร กิตติวนิชย์กุล

วิทยานิพนธ์นี้เป็นส่วนหนึ่งของการศึกษาตามหลักสูตรปริญญาวิทยาศาสตรดุษฎีบัณฑิต
สาขาวิชาสัตววิทยา ภาควิชาชีววิทยา
คณะวิทยาศาสตร์ จุฬาลงกรณ์มหาวิทยาลัย
ปีการศึกษา 2559

EFFECTS OF *Pueraria mirifica* Airy Shaw et Suvatabandhu AND ITS MECHANISMS OF ACTIONS ON OSTEOPOROSIS IN AGED CYNOMOLGUS MONKEYS: *IN VITRO* AND *IN VIVO* APPROACHES

Miss Donlaporn Kittivanichkul

A Dissertation Submitted in Partial Fulfillment of the Requirements
for the Degree of Doctor of Philosophy Program in Zoology
Department of Biology
Faculty of Science
Chulalongkorn University
Academic Year 2016

Thesis Title	EFFECTS OF *Pueraria mirifica* Airy Shaw et Suvatabandhu AND ITS MECHANISMS OF ACTIONS ON OSTEOPOROSIS IN AGED CYNOMOLGUS MONKEYS: *IN VITRO* AND *IN VIVO* APPROACHES
By	Miss Donlaporn Kittivanichkul
Field of Study	Zoology
Thesis Advisor	Professor Suchinda Malaivijitnond, Ph.D.
Thesis Co-Advisor	Professor Narattaphol Charoenphandhu, M.D., Ph.D.
	Professor Baruch Frenkel, D.M.D., Ph.D.

Accepted by the Faculty of Science, Chulalongkorn University in Partial Fulfillment of the Requirements for the Doctoral Degree

.....Dean of the Faculty of Science
(Associate Professor Polkit Sangvanich, Ph.D.)

THESIS COMMITTEE

.....Chairman
(Assistant Professor Duangkhae Sitthicharoenchai, Ph.D.)
.....Thesis Advisor
(Professor Suchinda Malaivijitnond, Ph.D.)
.....Thesis Co-Advisor
(Professor Narattaphol Charoenphandhu, M.D., Ph.D.)
.....Thesis Co-Advisor
(Professor Baruch Frenkel, D.M.D., Ph.D.)
.....Examiner
(Assistant Professor Noppadon Kitana, Ph.D.)
.....Examiner
(Assistant Professor Sukanya Jaroenporn, Ph.D.)
.....Examiner
(Assistant Professor Sittiporn Pattaradilokrat, Ph.D.)
.....External Examiner
(Professor Boonsong Ongphiphadhanakul, M.D.)

ดลพร กิตติวนิชย์กุล : ผลและกลไกการรักษาภาวะกระดูกพรุนของกวาวเครือขาว *Pueraria mirifica* Airy Shaw et Suvatabandhu ในลิงแสมวัยแก่: การศึกษาในหลอดทดลองและในสัตว์ทดลอง (EFFECTS OF *Pueraria mirifica* Airy Shaw et Suvatabandhu AND ITS MECHANISMS OF ACTIONS ON OSTEOPOROSIS IN AGED CYNOMOLGUS MONKEYS: *IN VITRO* AND *IN VIVO* APPROACHES) อ.ที่ปรึกษาวิทยานิพนธ์หลัก: ศ. ดร. สุจินดา มาลัยวิจิตรนนท์, อ.ที่ปรึกษาวิทยานิพนธ์ร่วม: ศ. นพ. ดร. นรัตถพล เจริญพันธุ์, ศ. ทพ. ดร. บารุค แฟรงเคล, 123 หน้า.

ได้ศึกษาผลและกลไกลการออกฤทธิ์ของผงกวาวเครือขาว (*Pueraria mirifica*; PMP) ต่อการเกิดโรคกระดูกพรุนในลิงแสมวัยหมดประจำเดือน ในการทดลองชุดแรก เป็นการศึกษาแบบตัดขวาง ในลิงวัยก่อนหมดประจำเดือน ลิงที่กำลังเข้าสู่วัยหมดประจำเดือน และลิงวัยหมดประจำเดือนในระยะแรก (0 ถึงน้อยกว่า 5 ปี), ระยะกลาง (5 ถึง 10 ปี) และระยะท้าย (มากกว่า 10 ปี) ทำการตรวจวัดค่าความหนาแน่นกระดูก (BMD) และมวลกระดูก (BMC) ที่กระดูกปลายแขนและกระดูกหน้าแข้ง ส่วนเมตาไฟซิสและไดอะไฟซิสด้วยเครื่องวัดมวลกระดูก (pQCT) รวมถึงตรวจวัดระดับฮอร์โมนและดัชนีชี้วัดการผลัดเปลี่ยนหมุนเวียนกระดูกในซีรั่มและปัสสาวะ พบว่าลิงสูญเสียกระดูกเนื้อโปร่งที่บริเวณเมตาไฟซิสอย่างฉับพลันเมื่อเข้าสู่วัยหมดประจำเดือน ในขณะที่กระดูกเนื้อแข็งจะค่อย ๆ ลดลงอย่างต่อเนื่องและสัมพันธ์กับระยะหมดประจำเดือน โดยการสูญเสียเนื้อกระดูกในลิงวัยหมดประจำเดือนระยะแรกและระยะกลาง สัมพันธ์กับการเพิ่มสูงขึ้นของระดับฮอร์โมนฟอลลิเคิลสติมูเลติงในซีรั่ม แต่ในลิงวัยหมดประจำเดือนระยะท้าย สัมพันธ์กับการลดลงของฮอร์โมนเอสตราไดออลในซีรั่ม และพบว่าระดับ BAP ในซีรั่ม และระดับ NTX ในปัสสาวะ มีความสัมพันธ์แบบผกผันกับ BMC ของกระดูกเนื้อโปร่งส่วนเมตาไฟซิส ในขณะที่ระดับ osteocalcin ในซีรั่มมีความสัมพันธ์แบบผกผันกับ BMC ของกระดูกเนื้อแข็งส่วนไดอะไฟซิส จากนั้นได้ทำการทดลองในชุดที่สอง ศึกษาผลของการให้ PMP นาน 16 เดือน ในลิงแสมวัยหมดประจำเดือนและอยู่ในภาวะกระดูกพรุน พร้อมกับวัดการแสดงออกของยีน *ALP*, *RANKL* และ *OPG* ด้วยเทคนิค qRT-PCR จากเซลล์สร้างกระดูกที่เก็บจากกระดูกเชิงกราน (iliac crest biopsy) โดยแบ่งลิงออกเป็นสองกลุ่ม คือ กลุ่ม PMP0 (ได้รับอาหารเม็ดปกติ) และกลุ่ม PMP1000 (ได้รับอาหารเม็ดผสม PMP ในขนาด 1000 มก/กก. น้ำหนักตัว/วัน) ติดตามวัดพารามิเตอร์ต่าง ๆ เช่นเดียวกับการทดลองชุดแรก และติดตามการเปลี่ยนแปลงทางเรขาคณิตของกระดูก (พื้นที่และความหนาของกระดูกเนื้อแข็ง และเส้นรอบวงด้านนอกและด้านในของกระดูก) ทุก ๆ 2 เดือน พบว่า BMD และ BMC ของกระดูกเนื้อแข็งในลิงกลุ่ม PMP0 ลดลงอย่างต่อเนื่อง ตลอดระยะ 16 เดือนของการทดลอง การให้กวาวเครือขาวสามารถลดการสูญเสียกระดูกเนื้อแข็งส่วนไดอะไฟซิส โดยไปลดอัตราการผลัดเปลี่ยนหมุนเวียนกระดูก โดยที่การเปลี่ยนแปลงทางเรขาคณิต (พื้นที่และความหนา) ของกระดูกเนื้อแข็ง เป็นไปในทิศทางเดียวกันกับการเปลี่ยนแปลงของ BMC และ BMD และเมื่อตรวจวัดการแสดงออกในระดับเอ็มอาร์เอ็นเอของเซลล์สร้างกระดูก พบว่ามีการลดลงของ *RANKL/OPG* ในลิงกลุ่ม PMP1000 มากกว่าลิงกลุ่ม PMP0 ในการทดลองชุดสุดท้าย จากที่ได้มีการผ่าตัดกระดูกเชิงกรานเพื่อเก็บเซลล์สร้างกระดูก จึงได้ติดตามผลของการให้ PMP ต่อการประสานของเนื้อกระดูก ด้วยวิธีถ่ายภาพรังสีเอกซ์เรย์ (X-ray radiograph) เอกซเรย์คอมพิวเตอร์ (3D-CT Scan) และตรวจทางมิญชวิทยา พบว่า PMP สามารถเร่งกระบวนการประสานของเนื้อกระดูกได้ โดยไปกระตุ้นการสร้างเนื้อกระดูกใหม่และลดจำนวนเซลล์คอนโดรไฟโบรบลาสท์ โดยสรุปลิงแสมวัยหมดประจำเดือนเป็นสัตว์ทดลองที่เหมาะสำหรับการวิจัยโรคกระดูกพรุนที่ต้องการนำข้อมูลไปประยุกต์ใช้ในผู้หญิงวัยหมดประจำเดือน และการให้ PMP สามารถเพิ่มปริมาณและทำให้คุณภาพของเนื้อกระดูกดีขึ้น และยังช่วยเร่งการประสานของเนื้อกระดูกโดยคาดว่าไปลดการผลัดเปลี่ยนหมุนเวียนกระดูกผ่านระบบ RANKL/RANK/OPG ดังนั้นข้อมูลที่ได้จากงานวิจัยนี้จึงสนับสนุนแนวคิดที่จะพัฒนากวาวเครือขาวเป็นสมุนไพรทางเลือกเพื่อใช้รักษาโรคกระดูกพรุนและการประสานกันของกระดูกที่หักสำหรับสตรีวัยหมดประจำเดือน

ภาควิชา ชีววิทยา
สาขาวิชา สัตววิทยา
ปีการศึกษา 2559

ลายมือชื่อนิสิต .....
ลายมือชื่อ อ.ที่ปรึกษาหลัก .....
ลายมือชื่อ อ.ที่ปรึกษาร่วม .....
ลายมือชื่อ อ.ที่ปรึกษาร่วม .....

5572812023 : MAJOR ZOOLOGY
KEYWORDS: PUERARIA MIRIFICA, OSTEOPOROSIS, CYNOMOLGUS MONKEYS, BONE, BONE HEALING, NATURAL PRODUCT

DONLAPORN KITTIVANICHKUL: EFFECTS OF *Pueraria mirifica* Airy Shaw et Suvatabandhu AND ITS MECHANISMS OF ACTIONS ON OSTEOPOROSIS IN AGED CYNOMOLGUS MONKEYS: *IN VITRO* AND *IN VIVO* APPROACHES. ADVISOR: PROF. SUCHINDA MALAIVIJITNOND, Ph.D., CO-ADVISOR: PROF. NARATTAPHOL CHAROENPHANDHU, M.D., Ph.D., PROF. BARUCH FRENKEL, D.M.D., Ph.D., 123 pp.

The effects and mechanism of action of *Pueraria mirifica* powder (PMP) on the development of osteoporosis were assessed in cynomolgus monkeys undergoing menopause. Initially, a cross-sectional study was conducted using pre, peri, as well as early- (0 to less than 5 years), mid- (5 to 10 years), and late- (more than 10 years) postmenopausal monkeys. Bone mineral density (BMD) and content (BMC) were measured by peripheral Quantitative Computed Tomography (pQCT) of the metaphysis and diaphysis of the distal radius and proximal tibia. This cross-sectional study also included assessment of serum and urinary osteotropic hormones and bone turnover markers. An abrupt decrease in metaphyseal trabecular BMD was observed as monkeys entered the perimenopausal period and afterwards. Cortical bone was progressively lost as a function of menopausal status. Bone loss was associated with elevated serum follicle-stimulating hormone (FSH) levels at early- and mid-postmenopause and with decreased serum 17beta-estradiol level at the late-postmenopausal period. Serum BAP and urinary NTX levels were negatively correlated with the metaphyseal trabecular BMC, while serum osteocalcin levels showed a negative correlation with the diaphyseal cortical BMD. Ten osteoporotic postmenopausal monkeys were selected and used further for longitudinal 16-month study of the effects of PMP. The mRNA expression of *ALP*, *RANKL* and *OPG* quantitated by qRT-PCR in cultures of osteoblasts isolated from iliac bone biopsies of these monkeys were also determined. Monkeys were fed either control standard diet (PMP0) or diet containing 1000 mg/kg BW/day of PMP (PMP1000) and parameters of bone structure and function were measured every 2 months. In addition to BMD, BMC and hormones and markers measured in the cross-sectional study, bones of the PMP-treated and control monkeys were also analyzed for cortical area, thickness, and periosteal and endosteal circumferences. The cortical BMD and BMC of the PMP0 monkeys continuously decreased throughout the 16-month period. PMP treatment ameliorated the bone loss, mainly at the cortical diaphysis, and this was associated with a decrease in bone turnover markers. Changes of cortical bone geometry (cortical thickness and area) was in the same line with the cortical BMD and BMC. The mRNA analysis of osteoblast cultures isolated from the treated and control monkeys revealed a significant decrease in the *RANKL/OPG* ratio in the PMP1000 group and a similar but smaller decrease in the PMP0 group. Lastly, the effect of PMP on healing of the iliac crest defect created during the biopsy procedure was assessed. X-ray radiography and 3D-CT scans indicated accelerated bone healing in the PMP1000 group which was confirmed by a histological examination indicating increased new bone formation and decreased number of chondrofibroblast cells. In conclusion, the cynomolgus monkey is an ideal animal model for osteoporosis in menopausal women. Furthermore, since PMP improves bone quantity and structural properties and accelerates bone healing (in part through the RANKL/RANK/OPG system), this work advocates investigation of PMP as a therapeutic agent for prevention of osteoporosis and for treatment of fractures in postmenopausal women.

Department:	Biology	Student's Signature	.....
Field of Study:	Zoology	Advisor's Signature	.....
Academic Year:	2016	Co-Advisor's Signature	.....
		Co-Advisor's Signature	.....

ACKNOWLEDGEMENTS

I would like to express my deepest appreciation and gratitude to my advisor Professor Dr. Suchinda Malaivijitnond for her invaluable advice, support and encouragement which are not only the scientific matters but also about my daily life. Her guidance and dedication are incomparable and without it the completion of this thesis could have been impossible.

I wish to express my sincere thanks to my co-advisor, Professor Dr. Narattaphol Charoenphandhu from the Center of Calcium and Bone Research, Faculty of Science, Mahidol University, Thailand for his kind support and suggestions.

I would also like to extend my thanks to Professor Dr. Baruch Frenkel, my co-advisor from Department of Orthopaedic Surgery and of Biochemistry & Molecular Biology, Institute for Genetic Medicine, Keck School of Medicine, University of Southern California (USC), USA. It was a wonderful experience to conduct a bone research under your supervision which will be unforgettable for me.

I also express my appreciation to Professor Boonsong Ongphiphadhanakul from Division of Endocrinology and Metabolism, Department of Medicine, Faculty of Medicine, Ramathibodi Hospital, Mahidol University, Thailand, my thesis committee, for kind suggestions and guidance to improve the quality of the thesis. My thanks also go to Professor Dr. Gen Watanabe and Associate Professor Dr. Kentaro Nagaoka at Department of Veterinary Medicine, Faculty of Agriculture, Tokyo University of Agriculture and Technology (TUAT), Japan for your help and kindness while I did the research there.

I truly appreciate all staff and members of Primate Research Unit, Chulalongkorn University; Center of Calcium and Bone Research (COCAB), Faculty of Science, Mahidol University, Thailand; Veterinary Physiology Laboratory, Tokyo University of Agriculture and Technology, Japan and the Frenkel's laboratory, USC, USA for help, support and especially friendship which made everything become easier even during my hardest.

I thank the grant agency; the 90th Anniversary of Chulalongkorn University Fund for the research scholar and the Thailand Research Fund through the Royal Golden Jubilee PhD Program (PHD/0097/2557) for the Ph.D. enrollment as well as research fund.

Lastly, and most of all, I would so much like to thank my dearest family and boyfriend for all of their understanding, support, love and giving me energy to overcoming every obstacle, without them I would not be where I am today.

CONTENTS

Page

THAI ABSTRACT iv

ENGLISH ABSTRACT v

ACKNOWLEDGEMENTS vi

CONTENTS vii

LIST OF FIGURES ix

LIST OF TABLES xiii

LIST OF ABBREVIATIONS xiv

CHAPTER I GENERAL INTRODUCTION 1

CHAPTER II LITERATURE REVIEW 4

1. Principle of bone biology 4

1.1 Bone structure and function 4

1.2 Bone cells 7

1.3 Bone growth, modeling and remodeling 13

2. Regulation of bone homeostasis by estrogen 16

3. Postmenopausal osteoporosis 18

4. Osteoporotic fractures and bone healing 20

4.1 Principle of bone healing 20

4.2 Estrogen deficiency and bone healing 21

5. *Pueraria mirifica* 22

CHAPTER III CHANGES IN BONE MASS DURING THE PERIMENOPAUSAL TRANSITION IN NATURALLY MENOPAUSAL CYNOMOLGUS MONKEYS 23

Introduction 23

Materials and Methods 25

Results 29

Discussion 42

CHAPTER IV *PUERARIA MIRIFICA* ALLEVIATES CORTICAL BONE LOSS IN NATURALLY MENOPAUSAL MONKEYS 47

Introduction 47

Page

Materials and Methods.....49
Results.....58
Discussion.....71
CHAPTER V A POTENTIAL USE OF *PUERARIA MIRIFICA* FOR BONE HEALING IN OSTEOPOROTIC MONKEYS.....76
Introduction.....76
Materials and Methods.....78
Results.....82
Discussion.....88
CHAPTER VI *PUERARIA MIRIFICA* REGULATES BONE RESORPTION AND FORMATION IN MONKEY BONE CELLS PARTIALLY THROUGH RANKL/RANK/OPG SYSTEM.....92
Introduction.....92
Materials and Methods.....94
Results.....97
Discussion.....99
CHAPTER VII GENERAL DISCUSSION AND CONCLUSIONS.....101
REFERENCES.....105
VITA.....123

LIST OF FIGURES

Figure 2.1 Structure of bone from nano to macroscopic level 5

Figure 2.2 Fundamental structure of bone matrix 6

Figure 2.3 Osteoclast lineages and differentiation 8

Figure 2.4 Schematic diagram presents the intracellular mechanism of bone resorption within osteoclast 9

Figure 2.5 Differentiation of osteoblast lineage from mesenchymal stem cell 11

Figure 2.6 Schematic present some biomolecules form osteocytes 12

Figure 2.7 The basic multicellular units (BMUs) in bone remodeling process in trabecular and cortical bone 14

Figure 2.8 Coupling mechanism between three types of bone cells and bone matrix-derived signals to regulate bone remodeling 15

Figure 2.9 Model of estrogen regulation on bone turnover 18

Figure 2.10 Normal and osteoporotic trabecular bone 19

Figure 2.11 Schematic of bone fracture healing 21

Figure 3.1 Serum hormone levels of (A) 17-β estradiol, (B) follicle stimulating hormone (FSH), and (C) luteinizing hormone (LH) in pre, peri and early, mid and late postmenopausal monkeys 30

Figure 3.2 Total (A, C, E, G) bone mineral content (BMC) and (B, D, F, H) bone mineral density (BMD) of the (A-D) radius and (E-H) tibia at the (A, B, E, F) metaphysis and (C, D, G, H) diaphysis compartment in pre, peri and early, mid and late postmenopausal monkeys 33

Figure 3.3 Bone mineral content (BMC) of the (A-C) radius bone and (D-F) tibia bone at the (A, D) metaphysis trabecular, (B, E) metaphysis cortical and (C, F) diaphysis cortical in pre, peri and early, mid and late postmenopausal monkeys 34

Figure 3.4 Bone mineral density (BMD) of the (A-C) radius bone and (D-F) tibia bone at the (A, D) metaphysis trabecular, (B, E) metaphysis cortical and (C, F) diaphysis cortical in pre, peri and early, mid and late postmenopausal monkeys 35

Figure 3.5 Correlations between the bone mineral content (BMC) and time-course after menopause of the (A, C) radius and (B, D) tibia (A, B) metaphysis trabecular and (C, D) diaphysis cortical..... 37

Figure 3.6 Bone markers (A) serum bone-specific alkaline phosphatase (BAP), (B) serum osteocalcin (OC) and (C) urinary cross-linked N-telopeptide of bone type I collagen (NTX) of pre, peri and early, mid and late postmenopausal monkeys 38

Figure 3.7 Negative correlations between the bone mineral content (BMC) or bone mineral density (BMD) at the (A, C, E) radius and (B, D, F) tibia and bone marker levels of (A, B) serum bone-specific alkaline phosphatase (BAP), (C, D) urinary cross-linked N-telopeptide of bone type I collagen (NTX) and (E, F) serum osteocalcin (OC). 40

Figure 3.8 Positive correlation between the serum follicle stimulating hormone (FSH) levels and urinary cross-linked N-telopeptide of bone type I collagen (NTX) levels. 41

Figure 4.1 Bone mineral content (BMC) of the (A, C) radius and (B, D) tibia at the (A, B) metaphysis site and (C, D) diaphysis site of pre-menopausal monkeys and post-menopausal monkeys that were selected for this study 50

Figure 4.2 LC/MS/MS chromatogram for 100 μg/L of (A) puerarin, (B) miroestrol and (C) glycyrrhetinic acid. 52

Figure 4.3 Fragmentation mode of (A) puerarin, (B) miroestrol and (C) glycyrrhetinic acid. 53

Figure 4.4 Cross-section of bone cortex demonstrated measurement of bone geometry which are cortical area, cortical thickness, endosteal and periosteal circumference. 56

Figure 4.5 Total (A, B, G and H), trabecular (C and D) and cortical (E, F, I and J) bone mineral content (BMC) of the (A, C, E, G, I) radius and (B, D, F, H, J) tibia bone at (A–F) metaphysis and (G–J) diaphysis sites during the 16-month study period 61

Figure 4.6 The (A, B, G and H) total, (C, D) trabecular and (E, F, I and J) cortical bone mineral density (BMD) of the (A, C, E, G, I) radius and (B, F, H, J) tibia bone at (A–F) metaphysis and (G–J) diaphysis sites during the 16-month study period 62

Figure 4.7 Bone geometry, in terms of the cortical area, thickness, endosteal and periosteal circumference, at the metaphysis of the (A, C, E, G) radius and (B, D, F, H) tibia during the 16-month study period..... 65

Figure 4.8 Bone geometry, in terms of the cortical area, thickness, endosteal and periosteal circumference, at the diaphysis site of the (A, C, E, G) radius and (B, D, F, H) tibia bone during the 16-month study period..... 66

Figure 4.9 Level of bone turnover markers. The (A, B) plasma (A) bone-specific alkaline phosphatase (BAP) and (B) osteocalcin plus the (C) urinary cross-linked N-telopeptide of type I collagen (NTX) levels during the 16-month study period.. 68

Figure 5.1 Bone defects at the lateral ilium wing in each monkey..... 79

Figure 5.2 The (A) perimeter and (B) area of bone defect, as determined by X-ray radiography, during the 16-month experimental period. 83

Figure 5.3 The (A) area, (B) perimeter and (C) depth of the bone defect, as determined by 3D-CT scans at month 0, 8 and 16..... 85

Figure 5.4 Reconstructed 3D-CT scans at month 0, 8 and 16 of the representative PMP0 and PMP1000 monkeys. 86

Figure 5.5 Longitudinal plane histology section (stained with H&E) of the ilium biopsy at month 16 of the (A, C, E) PMP0 and (B, D, F) PMP1000 treated monkeys at (A, B) 25X, (C, D) 100X and (E, F) 200X magnification 87

Figure 6.1 The mRNA expression of (A) alkaline phosphatase (*ALP*), (B) nuclear factor κ-B ligand (*RANKL*), (C) osteoprotegerin (*OPG*) and (D) *RANKL/OPG* ratio at month 0 and moth 16 of the monkeys in PMP0 and PMP1000 group..... 98

LIST OF TABLES

Table 3.1 Number of animals, age, and body weight of the pre, peri and postmenopausal cynomolgus monkeys used in this study. 25

Table 4.1 Body weight, age, menopause period, and total bone mineral density (BMD) of the monkeys in each treatment group. 54

Table 4.2 Blood chemical analysis of postmenopausal cynomolgus monkeys at 0 and 16 months after treatment with PMP0 or PMP1000 58

Table 4.3 Correlations between the bone turnover markers (plasma BAP, OC and urinary NTX levels) and bone mass (BMD and BMC) or geometry (cortical area and thickness, endosteal and periosteal circumference) parameters. 70

Table 6.1 *Macaca fascisculari*s primers used in qRT-PCR analysis 96

LIST OF ABBREVIATIONS

ALT	Alanine aminotransferase
AST	Aspartate aminotransferase
BAD	Bcl-2 associated death promoter
BAP	Bone specific alkaline phosphatase
BMC	Bone mineral content
BMD	Bone mineral density
BMUs	Basic multicellular units
BSP	Bone sialoprotein
BUN	Blood urea nitrogen
BW	Body weight
COL1A1	Type I collagen
CT	Computed tomography
DEPC	Diethylpyrocarbonate
DKK1	Dickkopf1
DMP1	Dentin matrix acidic phosphoprotein 1
DMSO	Dimethylsulfoxide
E_1	Estrone
E_2	17β-estradiol
E_3	Estriol
ERα	Estrogen receptor alpha
ERβ	Estrogen receptor beta
ERT	Estrogen replacement therapy
FSH	Follicle stimulating hormone
IL	Interleukin
kVp	Kilovoltage peak
LC/MS/MS	Liquid chromatography tandem mass-spectrometry
LH	Luteinizing hormone
M-CSF	Macrophage colony-stimulating factor

mAs	Milliampere seconds
MSC	Mesenchymal stem cells
NF-κB	Nuclear factor-kappa B
NTX	Cross-linked N-telopeptide of bone type-1 collagen
OC	Osteocalcin
OPG	Osteoprotegerin
OVX	Ovariectomized
ORX	Orchidectomized
PM	*Pueraria mirifica*
PME	*Pueraria mirifi*ca extract
PMP	*Pueraria mirifica* powder
pQCT	Peripheral Quantitative Computed Tomography
RANKL	Nuclear factor κ-B ligand
RIA	Radioimmunoassay
SDF1	Stromal cell-derived factor 1
SEM	Standard error of the mean
SERMs	Selective estrogen receptor modulators
TGFβ	Transforming growth factor-β
TNF	Tumor necrosis factor
US-FDA	US Food and Drug Administration

CHAPTER I
GENERAL INTRODUCTION

Osteoporosis is a metabolic bone disease characterized by low bone density and deteriorated bone microarchitecture (NIH, 2001). The major consequence of osteoporosis is bone fracture, which occurs even with minimal trauma. Osteoporotic fracture has become a global public health problem with approximately 8.9 million fractures annually (Johnell and Kanis, 2006) and a total of 200 million patients across the globe were recorded (Kanis, 2007). Fractures occur at any skeletal site, but hip, spine and distal forearm are the most common sites of fracture (Pecina et al., 2007). Osteoporosis thus finally leads to morbidity, mortality and huge economic consequence. Twenty-five percent of hip fracture patients require long-term nursing and 15-30% of them die within the first year (World Health Organization, 2003). The annual cost of care and treatment for osteoporosis is approximately $17 billion U.S. dollars in USA and 5,408 million euros in UK (Svedbom et al., 2013).

The prevalence of osteoporosis increases with age since after reaching the peak bone mass during maturity bone mass continuously decreases (Eastell et al., 2016). As such, the number of osteoporotic patient is increased yearly following the increased life expectancy of the current global population trends (Christensen et al., 2009). As estimated, the numbers of 65 years old or older osteoporotic patients can be increased up to 1555 million in 2050 (Harvey et al., 2010).

Since osteoporosis primarily occurs in postmenopausal women, estrogen is thus counted as an important factor maintaining bone metabolism (Khosla et al., 2012). The prevalence of osteoporotic fracture in aging women reported is three times higher than the men (World Health Organization, 2003). Other than facing with a high risk of osteoporotic fracture, postmenopausal women also delay in bone healing after fractured because estrogen deficiency also directly affects to all stages of bone healing (Giannoudis et al., 2007). Unlike normal subject, poor bone quantity and quality in osteoporotic patients lead to difficulty in surgery or stabilized fixation.

Estrogen replacement used to be the first-line treatment for postmenopausal osteoporosis. However, it was retracted after a randomized control study found that women taking estrogen/progestin had significantly increased risk of breast cancer (Beral and Million Women Study, 2003; Chlebowski et al., 2003). Use of estrogen is also associated with increased risks of endometrial cancer (Grady et al., 1995) and venous thromboembolism (Douketis et al., 2005). As such, selective estrogen receptor modulators (SERMs), estrogen receptor (ER) ligands that exert selective agonist or antagonist effects on estrogen targeted tissues (Riggs and Hartmann, 2003), have attracted attention. A previous study suggested that phytoestrogens, estrogen-like compounds found in plants and exhibit SERM-like activity, should be considered as an alternative to estrogen replacement therapy (Brzezinski and Debi, 1999).

Pueraria mirifica (PM) is a leguminous plant, which is endemic to Thailand. It has been reported that PM contains at least 17 phytoestrogenic substances such as miroestrol, puerarin, daidzin, daidzein, genistin and genistein (Malaivijitnond, 2012). In the past decades, the estrogenic activities of PM have been tested both *in vitro* and *in vivo* (rodents, monkeys and humans) (Malaivijitnond, 2012). In *in vitro* study, the anti-osteoporotic effect of PM has also been elucidated both *in vivo* and *in vitro*. PM stimulated differentiation of UMR 106 rat osteoblast-like cells (indicating by increased alkaline phosphatase (*Alp*) mRNA level) and baboon primary osteoblasts (indicating by increased *ALP* and type I collagen mRNA levels (*COL1A1*)). Furthermore, PM directly suppressed proliferation, differentiation, fusion and resorbing function of osteoclasts (Suthon et al., 2016b) and indirectly via the reduction of receptor activator of NFκ-B ligand (*RANKL*)/ osteoprotegerin (*OPG*) mRNA expression ratio (Tiyasatkulkovit et al., 2012; 2014). In *in vivo* study, PM effectively prevented bone loss by increasing both bone mineral density (BMD) and bone mineral content (BMC) in ovariectomized (OVX) and orchidectomized (ORX) rats (Urasopon et al., 2007; 2008), and maintained bone mass in osteopenia ovariectomized rats (Suthon et al., 2016a).

Although many positive results of PM on osteoporosis have been reported, there is still not sufficient supporting data for PM development as an anti-osteoporotic drug for human use. This is because the experiments were mainly done in rats. Based upon the fact that rats and humans are different in anatomical and physiological

characteristics; that is, rats lack Harversian remodelling as the humans do, and the progress of osteoporosis in rats is slower than that in humans (Jee and Yao, 2001; Lelovas et al., 2008). Thus, results gained from the rats are not able to transfer directly to humans. Moreover, following the US-FDA guideline, at least two animal species are required for assessment of the safety of any substances which will be applied to postmenopausal osteoporotic patients (Thomson et al., 1995). The animal species, particularly aged individuals who have bone mass and structures, and hormonal profile similar to those of humans should be used. Cynomolgus monkeys (*Macaca fasicularis*), a non-seasonal breeding non-human primate, should be a representative animal model of choice for this study. The physiological systems of cynomolgus monkeys, including hormonal patterns (Goodman et al., 1977), reproductive functions (Weinbauer et al., 2008) and bone structures (Schaffler and Burr, 1984) are similar to those of humans. Thus, aged female cynomolgus monkeys were selected as animal subjects to investigate the effect of estrogen deficiency on bone loss, and the therapeutic effects of PM on osteoporosis and bone healing fracture in this study.

Objectives

1. To evaluate the effects of estrogen deficiency on bone mass in perimenopausal and postmenopausal cynomolgus monkeys.
2. To investigate the therapeutic effects of PM on bone loss in postmenopausal monkeys.
3. To determine the efficacy of PM on healing process of bone fracture in postmenopausal monkeys.
4. To understand the mechanism of actions of PM on bone resorption and formation in monkey bone cells.

CHAPTER II
LITERATURE REVIEW

1. Principle of bone biology

1.1 Bone structure and function

Bone is a specialized connective tissue that has an important role in mechanical support, protection of the body, locomotion, mineral homeostasis, and hematopoiesis within the marrow (Florencio-Silva et al., 2015). Recently, bone is counted as an endocrine organ where the bone cells secrete hormones involving in energy balance and mineral ion homeostasis (DiGirolamo et al., 2012). Therefore, to achieve those functional purposes, bone specially and delicately organizes their structures; from nano to macroscopic levels (Figure 2.1). At macroscopic level, bone divides into cortical and trabecular part. Cortical bone is a dense solid material surrounding the outer shell of the bone, whereas trabecular bone comprises honeycomb-like network positioning near marrow cavity or at the end shaft of long bone. Adult skeleton consists of 80% and 20% of cortical and trabecular bones, respectively (Clarke, 2008). Cortical bone organizes in microstructure of osteon or so-called Haversian system, where bone resorption and formation in cortical bone occur. The central of each osteon, Harversian canal, is a nutrient perforating canal, consisting of blood vessel, nerves, and lymphatic vessels, which is surrounded by layers of concentric lamellae (Kim et al., 2015). On the other hand, the lamellae of trabecular bone run parallel to the trabecular surface. However, both cortical and trabecular bones share a similar nano and ultrastructure of bone matrix.

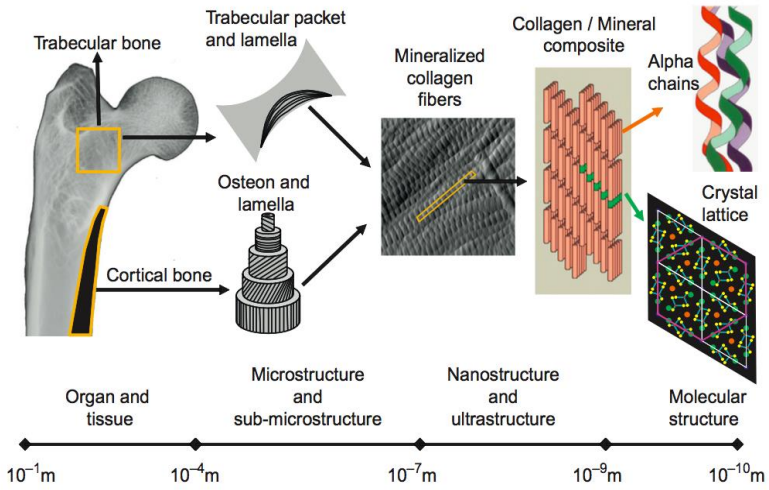

Figure 2.1 Structure of bone which is specifically and delicately organized from nano- to macroscopic level (Source: Burr and Akkus, 2014, re-use with permission form Elsevier)

Bone matrix composes of approximately 65% of inorganic materials, mainly carbonated apatite, 20-25% of organic component, primarily Type I collagen or noncollagen protein, and 10-15% of water which is bound to collagen-mineral composite or unbound water free flowing in canaliculi and vascular of bone (Burr and Akkus, 2014). Fundamental structure of bone is a triple helix Type I collagen formed by two α1 chains and a single α2 chain. The triple helix contains propeptides at the terminal known as procollagen. Subsequently, peptide regions are enzymatically cleaved and form mature collagen molecules containing helical triple helix and non-helical N- or C- telopeptides at N- or C-terminus, respectively. The mature collagens aggregate into collagen fibrils and fibers. Collagen fibrils connect differently which predominantly affect the material properties of tissue and mechanical behavior of the bone. The carbonate apatite, a primary mineral of bone matrix, nucleates within the gap region of the collagen fibrils known as a hole zone. Initially, amorphous calcium phosphate deposit along with large amount of calcium carbonate. As bone tissue matures, the carbonate content is reduced and become plate-like structure oriented parallel to the collagen fibrils (Figure 2.2). Other than that, the bone matrix also contains numerous noncollagen proteins which play an important role in embryogenesis

and development, regulate the formation and size of collagen fibrils, control mineralization, and provide conduits for cellular signaling and attachment. The critical noncollagen molecules in bone matrix are such as alkaline phosphatase (ALP), bone sialoprotein, osteocalcin (OC) and osteonectin. ALP is an enzyme that hydrolyzes pyrophosphatase which inhibits mineral deposition by binding to mineral crystals and is used as biomarker for osteoblast cells. Bone sialoprotien, also known as osteopontin, is secreated by osteoblasts and acts as glue in the bone providing fiber matrix bonding. OC is expressed in osteoblasts and osteocytes, which plays a critical role in enhancing calcium binding and controlling mineral deposition. Osteonectin locating in mineral matrix of the bone promotes nucleation of new mineral crystal as well as regulates osteoblast proliferation.

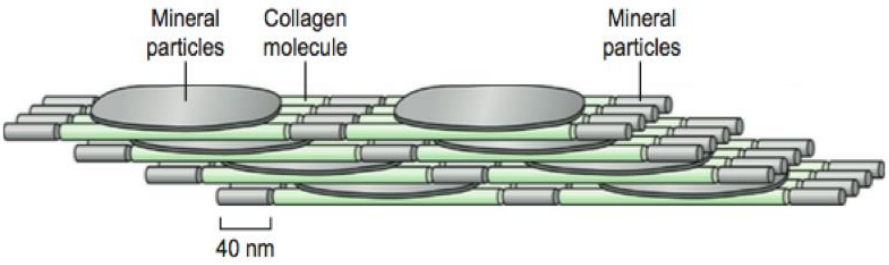

Figure 2. 2 Fundamental structure of bone matrix which comprises collagen molecules and minerals (hydroxyapatite) within hole zones. (Source: Burr and Akkus, 2014, re-use with permission form Elsevier)

1.2 Bone cells

1.2.1 Osteoclasts

Osteoclasts are multinucleated giant cells known to be responsible for bone resorption. The osteoclasts are originated from pluripotent hematopoietic stem cells which can be differentiated to be granulocytes, megakaryocytes, monocytes-macrophages and osteoclasts (Marks and Walker, 1981). The earliest factor identification of the hematopoietic precursor-derived osteoclasts is the colony forming unit-granulocyte/macrophage cell (CFU-GM) (Menaa et al., 2000). The CFU-GM will proliferate in response to hematopoietic growth factor such as IL-3, GM-colony-stimulating factor (CSF), and especially macrophage colony stimulating factor (M-CSF) (Roodman, 2006). Not only proliferation but M-CSF also plays an important role in differentiation, survival, and apoptosis of osteoclast precursors and also survival and cytoskeletal rearrangement of osteoclast bone resorption. M-CSF found mainly in bone marrow stromal and osteoblast in both membrane-bound and soluble forms. Therefore, osteoblast and stromal cells are needed in osteoclastogenesis process (Teitelbaum and Ross, 2003). However, M-CSF alone cannot complete the osteoclastogenesis. Between 1981 to mid 1990s, RANKL was discovered. RANKL is a type II homotrimeric transmembrane protein that found in membrane-bound form or secreted protein from stromal cells and osteoblast lineages. The RANKL binds with its receptor, RANK, locating on osteoclast cell surface, which requires committing the maturation and function of osteoclasts by inducing several pathways such as p38 MAP kinase, JNK, and *c-Src* (Roodman, 2006). Indeed, RANKL and RANK receptor widely express in other tissues such as mammary gland (Fata et al., 2000), breast cancer (Kim et al., 2006) and prostate cancer (Chen et al., 2006). Furthermore, the OPG which is a decoy receptor protein for the RANKL also expresses in osteoblasts and many tissues such as heart, kidney, liver, spleen and bone marrow, thus it functions to limiting osteoclast bone resorption (Wada et al., 2006) (Figure 2.3).

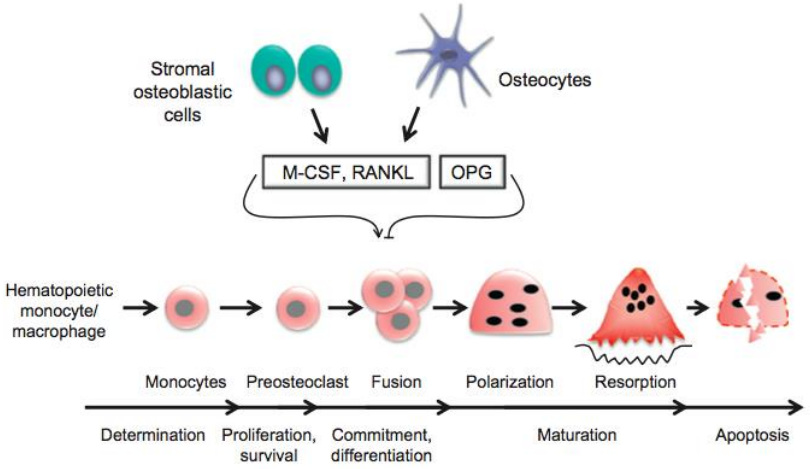

Figure 2.3 Osteoclast lineages and differentiation. Hematopoietic cell commits to osteoclast by induction of macrophage colony- stimulating factor (M-CSF), receptor activator of NFκB ligand (RANKL) and also other cytokines secreted by osteoblast and osteoclast. Osteoprotegerin (OPG) acts as decoy receptor for the RANKL to reduce osteoclast differentiation. (Source: Bellido et al., 2014, re-use with permission form Elsevier)

It is not known exactly how osteoclasts are guided to the resorption sites. At least the first sign is the retraction of bone-lining cells at the bone matrix (Jones and Boyde, 1976). After removal, the osteoclasts attach to the bone matrix via integrin receptor on osteoclast membrane which binds to RGD (arginine, glycine and asparagine)-containing peptide at the surface of bone matrix. Subsequently, the matrix-derived signals transduction through integrins resulting in ring like structure's formation, called actin ring, at sealing zone, that isolates the resorptive microenvironment (between the osteoclast and the underlying bone matrix) from other. Osteoclast develops ruffled border to secrete H^+ ions via H^+-ATPase channel and Cl^- via chloride channel, to solubilize crystalline hydroxyapatite in low pH. Subsequently, the organic matrix of bone is degraded and removed by enzymes such as tartrate-resistant acid phosphatase, cathepsin K, matrix metalloproteinase (MMP)-9 and gelatinase from cytoplasmic lysosome (Clarke, 2008). The resorption of osteoclast resulting in saucer-shape in the bone called Howship's lacuna or Harversian canals in

trabecular and cortical bone, respectively. After osteoclast fulfills the resorption task it undergoes apoptosis (Vaananen et al., 2000) (Figure 2.4).

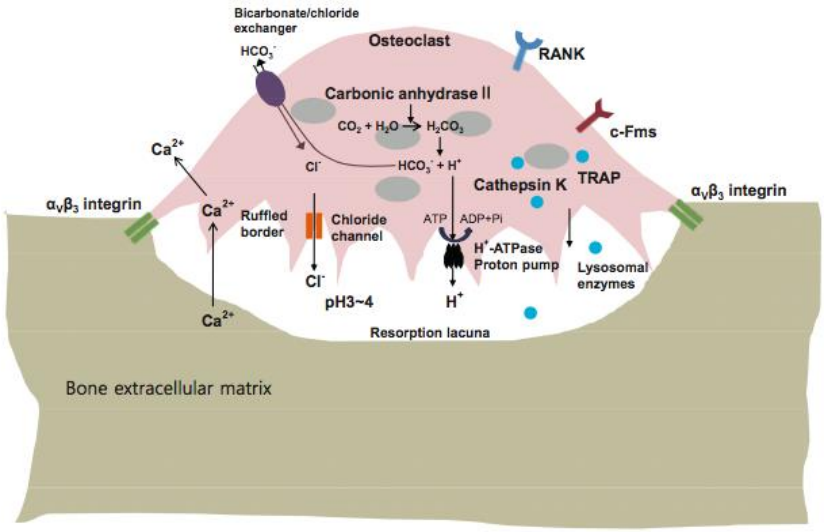

Figure 2.4 Schematic diagram presents the intracellular mechanism of bone resorption within osteoclast. Osteoclast attaches to the bone matrix by binding to integrin and is induced to secrete H^+ ions via H^+-ATPase channel and Cl^- via chloride channel, to solubilize crystalline hydroxyapatite in low pH (Source: Lee, 2010)

1.2.2 Osteoblasts

Osteoblast is a bone forming cell derived from multipotent stem cells known as stromal cells, mesenchymal stromal cells, skeletal stem cells, stromal fibroblastic stem cells, and most recently, mesenchymal stem cells (MSCs). The stem cells can differentiate to several kinds of cells which are myoblast, chondrocytes, adipocytes and osteoblasts depending on the regulation of various transcription factors and signaling proteins (Figure 2.5). Indian Hedhehog (Ihh) which belongs to the Hedgehog family is required for the expression of RUNX2 (or so-called core binding factor a1, Cbfa1) which is the master transcription factor of osteogenesis (Vimalraj et al., 2015). RUNX2 stimulates the MSC to preosteoblast by activating osteoblast-specific genes such as osteopontin, bone sialoprotein, type I collagen, and OC (Manolagas, 2000). Thus, deletion of RUNX2 fails to form any bone in mice (Komori, 2006). Subsequently, Osterix, zinc finger protein, acts as downsteam of RUNX2 (Sinha and Zhou, 2013) to stimulate preosteoblastic cell into mature osteoblast (Zhang, 2012). Other transcription factors involved in osteoblast differentiation are Wnt/β-catenin signaling pathway, Twist1, ATF4, SatB2, Shn3, and Dlx5 (Zhang, 2012) (Figure 2.5). After the commitment into osteoblast lineage, the cells undergo proliferation and express osteoblastic marker genes which are *ALP*, bone sialoprotein (*BSP*) and *COL1A1*. The mature osteoblast also secretes extracellular matrix such as OC and osteopontin which constitute 40-50% of noncollagenous protein in the bone matrix. In addition to osteoid matrix, osteoblasts also regulate local concentration of calcium and phosphate and form hydroxyapatite. The hydroxyapatites are deposited by osteoblast in the mineralization process (Boskey, 1996). Matrix synthesis indicates bone volume but not its density. On the other hand, mineralization of the matrix increases the density of bone by displacing water, but does not alter its volume (Manolagas, 2000).

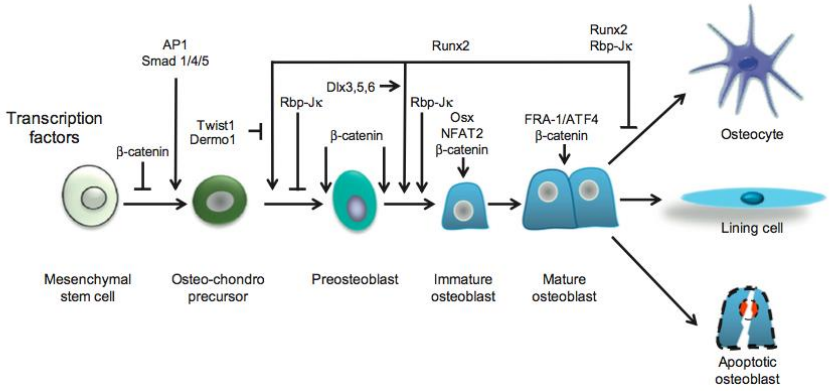

Figure 2.5 Differentiation of osteoblast lineage from mesenchymal stem cell. The scheme illustrates transcription factors that regulate proliferation and differentiation of osteoblast in each stage. (Source: Bellido et al., 2014, re-use with permission form Elsevier)

1.2.3 Osteocytes

Osteocyte is osteoblast which is buried within mineralized matrix of the bone. Osteocyte is the most abundance cell type in bone, which is about 10 times higher than comparing to the osteoblast (Parfitt, 1977). Morphology of osteocytes is stellate shape with cytoplasmic process radiating in all directions. The osteocyte's cell body is enclosed in spaces called lacuna. The process of osteocytes expands through the bone matrix to the neighboring osteocytes, lining cells and cells within bone marrow via small canals, called the canaliculi. As bone mass and architecture are affected by the external mechanical loading during physical activity which happens all the time, the bone has to self-organize or adapt in response to those stimuli. Mechanical load drives an interstitial fluid flow in the bone matrix through the pericellular matrix surrounding osteocytes and their process (Klein-Nulend et al., 2013). Osteocytes sense the mechanical stimuli via communication network, such as gap junction, which is transmembrane channels connecting the cytoplasm of two adjacent osteocytes and passes the molecules less than $1kD_a$ (Goodenough et al., 1996). Moreover, hemichannel locating on osteocyte surface play a role in mediating extracellular communication within osteocyte network. After mechanosensation, the mechanical signals convert into chemical signals to orchestrate bone formation or resorption via osteoblast and

osteoclast, respectively (Figure 2.6). Other than that, osteocyte also plays an important role in blood-calcium/phosphate homeostasis as it highly expresses dentin matrix acidic phosphoprotein 1 (*DMP1*). Previously, deletion or mutation of *DMP1* results in hypophosphatemic rickets (Feng et al., 2006). Lifespan of osteocyte can span a decade, depending on osteoclast bone resorption and bone turnover rate. Interestingly, apoptosis of embedded osteocyte, inducing by immobilization, microdamage, estrogen deprivation, elevated cytokines, glucocorticoid treatment, osteoporosis, osteoarthritis and aging, leads to bone resorption (Klein-Nulend et al., 2013)

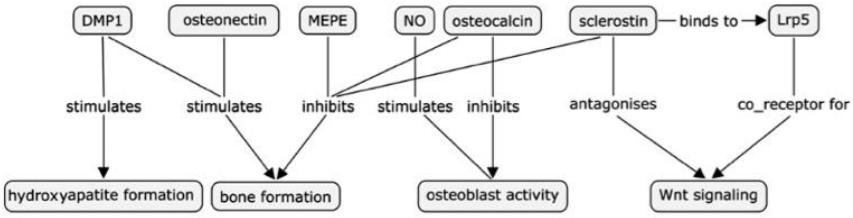

Figure 2.6 Schematic present some biomolecules form osteocytes involving in bone formation and bone resorption via osteoblast and osteoclast, respectively. (Source: Klein-Nulend et al., 2013, re-use with permission form Elsevier)

1.2.4 Lining cells

Bone lining cell is a lineage of osteoblast lineage which rests on endosteal and trabecular surfaces. The lining cell has flat morphology, little cytoplasm or endoplasmic reticulum, largely lost their synthetic function, less cytoplasmic basophilia and ALP activity than matrix-synthesizing osteoblasts. As the lining cells cover the mineralized bone surface, they play an important role to serve as a barrier to osteoclasts and participate in other aspects of intercellular signaling.

1.3 Bone growth, modeling and remodeling

During skeletal development in the childhood, there are two types of bone formation or osteogenesis. Intramembranous ossification is a bone forming in skull or flat bone of which new bone is directly formed by mesenchymal stem cells. In contrast, longitudinal bone growth occurring at metaphysis of long bone needs a prior chondrocyte proliferation. Subsequently, the invasion of osteoclasts assists in the removal of chondrocytes and osteoblasts come to create bone matrix (Mackie et al., 2008).

Modeling is the process in which shape of bone is changed in both of longitudinally or radially growth in response to physiological influences or mechanical loading. For example, the widening of bone is normally observed in age individuals owing to bone resorption at endosteal site. Therefore, the compensation of stress causes the increase in periosteal apposition (Szulc et al., 2006). During bone modeling, bone formation and resorption are not tightly coupled.

Bone remodeling occurs throughout adult life which is responsible for maintenance of mineral homeostasis and repairing microdamage within the bone. The bone remodeling occurs at distinct sites throughout the body in terms of basic multicellular units (BMUs). However, the BMUs in cortical and trabecular bone are differences. The BMUs in trabecular locate at the bone surface and cover with mesenchymal stem cell, called canopy. The remodeling initiates when osteoclast precursors from the monocyte–macrophage lineage are recruited, and then attach to the bone matrix to create a sealing zone. Within this compartment, the osteoclast plays an important role to resorb mineral and organic components of bone by producing proton pumps and enzymes such as metalloproteases. Subsequently, osteoblast precursors differentiate to active osteoblast and fill up the resorption pit with new bone matrix. In cortical bone, osteoclast proceeds resorption through the bone cortex to create a cutting cone followed by differentiating osteoblast (Sims and Martin, 2014) (Figure 2.7).

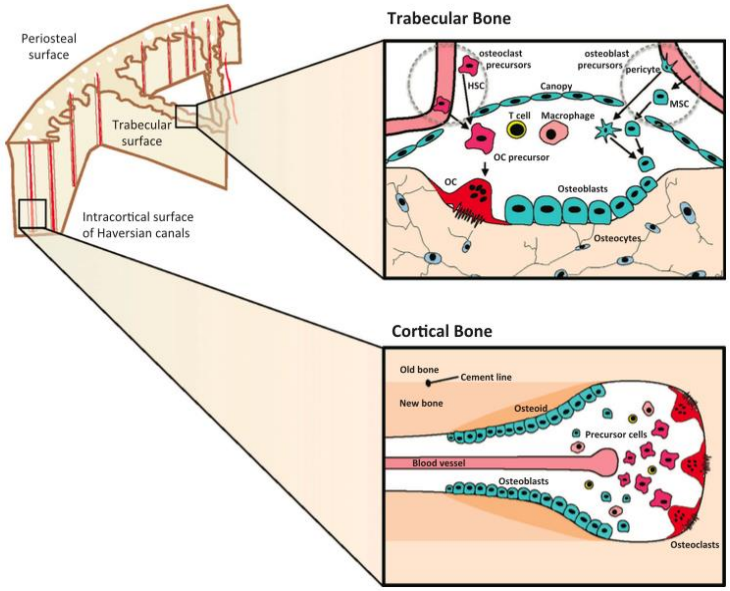

Figure 2.7 The basic multicellular units (BMUs) in bone remodeling process in trabecular bone (upper panel) ad cortical bone (lower panel). (Source: Sims and Martine, 2014, re-use with permission from Macillan Publisher Ltd.)

The bone remodeling is stringently regulated by communications between osteoclasts, osteoblasts and osteocytes. Osteocytes express sclerostin which inhibits osteoblast-mediated Wnt/β-catenin signaling pathway. Mechanical loading can decrease sclerostin expression in association with increased bone formation while the unloading increases sclerostin and inhibits bone formation (Moustafa et al., 2012). Osteocyte also produces another Wnt/β-catenin inhibitor which is dickkopf 1 (DKK1). Both sclerostin and Dkk1 can act synergistically to inhibit osteoblast activity. Conversely, osteocyte apoptosis triggers osteoclast bone resorption via RANKL/RANK/OPG pathway. As mentioned above, RANKL is a critical factor promoting osteoclastogenesis by binding with RANK receptor on osteoclast precursor's membrane and stimulating differentiation and function of osteoclast, whereas OPG, a decoy receptor of RANKL, suppresses osteoclastogenesis. Osteocyte apoptosis leads to loss of OPG production and at the same time to increase RANKL

expression of neighboring osteocytes (Chen et al., 2015). Osteoblast also plays a crucial role to regulate osteoclast bone resorption by RANKL/RANK/OPG pathway. When osteoblast cell numbers increase, more RANKL is available to stimulate osteoclastogenesis. On another hand, osteoclast also regulates osteoblast bone formation. Osteoclast expresses Sema4D to bind with their receptors, Plexin-B1, on osteoblast's membrane, and induces a negative feedback to reduce osteoblast differentiation (Cao et al., 2011). In addition, osteoclast also directly recruits osteoblast via cell-cell contact by expressing transmembrane protein, ephrinB2, which binds to its receptor, EphB4, on osteoblast's membrane (Matsuo and Otaki, 2012). Bone matrix also generates signal to regulate bone remodeling. Releasing of transforming growth factor-β (TGFβ) and insulin-like growth factors from bone matrix promote recruitment of MSCs which then stimulate bone formation at the resorption site (Sims and Martin, 2014) (Figure 2.8).

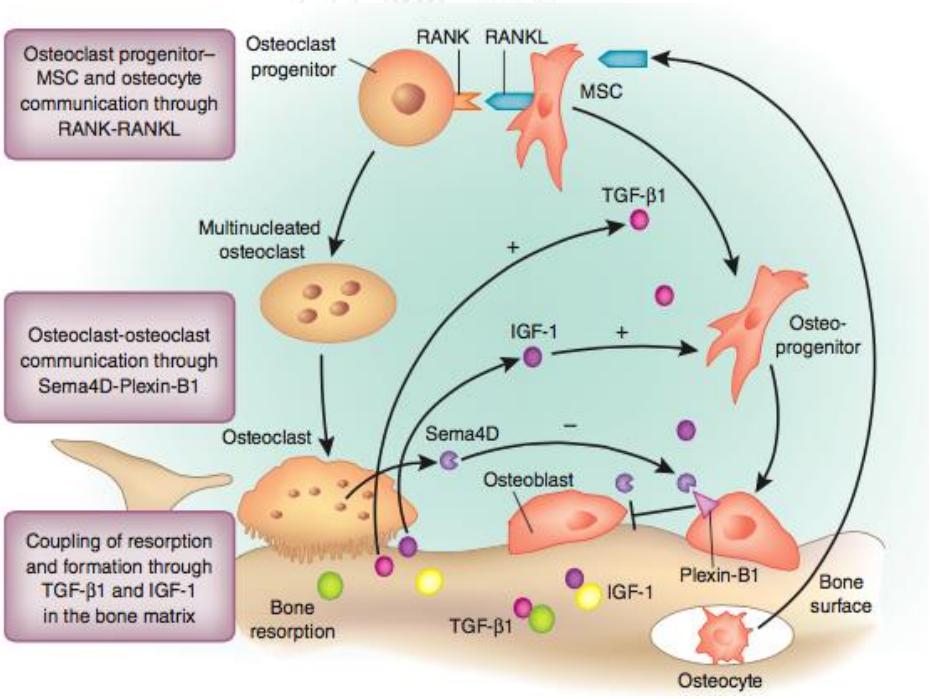

Figure 2.8 Coupling mechanism between three types of bone cells; osteocyte, osteoblast and osteoclast, and bone matrix-derived signals to regulate bone remodeling. (Source: Cao, 2011, re-use with permission from Macillan Publisher Ltd.)

2. Regulation of bone homeostasis by estrogen

Estrogen is a steroid hormone produced primarily by female's ovaries and male's testes. There are three major types of estrogen, estrone (E_1), 17β-estradiol (E_2) and estriol (E_3). Among these three types, E_2 is the most potent form. Estrogen is necessary hormone for growth, development and physiological functions of the reproductive system. The biological function of estrogen mediates by binding to its receptors which are estrogen receptor alpha (ERα) and beta (ERβ) (Lee et al., 2012). These two types of ERs distribute in many tissues in the body such as central nervous system, breast, cardiovascular system, and bone.

In bone, estrogen is the key hormonal regulator for maintaining the balance of bone remodeling. As such, ER expression is found in osteoblast, osteoclast and osteocyte (Weitzmann and Pacifici, 2006). Estrogen deficiency associated with both cortical and trabecular bone loss in post-menopausal women and even in men (Falahati-Nini et al., 2000). The determination of bone turnover markers indicates that estrogen withdrawal increases bone resorption as well as bone formation markers. However, the formation cannot couple with the resorption and leads to the net bone loss. It has been showed that E_2 lower than 5 pg/ml is associated with 2.5-fold increase in vertebral fractures in elderly women (Cauley, 2015).

Estrogen deficiency leads to a 4-fold increase in osteocyte apoptosis in both trabecular and cortical bones (Tomkinson et al., 1998). Subsequently, it has been found that estrogen protects osteocyte apoptosis via activation of the nitric oxide/cGMP/cGMP-dependent protein kinase cascade which stimulates pro-survival signaling via phosphorylation of the pro-apoptotic protein Bcl-2 associated death promoter (BAD). Moreover, as osteocyte is a crucial source of RANKL, the apoptosis of osteocyte might play a part to increase RANKL in bone microenvironment which results in increased bone resorption.

In osteoclast, direct effect of estrogen is mediated through ERα. ERα specific deletion in osteoclast creates loss of trabecular bone (Martin-Millan et al., 2010). Estrogen regulates apoptosis of osteoclast by blocking RANKL/M-CSF-induced activator protein-1-dependent transcription, through a reduction of c-jun activity.

Moreover, estrogen suppresses RANKL-induced osteoclast differentiation by sequestering tumor necrosis factor (TNF) receptor associated factor 6 (Robinson et al., 2009). Other than that, estrogen also regulates osteoclast indirectly by modulating production of cytokines involving in osteoclast formation and activity. Recently, B- cell but not T-cell lineage deleted RANKL prevents increasing in osteoclast differentiation and trabecular bone loss in OVX mice (Onal et al., 2012). In addition, other bone resorbing cytokines including interleukin (IL)-1, IL-6, TNF-α, M-CSF, and prostaglandins are modulated by estrogen (Khosla et al., 2012).

In part of bone formation, estrogen inhibits osteoblast apoptosis via Src/Shc/ ERK signaling pathway (Kousteni et al., 2001) and downregulates JNK pathway. Study in human reveals that estrogen modulates level of circulating sclerostin, which is an inhibitor of bone formation, in postmenopausal women (Modder et al., 2011). In addition, estrogen deficiency also stimulates nuclear factor-kappaB (NF-κB) activity in osteoblasts which leads to a decreased expression of transcription factor essential for bone matrix (Chang et al., 2009). However, the recent study revealed that deletion of ERα in osteoblast cells (*Col1a1*-Cre recombinase system) have no effect on bone (Almeida et al., 2013). Surprisingly, ERα deletion in osteoprogenitor cells (*Prx1*-Cre recombinase system) produces a loss of cortical but no trabecular bone (Almeida et al., 2013). However, the exact mechanism of estrogen in different bone compartment is still poorly understood.

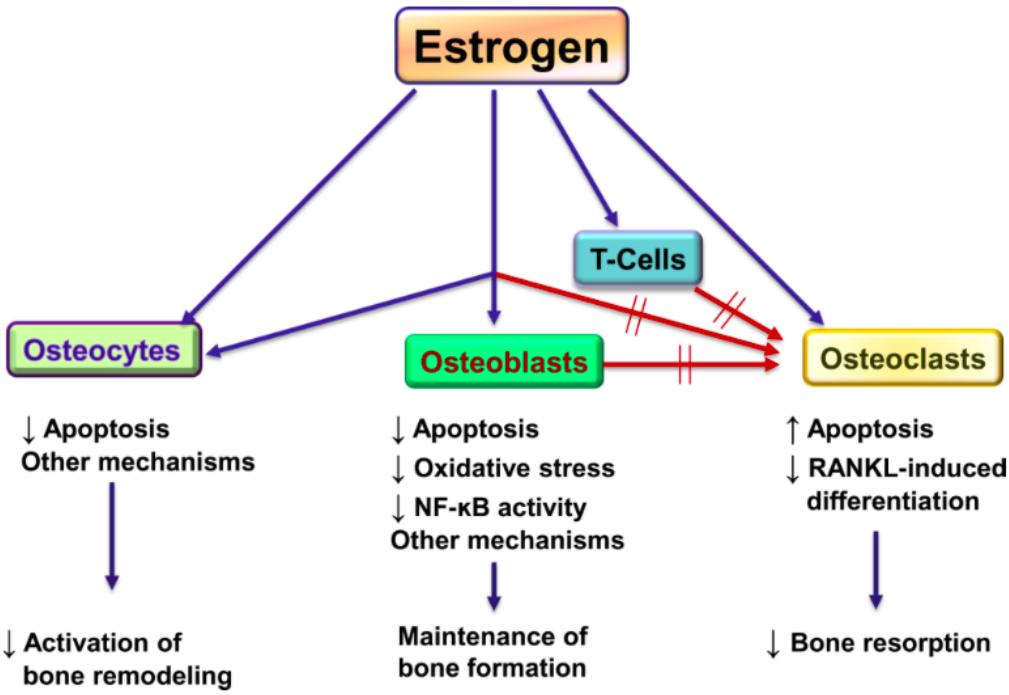

Figure 2.9 Model of estrogen regulation on bone turnover which is mediated through osteocytes, osteoblast, osteoclast and T-cells. (Source: Khosla et al., 2012, re-use with permission from Elsevier)

3. Postmenopausal osteoporosis

Osteoporosis is a major public health problem characterized by low bone mass and microarchitecture deterioration of bone tissue resulting in increased bone fragility (Figure 2.10). Bone fractures are serious and important consequences of osteoporosis which occurs with minimal trauma. Based on the fact that skeletal changes throughout life, bone mass increases and reaches the peak at a second decade of life. It is believed that at the middle age both men and women can maintain bone mass without loss or change in microarchitecture. However, current study revealed that decreasing of bone mineral density begins as early as the third decade of life (Riggs et al., 2004). As mentioned above that estrogen is a key critical hormone in regulation of bone homeostasis, thus changes in estrogen levels directly or indirectly affect the balance of bone turnover as well as bone mass. In women, the acceleration of trabecular and cortical bone loss occurs during menopausal transition period (Riggs et al., 2004) which usually happens around the fourth or five decade of life (Khosla and Riggs, 2005).

Based on the fact that men do not undergo the menopause transition as well as no clear point of estrogen deficiency, the progressive of bone loss in men is less comparing to the age-matched women. Therefore, postmenopausal osteoporosis or so-called a primary osteoporosis is a common type of the disease in women. Currently, approximately 8.9 million fractures are reported annually (Pisani et al., 2016). According to the current global population trends of the increased life expectancy, the number of elderly together with the number osteoporotic patients increases yearly. Based on the estimation, the numbers of osteoporotic patients, aged 65 years old or older, can be increased from 323 million to 1555 million in 2050 (Harvey et al., 2010), especially the hip fracture patients will be increased from 1.66 million in 1950 to 6.26 million in 2050 (Cooper et al., 1992). The impact of osteoporosis on the quality of the patient's life is mortality, morbidity and economic burden.

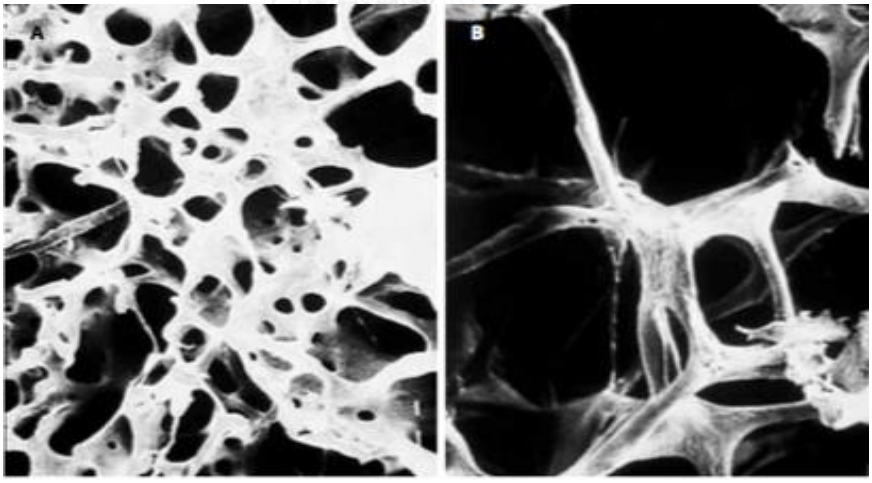

Figure 2.10 Normal (left) and osteoporotic (right) trabecular bone (Source: Reid, 2011, re-use with permission from Springer)

4. Osteoporotic fractures and bone healing

4.1 Principle of bone healing

The goal of bone healing is to restore the mineralized tissue, mechanical strength and integrity of the injured bone at the fracture site. Symphony of bone healing is more complicated than osteoporotic bone remodeling which depends on the coordination of various cell types such as inflammatory cells, mesenchymal progenitor cell, endothelial cell, chondroblast, osteoblast and osteoclast cells. Immediately after fracture, a hematoma formation stage starts of which inflammatory cells are crucial for bone regeneration. The inflammatory cytokines such as TNF, IL-1, IL-6, IL-11 and IL-18 play an important role in promoting angiogenesis, inducing osteogenic lineage differentiation of MSCs and acting as a chemotactic substance to employ necessary cells (Marsell and Einhorn, 2011). Subsequently, the fibrocartilaginous callus formation occurs when collagen is deposited and fibrocartilage converts granulation tissue to a soft callus. The matrix is composed mainly collagen type II, X and glycosaminoglycans. At this stage, the soft callus is vascularized. However, the proangionenic factors such as vascular endothelial growth factor (VEGF), bone morphogenetic proteins (BMPs), TGF-β and fibroblast growth factor (FGF) are essential to revascularization of fractures site (Oryan et al., 2013). Afterward, the cartilage is calcified and replaced by osteoblasts to be a woven, poorly organized bone. Lastly, angiogenesis invades the callus following which remodeling of osteoclast and formation of new bone by osteoblast to be well organized lamellar bone (Marsell and Einhorn, 2011) (Figure 2.11).

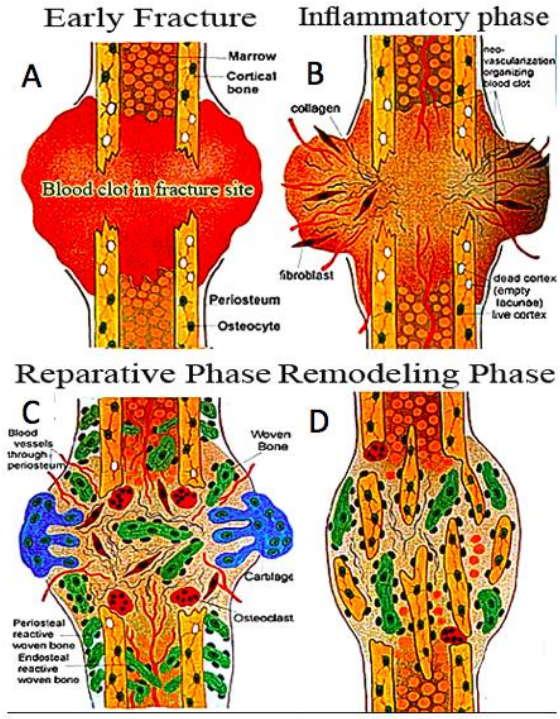

Figure 2.11 Schematic of bone fracture healing; (A) early fracture occurring with hematoma formation, (B) inflammatory cells migrating to the fracture site, (C) fibrocartilage and woven bone formation (D) woven bone remodeling to mature lamella bone (Source: Oryan et al., 2013)

4.2 Estrogen deficiency and bone healing

The study in estrogen deficient mice indicated an impaired periosteal callus formation, diminished chondrocytes and less mineralization in early stage of bone healing. In the late stage, the animals showed thin and porous cortex comparing to the control. As expected, estrogen treatment could enhance fracture healing indicating by a greater chondrocyte area, an increased mineralization and a thicker cortex (Beli et al., 2010). Moreover, the DNA microarray-based experiment from fracture callus discovered 52 gene candidates which down-regulated in estrogen-deficient rats and restored by estrogen treatment rats. Among those 52 genes, 4 genes which are collagen type 2, extracellular superoxide dismutase, urokinase-type plasminogen activator, and ptk-3 have been confirmed to be regulated by estrogen (Hatano et al., 2004). However, the molecular mechanisms of estrogen deficiency and bone fracture healing have not been clearly understood.

5. *Pueraria mirifica*

PM, locally named Kwao Krua Kwao, belongs to the Family Leguminosae, subfamily Papilionoideae (Malaivijitnond, 2012). It has been used in folklore medicine for its rejuvenating qualities in menopausal women for a long time. There are at least 17 chemical substances exhibiting estrogenic activities in PM. The compound can be categorized into three groups; isoflavonoids, coumestrans and chromenes. In the past decades, many publications clearly demonstrated the estrogenic activity of PM both *in vitro* and *in vivo*. Oral treatment with PM at a dose of 1,000 mg/kg BW/day for 14 days in OVX rats attenuated the increase in serum follicle stimulating hormone (FSH) and luteinizing hormone (LH) levels, and stimulated the proliferation of uterine and vagina (Malaivijitnond et al., 2004). Consistent with the experiment in rats, PM decreased the serum levels of FSH, LH, estradiol and progesterone in adult female cynomolgus monkeys (Trisomboon et al., 2005). The effect of PM on bone was currently evaluated. PM at doses of 10-1,000 mg/day fed daily in cynomolgus monkeys significantly decreased serum levels of parathyroid hormone and calcium (Trisomboon et al., 2004a). PM at doses of 10-1,000 mg/kg BW/day orally treated to OVX and ORX rats for 90 days could effectively prevent bone loss (Urasopon et al., 2007; 2008). When the rats were OVX, kept for 4 weeks to induce bone loss, and fed with 50 mg/kg BW/day of PM for 12 weeks, bone mass could be retained to the baseline level (Suthon et al., 2016a). *In vitro* study in rat osteoblast-like UMR 106, PM extract at the doses of 1, 10 and 100 μg/ml as well as its major isoflavone component, puerarin at the dose of 10 and 1000 nM, were likely to enhance bone formation by promoting osteoblast differentiation indicating by increased *Alp* mRNA level (Tiyasatkulkovit et al., 2012). Moreover, PM extract and puerarin also exhibited anti-osteoclastogenesis effect by suppressing differentiation and fusion of pre-osteoclast cells (Suthon et al., 2016b). Other than the rodent studies, 1000 nM of PM extract and puerarin increased cell proliferation as well as expression of *ALP* and *COL1A1* genes while decreased *RANKL/OPG* ratio in primary baboon osteoblast cells (Tiyasatkulkovit et al., 2014).

CHAPTER III
CHANGES IN BONE MASS DURING THE PERIMENOPAUSAL TRANSITION IN NATURALLY MENOPAUSAL CYNOMOLGUS MONKEYS

Introduction

Postmenopausal women are at the highest risk for osteoporosis due to estrogen deficiency (Clarke and Khosla, 2010). Thus, in the past two decades, there have been many attempts to establish or develop medication to prevent or treat osteoporosis in estrogen-deficient postmenopausal women. However, any preclinical evaluation of agents to be used in the intervention of postmenopausal osteoporotic humans must first be performed in nonhuman animal models (Thompson et al., 1995), of which the most commonly used is OVX rats (Turner, 2001). The advantages of the OVX rodent model are that they are inexpensive, easy to handle, and there is a wealth of existent knowledge on their reproductive physiology. However, the OVX rat is not an ideal representative animal model for humans as it has many different features compared to humans. For example, in contrast to humans, OVX rats lack Harversian or intracortical remodeling, and some bones in rats have a nonfused epiphysis and retain growth throughout life (Jee and Yao, 2001; Lelovas et al., 2008). Apart from the rodent model, the US Food and Drug Administration (US-FDA) announced that before the clinical trials of antiosteoporotic agents, the compounds must first be verified in a second animal species that has similar cortical remodeling to humans (Thompson et al., 1995).

Nonhuman primates are currently extensively used in postmenopausal osteoporosis research. Among many candidate primate species, cynomolgus monkeys (*Macaca fasicularis*) are often used with respect to their reproductive physiology and musculoskeletal biology as they share similarities in their hormone pattern (Goodman et al., 1977), reproductive function (Weinbauer et al., 2008), and skeletal biology (Schaffler and Burr, 1984) to humans. The duration of the ovarian cycle in cynomolgus monkeys is 30.4±4.7 days, whereas the follicular phase, ovulatory interval and luteal phase last for 12-14, 3, and 14-16 days (Weinbauer et al., 2008), respectively. After

ovariectomy, the serum FSH and LH levels are elevated, and serum E_2, inhibin B, and antimullerian hormone levels are decreased (Jerome and Peterson, 2001; Bellino and Wise, 2003). Similar to humans, cynomolgus monkeys have Haversian osteonal remodeling in their cortical bone (Burr, 1992).

Generally, OVX cynomolgus monkeys have frequently been used as an animal model for bone loss in association with estrogen depletion (Smith et al., 2011). Nevertheless, the estrogen levels fall abruptly after OVX, and the other organs that are involved in bone metabolism such as the adrenal gland, pituitary gland, hypothalamus and cytokine organs, are not senile. Thus, OVX monkeys might not completely reflect bone loss in naturally postmenopausal women (Bahar et al., 2011). In addition, the perimenopausal transition also plays a critical role in the pathological change in postmenopausal osteoporosis. A previous study proposed that the perimenopausal period might be a ‘‘critical window’’ to reduce the postmenopausal disease burden (Appt and Ethun, 2010). Accordingly, the OVX monkey model fails to represent the progression of osteoporosis in the perimenopausal transition status. From the lack of a primate model of the perimenopausal transition in naturally occurring menopause, the understanding of progression in osteoporosis from premenopause, perimenopause, and postmenopause in monkeys is poor. However, this important basic information is accessible by the use of naturally menopausal cynomolgus monkeys. Therefore, this study was performed to evaluate how the skeletal system changes during the perimenopausal transition and different time-courses after postmenopause in older female cynomolgus monkeys. The overall purpose of this study was: (1) to determine the serum E_2, LH and FSH, and bone marker levels during the premenopause, perimenopause, and early, mid, and late postmenopausal period; (2) to measure the differences in BMD and BMC at the distal radius and proximal tibia in both metaphysis and diaphysis during the premenopause, perimenopause, and early, mid, and late postmenopausal period; and (3) to evaluate the changes in bone mass in relation to changes in the serum hormone and bone marker levels

Materials and Methods

Animals

Seventy-nine female cynomolgus monkeys were used in this study. They were divided into three groups based on their menstrual records: premenopause, perimenopause, and postmenopause (Table 3.1). Premenopausal monkeys (n=33) were fully mature animals with at least three consecutive regular menstrual cycles before the study onset. Perimenopausal monkeys (n=12) were those that had irregular menstrual cycles within one year before the study onset. Postmenopausal monkeys (n=34) were those that had a complete cessation of menstrual bleeding for at least one year before the study period, and these were further divided into three subgroups of early-menopause (0 to less than 5 years of cessation of menstrual bleeding; n=18), mid-menopause (5 to 10 years; n=11), and late-menopause (more than 10 years; n=5). The postmenopausal stage in these monkeys was verified by their low serum estradiol and high serum FSH and LH levels (Kavanagh et al., 2005).

Table 3.1 Number of animals, age, and body weight of the pre, peri and postmenopausal cynomolgus monkeys used in this study.

Menopause status	Number of animals	Age[a] (y)	Body weight[a] (kg)
Premenopause	33	13.25 ± 9.55 (6.50-20.00)	5.11 ± 0.83 (4.00-6.50)
Perimenopause	12	25.38 ± 2.79 (22.39-29.72)	6.40 ± 1.21 (4.00-7.88)
Postmenopause	34	28.50 ± 4.61 (20.00-33.54)	5.90 ± 1.24 (3.34-8.89)

[a]Data are shown as the mean ±SEM, with the range in parenthesis

The naturally peri and postmenopausal monkeys were housed in individual cages at the Primate Research Unit, Faculty of Science, Chulalongkorn University. The premenopausal monkeys were reared in communal cages (4-8 animals/cage) at the Krabok-Koo Wildlife Breeding Center, Chachoengsao Province, Thailand. The monkeys were exposed to a 12:12h light-dark cycle at ambient temperature and fed daily with monkey chow diet (Perfect Companion Group Co., Ltd., Samut Pakran, Thailand) in the morning (08:00-09:00 am) and supplemented with fresh fruits in the

afternoon (01:00-02:00 pm). All monkeys had historical records. Two-thirds of the monkeys were born in the breeding unit, and one-third was caught from the wild in Thailand. Monkeys originally caught from the wild were estimated for their age from their dental eruption and body size (Hamada et al., 2005). Menstrual bleeding of monkeys was checked daily using a vaginal cotton swab. Health checks were routinely performed by veterinary staff and animal caretakers for any sign of illness.

Blood and urine collections

Animals were fasted overnight (06:00 pm to 06:00 am) before the blood and urine collections. A mixture of ketamine hydrochloride (Sankyo Co, Ltd, Tokyo, Japan) and medetomidine hydrochloride (Vetcare, Inc, Jonesboro, AR, USA) at 10 and 0.1 mg/kg body weight, respectively, was administered intramuscularly for anesthetization. Blood samples were collected from the femoral vein between 08:00 to 11:00 am, and centrifuged at 4°C 1,700g for 20 minutes. The sera were harvested and kept at -20 ºC until assayed for hormone and bone formation marker levels. To ease the fluctuation of the serum hormone levels in premenopausal and perimenopausal monkeys, blood collections were performed during day-1 to day-3 of the menstrual cycle or early follicular phase, when the first day of detection of the menstrual bleeding was counted as day-1 of the menstrual cycle. The monkeys were antisedated with atipamezole (≤0.1mg/kg body mass) after the procedures were completed.

The 12-h urine samples were collected on the same day as the blood collection by placing a stainless steel tray, covered with iron mesh, to prevent feces contamination, under the monkey cage at 6:00 pm and removing it at 6:00 am of the following day. Urine samples were centrifuged at 4°C and 1,700g for 20 minutes. The supernatants were harvested and kept at -80°C until assayed for bone resorption marker levels.

All animal activities in this study were approved in accordance with the guide for the care and use of laboratory animal prepared by the Animal Care and Use Committee of the Faculty of Science, Chulalongkorn University (CU-ACUC; Protocol review no. 1123015).

Serum hormone levels

To avoid interassay variations, all samples were measured for serum E_2, FSH, and LH levels in a single run. Serum E_2 levels were assessed by a double-antibody radioimmunoassay (RIA) using ^{125}I labeled radioligands (MPBio 07138226) as described previously (Trisomboon et al., 2004b). Antisera against E_2 were diluted with phosphate buffer saline (PBS) containing 0.05M ethylene diamine tetra-acetic acid, disodium salt, and 0.025% (v/v) normal sheep serum. Rabbit antisheep gamma globulin serum was diluted with 5% (w/v) polyethylene glycol in 0.05M PBS. Standard concentrations were 640 to 0.0781pg/tube. The intra-assay coefficient variation was 1.47%.

Serum FSH and LH levels were evaluated by a heterologous RIA system as described previously (Trisomboon et al., 2004b), using the iodinated NIDDK-rat FSH-I-5 and rat LH-I-5 and antiovine FSH (NIDDK-H-31) and antiovine LH (YM#18) antisera. The results are shown in terms of NIDDK rat FSH-RP-2 and rat LH-RP-2. The intra-assay coefficients were 3.22% for FSH and 2.03% for LH.

Serum bone formation marker levels

Serum bone specific alkaline phosphatase (BAP; Quidel, San Diego, CA, USA Catalog no. 8012) and OC (Quidel, San Diego, CA, USA Catalog no. 8002) were measured following the manufacturer's protocol. The intra and interassay coefficients were 13.2% and 16.4% for BAP, and 9.86% and 10.8% for OC, respectively.

Urinary bone resorption marker level

The urinary level of cross-linked N-telopeptide of bone type-1 collagen (NTX; Wampole Labs, Princeton, NJ, USA Catalog no. OST0001) was measured following the manufacturer's protocol. The levels of NTX were normalized with urinary creatinine levels following the Jaffe kinetic method (Legrand et al., 2003). The intra and interassay coefficients were 13.2% and 14.2%, respectively.

Measurement of the BMD and BMC

After blood withdrawal, the BMD and BMC were measured in the radius and tibia at both the metaphysis (comprised of the trabecular and cortical bones) and diaphysis (mainly in the cortical bone) using the peripheral Quantitative Computed Tomography (pQCT; Norland Stratec XCT Research SA+ pQCT, Startec, Pforzheim, Germany). Before measurement, the total lengths of the radius and tibia were measured with measuring tape. The monkey was placed in a left lateral recumbent position and the radius or tibia was fixed with tape to avoid movement. A scout scan was performed at 30 mm/s with a scan line spacing of 1 mm to properly locate the reference line. The reference line was set at the center of the epiphyseal plate in both the radius and the tibia. Compared to the reference line, the computed tomography (CT) scan was positioned at 3% (for metaphysis) and 50% (for diaphysis) of the total bone length, with a voxel size of 0.1 mm^3 and CT speed of 15mm/s. Each site was scanned three times consecutively, with a line spacing of 0.5 mm for metaphysis and 1 mm for diaphysis, respectively, and the averaged value of three time scans was used to analyze the BMD and BMC at all sites of each bone using the XCT-5.50E software (Stratec).

Statistical analysis

Data are expressed as the mean±standard error of the mean (SEM). The BMC, BMD, serum hormone and BAP levels, and the urinary NTX levels all had heterogeneous variances and so were analyzed by the Kruskal-Wallis test. The serum OC levels had homogenous variance and so were tested by one-way analysis of variance (ANOVA) with the least significant difference post-hoc test. Statistical analyses were performed using the IBM SPSS version 20 software (IBM Crop., Armonk, NY, USA). Correlation analysis was performed using the Spearman's test in GraphPad Prism (v5.01). Significance was accepted at the *p* less than 0.05 level.

Results

Serum hormone levels during perimenopause

The basal serum E_2 level was highest in premenopausal monkeys (152.4±27.0 pg/ml) and started to decrease, albeit statistically insignificantly ($p = 0.23$), when the monkeys entered into the perimenopausal period (89.0±14.1 pg/ml) (Figure 3.1A). Serum E_2 levels remained low throughout the perimenopausal and postmenopausal period, with a significant decrease (only) in the late-menopausal period (42.8±13.7 pg/ml; $p = 0.023$).

In contrast to the serum E_2 level, the serum FSH level in perimenopausal monkeys was essentially the same as in the premenopausal monkeys (548.8±159.7 pg/ml for premenopause and 507.3±145.5 pg/ml for perimenopause). However, a significant (1.82-fold) increase was detected when the monkeys entered early menopause (925.3±159.4 pg/ml; $p = 0.013$) and was highest in the mid-menopause (1100.7±177.071 pg/ml; $p = 0.02$) before returning to almost the same level as the premenopausal monkeys at the late-menopausal period (645.1±178.4 pg/ml) (Figure 3.1B).

The pattern of changes in serum LH levels resembled that of serum FSH, with the highest level detected in mid-menopausal monkeys (4793.1±1245.6 pg/ml; $p = 0.015$). However, the increase in serum LH level started from the perimenopausal period (3831.8±1003.3 pg/ml), and was not significantly different ($p = 0.12$) compared with the premenopausal period (2264.5 ±422.1 pg/ml) (Figure 3.1C).

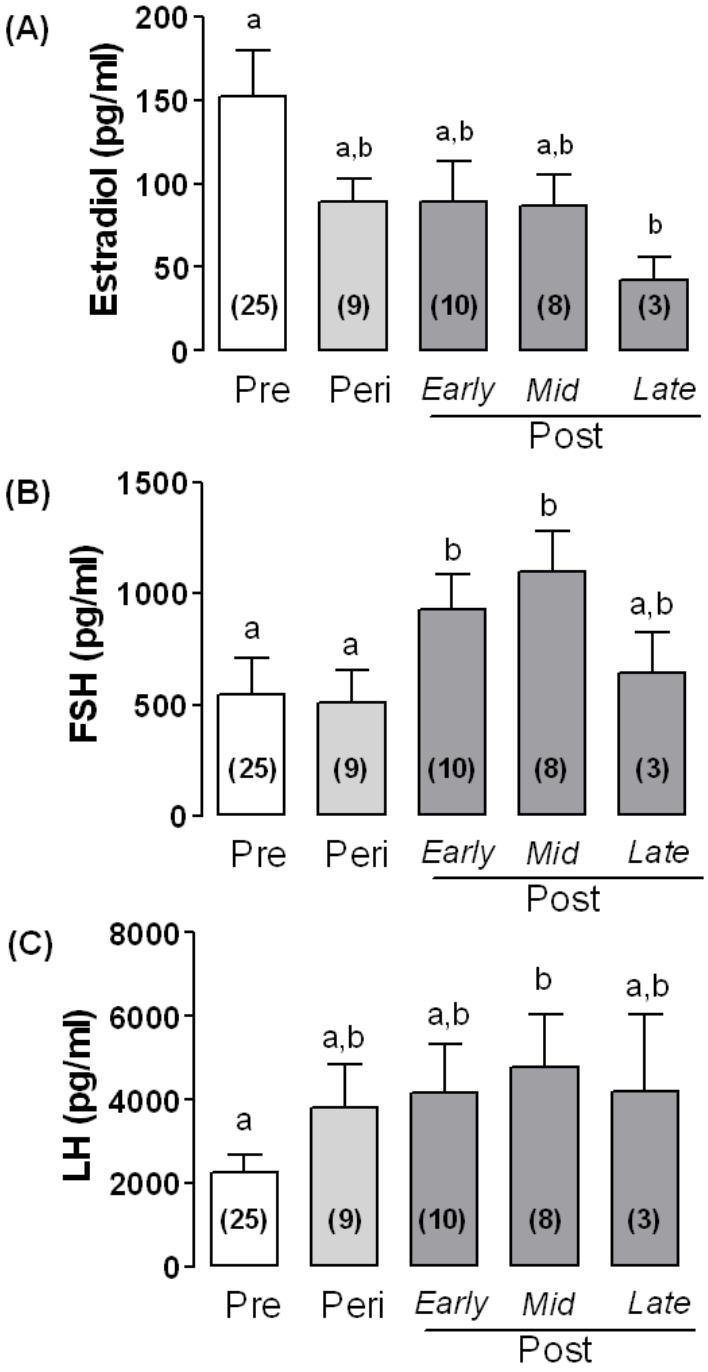

Figure 3.1 Serum hormone levels of (A) 17-β estradiol, (B) follicle stimulating hormone (FSH), and (C) luteinizing hormone (LH) in pre, peri and early, mid and late postmenopausal monkeys. Data are shown as the mean ± SEM. Means with different lowercase letters are statistically significant difference ($p < 0.05$).

BMC and BMD during perimenopause

The pattern of changes in metaphyseal and diaphyseal total BMC and BMD was roughly similar between the radius and the tibia (Figure 3.2). The total BMC and BMD tended to slightly decrease, although with some fluctuation during the premenopausal, perimenopausal, and postmenopausal periods for the metaphysis, they gradually and significantly lowered when the monkeys entered into the postmenopausal period for diaphysis. The metaphysis consisted of cortical and trabecular bones, thus the total BMD and BMC analysis may have masked opposing changes in each component. Accordingly, the cortical bone was analyzed separately from the trabecular bone for the metaphysis.

The separate analysis of the cortical and trabecular bone in metaphysis clearly revealed that the trabecular BMCs at the metaphysis site in both the radius and tibia abruptly and significantly lowered in the perimenopausal period compared with the premenopausal period ($p < 0.0001$ for both radius and tibia) and then remained consistently low throughout the three postmenopausal periods (Figure 3.3A and D). In contrast, no significantly lowered cortical BMC was detected at the metaphysis sites of the radius or tibia (Figure 3.3B and E). Conversely, the cortical BMC at the diaphysis site of both the radius and the tibia gradually and continuously lowered as the monkeys entered into the perimenopausal period and then markedly and significantly lowered in the late postmenopausal period ($p < 0.0001$ for both the radius and the tibia) (Figure 3.3 C and F).

Although not as prominent as that observed in the BMCs, the change in BMD between the radius and the tibia at the trabecular and cortical compartments of metaphysis and at the cortical compartment of diaphysis showed the same trends as those observed in BMC (Figure 3.4). The lowered trabecular BMD at the tibia metaphysis was found in perimenopausal as well as postmenopausal monkeys (Figure 3.4D), whereas a significantly lowered metaphysis site of the radius was only detected at the early postmenopausal period ($p = 0.019$) (Figure 3.4A). Interestingly, the cortical BMD at the metaphyseal compartment of the radius was significantly higher in perimenopausal and postmenopausal monkeys ($p = 0.0001$, 0.0001, and 0.013 for perimenopausal, early, and mid postmenopausal monkeys, respectively) (Figure 3.4B),

but could only be observed in the mid-menopause of postmenopausal monkeys for the tibia bone $p = 0.021$) (Figure 3.4E). Conversely, the cortical BMD at the diaphysis of both the tibia and the radius gradually and continuously lowered as the monkeys entered into the perimenopausal and postmenopausal periods (Figure 3.4C and F).

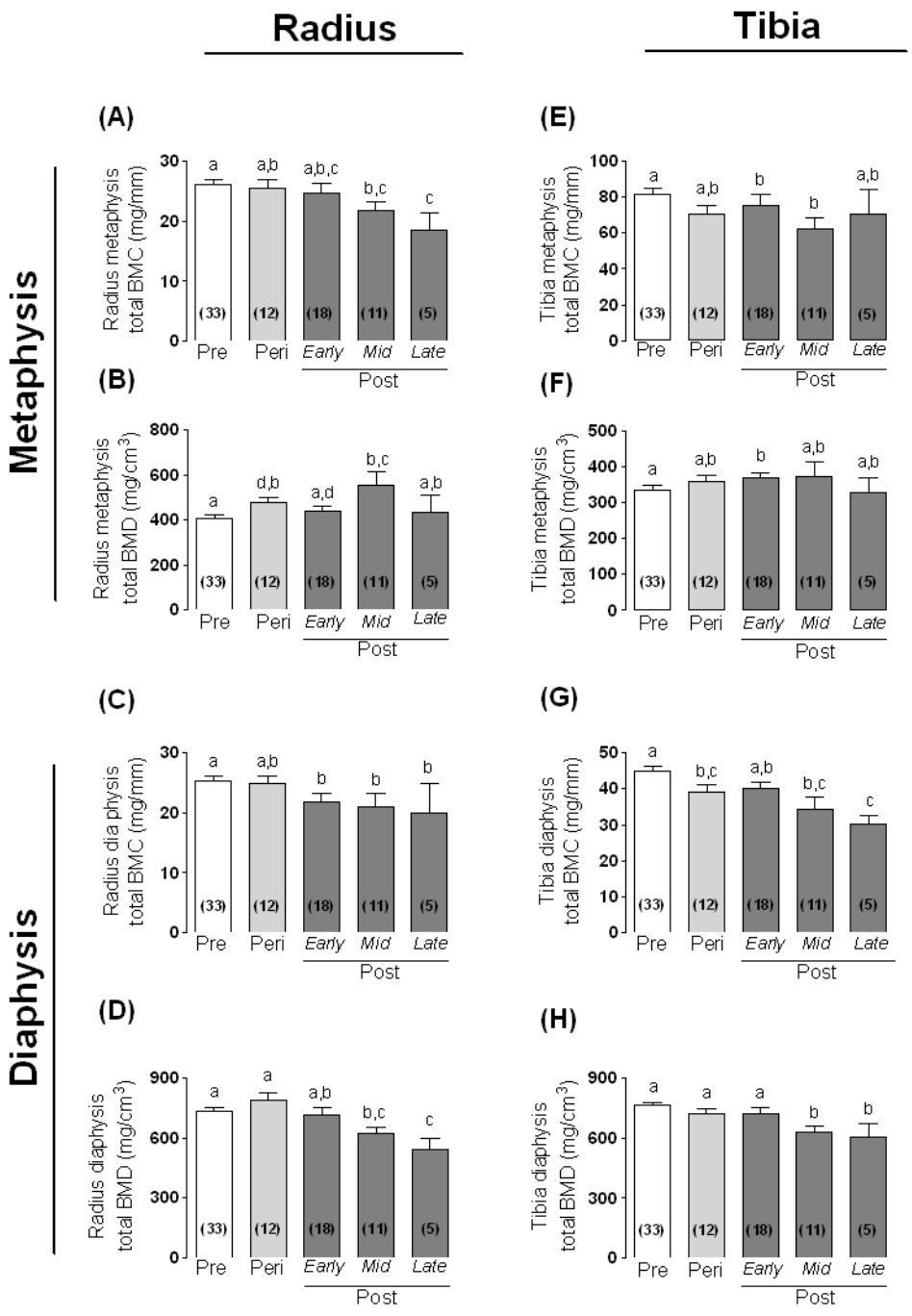

Figure 3.2 Total (A, C, E, G) bone mineral content (BMC) and (B, D, F, H) bone mineral density (BMD) of the (A-D) radius and (E-H) tibia at the (A, B, E, F) metaphysis and (C, D, G, H) diaphysis compartment in pre, peri and early, mid and late postmenopausal monkeys. Data are shown as the mean ± SEM. Means with a different lowercase letter are significantly different ($p < 0.05$).

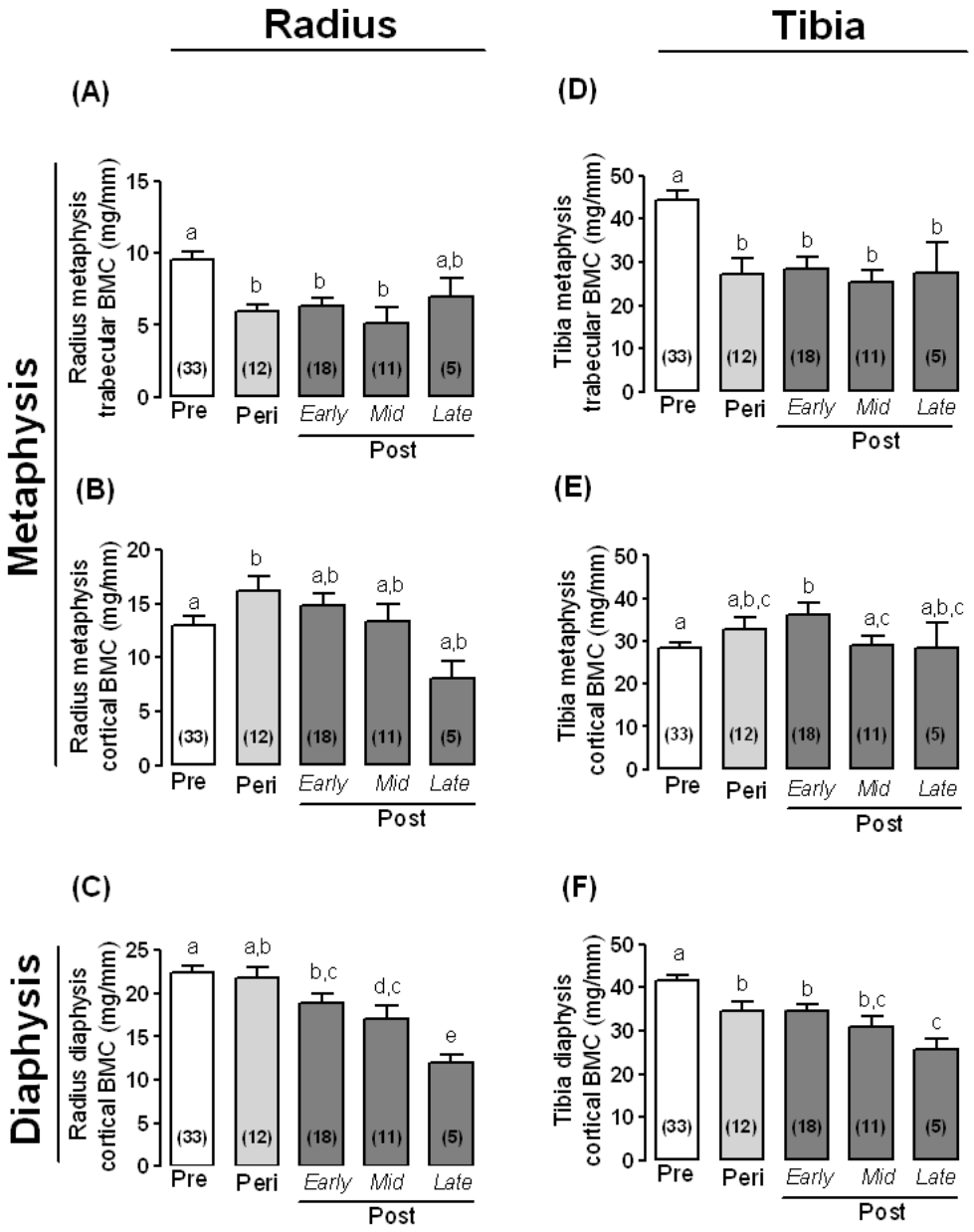

Figure 3.3 Bone mineral content (BMC) of the (A-C) radius bone and (D-F) tibia bone at the (A, D) metaphysis trabecular, (B, E) metaphysis cortical and (C, F) diaphysis cortical in pre, peri and early, mid and late postmenopausal monkeys. Data are shown as the mean±SEM. Means with a different lowercase letter are significant different ($p< 0.05$).

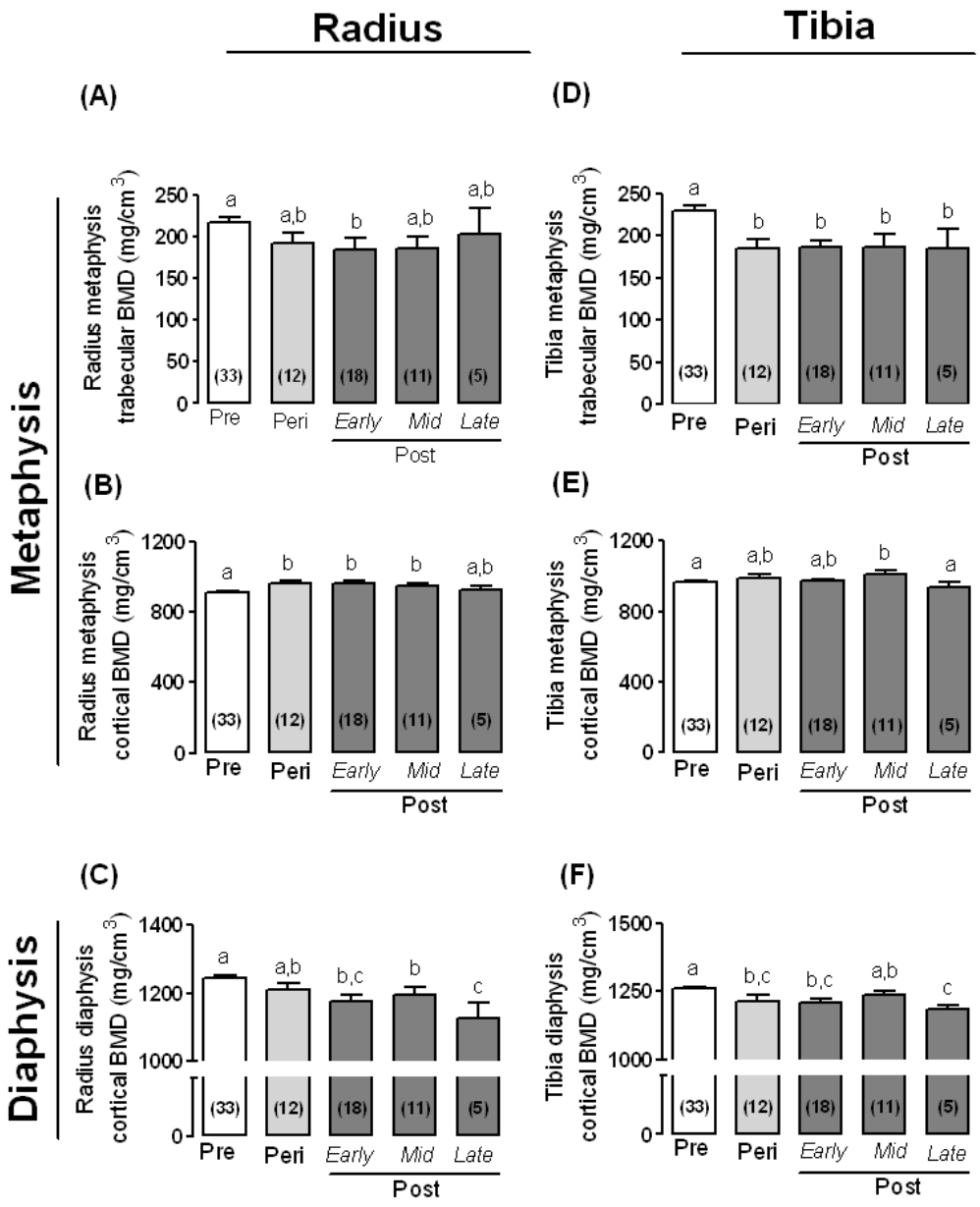

Figure 3.4 Bone mineral density (BMD) of the (A-C) radius bone and (D-F) tibia bone at the (A, D) metaphysis trabecular, (B, E) metaphysis cortical and (C, F) diaphysis cortical in pre, peri and early, mid and late postmenopausal monkeys. Data are shown as the mean±SEM, derived from. Means with a different lowercase letter are significant different ($p< 0.05$).

Correlation between the BMC and the postmenopause progression

Because the lowered BMC at the trabecular metaphysis and cortical diaphysis was protuberant and seemed to relate to the postmenopausal time, it was of interest to determine if there was any correlation between these two parameters. In agreement with the abruptly lowered BMC in the perimenopausal period, before remaining at a relatively stable low level throughout the three postmenopausal periods (Figure 3.3), the trabecular BMC at the metaphysis site did not significantly correlate with the time-course after postmenopause in both the radius and the tibia (p =0.84 and 0.53, respectively) (Figure 3.5A and B). On the contrary, from the gradually and continuously lowered BMC during the early, mid and late postmenopausal periods (Figure 3.3C), the cortical BMC at the diaphysis site showed a significant negative correlation with the postmenopause time (p =0.007, r^2=0.2103 for radius and p =0.04, r^2=0.1326 for tibia) (Figure 3.5C and D). In conclusion, when monkeys enter the postmenopausal period, they retain the stable low trabecular BMC with no further significant decrease, but the cortical BMC at the radius and the tibia is lowered further with the longer postmenopausal period.

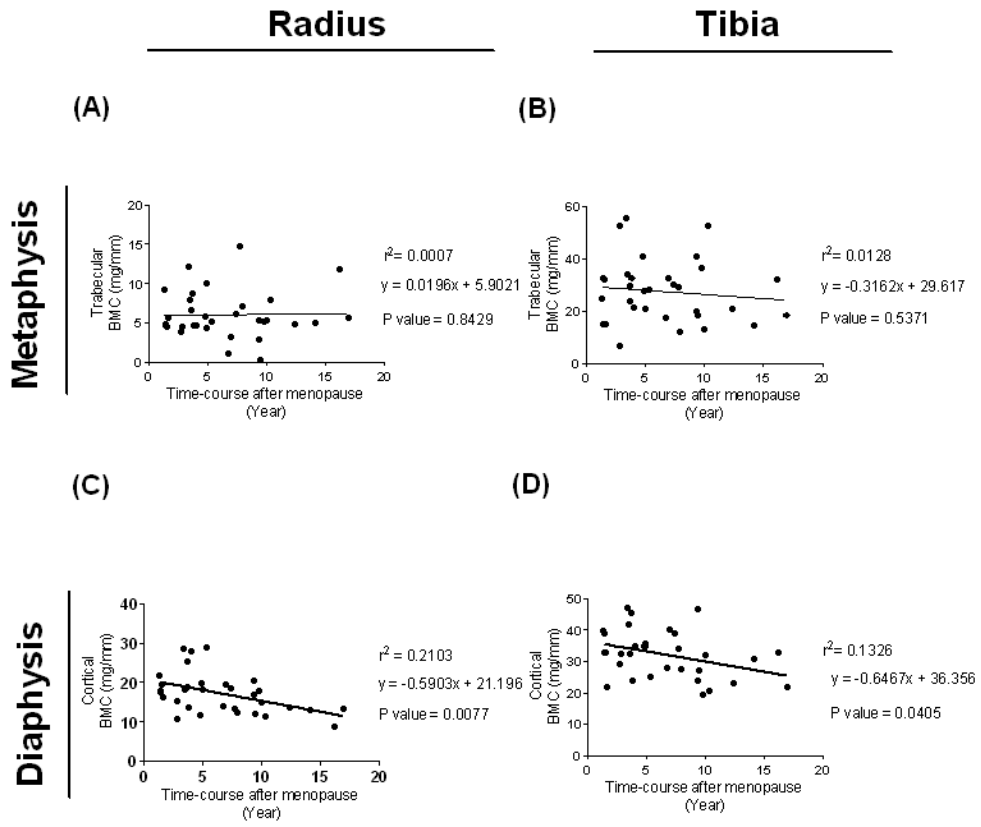

Figure 3.5 Correlations between the bone mineral content (BMC) and time-course after menopause of the (A, C) radius and (B, D) tibia (A, B) metaphysis trabecular and (C, D) diaphysis cortical.

Serum levels of bone formation (BAP) and turnover (OC) and urinary bone resorption (NTX) markers during menopause

Compared to the premenopausal levels, serum BAP levels were not significantly different in the perimenopausal and postmenopausal monkeys (Figure 3.6A). Conversely, a significant and abrupt decrease in the serum OC level was observed in the perimenopausal monkeys (p =0.002), and this then remained at a low level throughout the postmenopause periods (Figure 3.6B). Urinary NTX levels showed a gradual numerical decrease in the perimenopausal and postmenopausal monkeys, but this was not significantly different (Figure 3.6C).

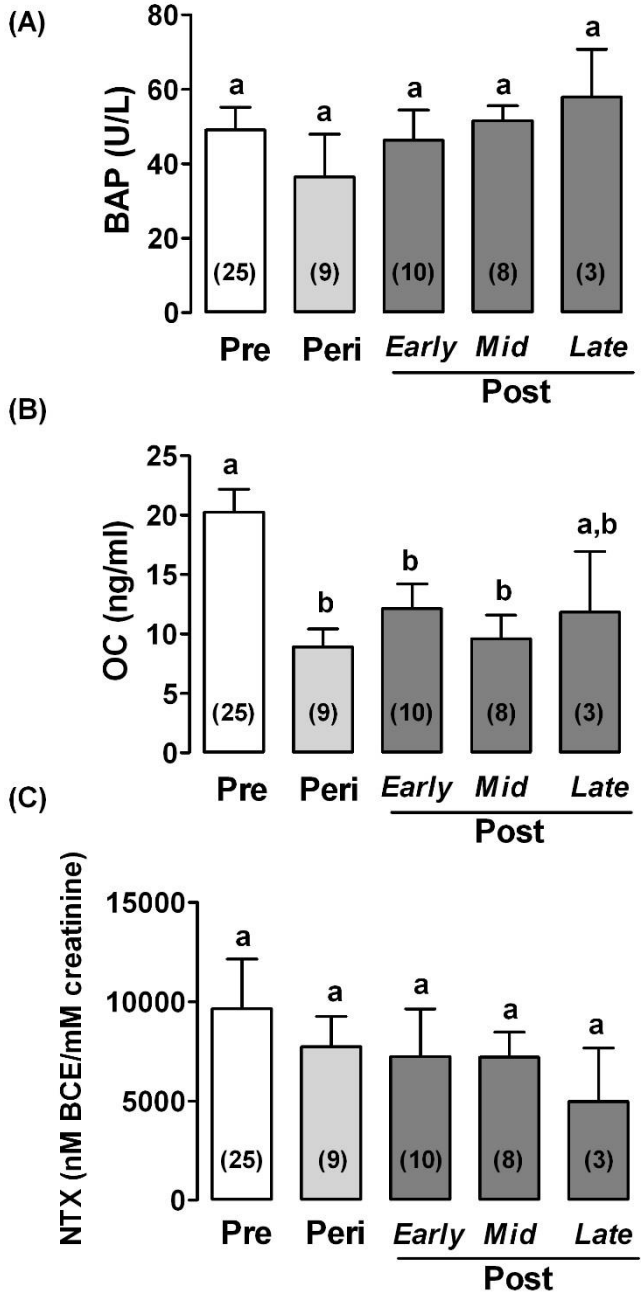

Figure 3.6 Bone markers (A) serum bone-specific alkaline phosphatase (BAP), (B) serum osteocalcin (OC) and (C) urinary cross-linked N-telopeptide of bone type I collagen (NTX) of pre, peri and early, mid and late postmenopausal monkeys. Data are shown as the mean±SEM. Means with a different lowercase letter are significant different ($p < 0.05$).

Correlation between the bone mass (BMC and BMD) and bone formation (BAP), turnover (OC), and resorption (NTX) markers

Because the lowered BMC and BMD in the trabecular compartment of metaphysis and the cortical compartment of diaphysis were different, the underlying mechanism of bone loss within these two bone compartments was assessed. The correlation between the bone mass (either BMC or BMD) and bone markers (BAP, OC, and NTX) was analyzed. The serum level of the bone formation (BAP) and turnover (OC) markers showed significant negative linear correlations with the bone mass, but in different bone compartments (Figure 3.7). The serum BAP levels were significantly negatively correlated with the trabecular BMC at the metaphysis site of both the radius and the tibia (p =0.007, r^2=0.1639 for radius and p =0.006, r^2=0.2315 for tibia) (Figure 3.7A and B), whereas the serum OC levels showed significant negative correlations with the cortical BMD at the diaphysis site of both the radius and the tibia (p = 0.015, r^2=0.1773 for radius and p = 0.023, r^2=0.1568 for tibia) (Figure 3.7E and F). In agreement with the serum BAP levels, the urinary NTX levels showed a significant negative correlation with the trabecular BMC at the metaphysis site of the radius (p = 0.045, r^2=0.2231), but were not significantly correlated in the tibia (p = 0.18, r^2=0.1754) (Figure 3.7C and D).

Correlation between the serum hormone (E_2, FSH, and LH) and bone marker (BAP, OC, and NTX) levels

Because the lowered trabecular metaphysis and cortical diaphysis were separately related to each bone marker, the correlation between the serum hormone and bone marker levels was evaluated. The only correlation found was a significant positive linear correlation between the serum FSH and urinary NTX levels (p = 0.012, r^2=0.1950) (Figure 3.8).

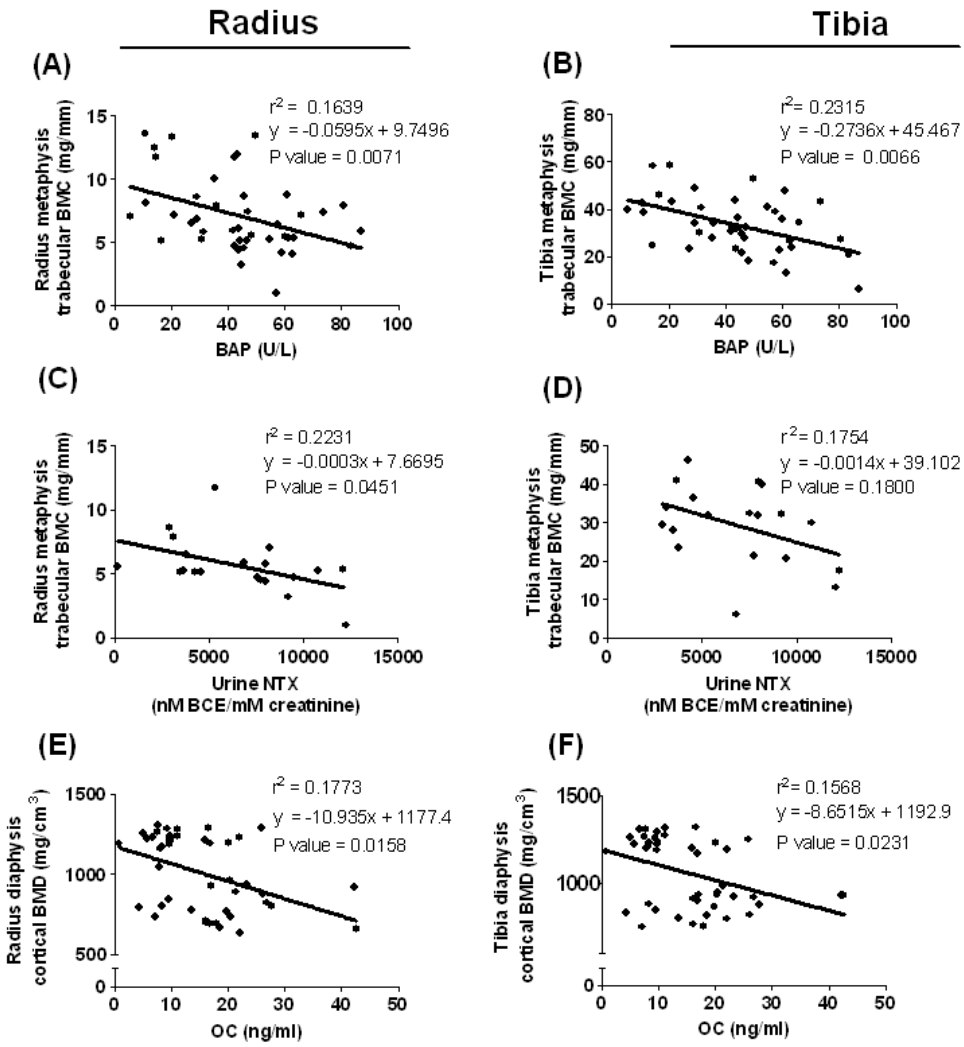

Figure 3.7 Negative correlations between the bone mineral content (BMC) or bone mineral density (BMD) at the (A, C, E) radius and (B, D, F) tibia and bone marker levels of (A, B) serum bone-specific alkaline phosphatase (BAP), (C, D) urinary cross-linked N-telopeptide of bone type I collagen (NTX) and (E, F) serum osteocalcin (OC).

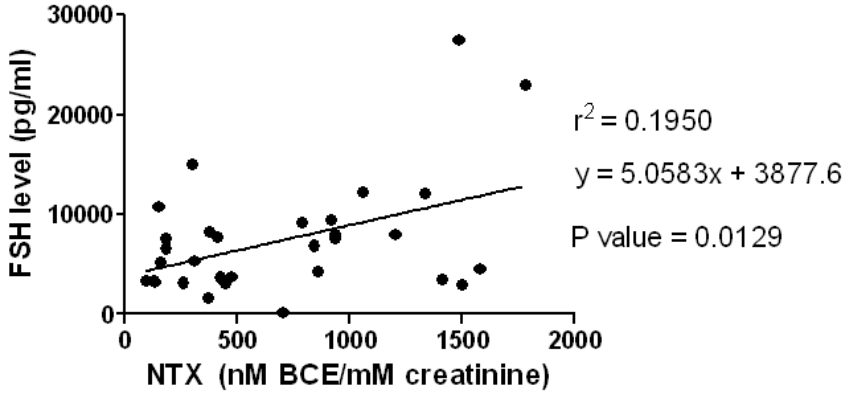

Figure 3. 8 Positive correlation between the serum follicle stimulating hormone (FSH) levels and urinary cross-linked N-telopeptide of bone type I collagen (NTX) levels.

Discussion

This study provided basic information on the differences in bone mass (BMD and BMC) in relation to bone markers (BAP, OC, and NTX) and serum hormone levels (E_2 and FSH) in female cynomolgus monkeys progressing through menopause. The decrease in serum E_2 levels during the perimenopausal transition in cynomolgus monkeys and humans are due to regression of most of the ovarian follicles, with only a few remaining dominant follicles to synthesize and secrete E_2 (Burger, 2008). Although the low serum E_2 level in perimenopausal cynomolgus monkeys in this study showed a subtle decrease compared with that of premenopausal monkeys, this could still abrogate the negative feedback on the hormonal regulation of the pituitary-ovary axis (and so cause a slight increase in the serum LH levels). This is because the hormone levels determined in this study were the basal levels in the early follicular phase, where the serum E_2 levels were typically low and so the slight decrease was sufficient to affect the animal's homeostasis.

Interestingly, serum FSH and LH levels in the late postmenopausal monkeys (aged about 30 years, equal to women aged 80-90 years) had reverted back to the premenopausal levels. This is consistent with a study in postmenopausal women, in which the highest serum FSH and LH levels were observed in young postmenopausal women, and then the levels progressively declined in the eighth and ninth decade postmenopausal women (Vaninetti et al., 2000). How and why this phenomenon occurs is not clearly understood. It has been suggested that the decreased capability of the pituitary in late postmenopause to secrete gonadotropins is involved (Zheng et al., 2007), but it might be that the increased serum FSH and LH levels from the pituitary gland that resulted from the loss of ovarian E_2 negative feedback could no longer stimulate the synthesis and secretion of E_2 from the ovary, and the animal has adjusted to an alternative (redundant) form of homeostasis.

Although there have been many reports on the effects of estrogen deficiency on bone loss, most of those experiments have been done in OVX animals, a popular model of postmenopausal women (Turner, 2001). Even though the ovaries are removed, the other organ systems function well and are not senescent, which is different to that of the naturally aged menopausal animals where all the other organs, including ovaries,

may show impaired function. Likewise, although the relationship between age and bone mass in female monkeys has been previously reported (Jayo et al.,1994), the estrogen status in these animals was questioned. In fact, monkeys at a younger age might have already entered into the perimenopausal or postmenopausal period, or an older animal may have remained in the premenopausal period. The relationship between only age and bone mass might not be able to be applied to naturally menopausal monkeys of which age, estrogen-deficient stage, and bone loss were all linked. It seems that this is the first study about the changes in BMD and BMC during the perimenopausal period in naturally menopausal monkeys.

It is well known that estrogen deficiency induces bone loss by enhancing the release of the inflammatory cytokines IL-1, IL-6, and TNFα from osteoblasts (Roggia et al., 2001; Cencil et al., 2003) and stimulating osteoclast differentiation by acting on bone-marrow precursors (Srivastava et al., 2001; Oursler, 2003). In addition to E_2 deficiency, it was recently demonstrated that FSH binding to its receptor on the cell membrane of mouse and human precursor or mature osteoclasts stimulated their differentiation and cell function (Sun et al., 2006). Thus, FSH can potentially directly stimulate osteoclast bone resorption. Moreover, treatment with anti-FSH antibody could stimulate bone formation both *in vivo* and *in vitro* in mice (Zhu et al., 2012). With a significant increase in the serum FSH levels during the early and mid-postmenopausal period, and a significant decrease in the serum E_2 level in the late postmenopause, this study hypothesized that the bone loss occurred in early and mid-menopausal monkeys was affected partly by FSH, whereas that in the late-menopausal monkeys was mainly caused by the lowered serum E_2 level.

It has been reported that in OVX monkeys, the trabecular bone loss is associated with estrogen deficiency (Itoh et al., 2002). However, the substantially lower serum E_2 level (<20pg/mL) after bilateral ovariectomy (Lelovas et al., 2008; Konstenuik dt al., 2009) was lower than that found in naturally postmenopausal monkeys in this study. Rather, this study revealed (1) a correlation between the time-course after menopause and the cortical degradation at diaphysis site and (2) an abruptly lowered trabecular metaphysis during the perimenopausal transition in naturally menopausal monkeys. This depicts the differences between the use of OVX and naturally menopausal,

estrogen-deficient monkeys as animal models for bone research. Overall changes in the OVX-animal model seem too dramatic compared to naturally menopausal monkeys. In addition, a gradual reproductive senescence in natural menopause leads to a gradual change in the bone, hormone levels, and bone marker levels. As observed previously, bone loss in oophorectomized women was more severe than in 10-year postmenopausal women (Mucowski et al., 2014). Another comparison to OVX rats, the most commonly used animal model for osteoporosis, is that ovariectomy rapidly lowered trabecular, but not cortical bone mass, whereas it increased the bone turnover in rats (Wronski et al., 1988). It is worth noting that cortical bone remodeling was not observed in the OVX-rat model (Jee and Yao, 2001), whereas it can clearly be observed in naturally menopausal cynomolgus monkeys. Another point which needs to be kept in mind when OVX animals are used for bone loss research is the site-specific bone loss, because the distal tibial metaphysis and caudal vertebrae are known to be resistant to OVX-induced bone loss (Li and Jee, 1991; Li et al., 1996; Miyakoshi et al., 1999). In conclusion, bone losses are different in regards to animal species, bone compartment, site and type, and estrogen state, and these need to be considered in the choice of animal as a model for bone research and in general extrapolation of any obtained results.

The suddenly lowered trabecular metaphysis during the perimenopausal period in cynomolgus monkeys might be due to the larger surface volume ratio of the trabecular bone compared to the cortical bone. The remodeling rate of the trabecular bone can be up to 10-fold higher than that of the cortical bone (Parfitt, 1988). The lowered cortical bone mass with a steady trabecular bone mass observed in naturally menopausal monkeys during the late postmenopausal period is consistent with that in humans, where cortical bone loss typically increased in women older than 60, which is about when the rate of trabecular bone loss decelerates (Riggs et al., 1981; Kanis et al., 2001). The lowered cortical density is strongly associated with decreased bone strength because the cortical bone provides the strength (Augat and Schorlemmer, 2006). Indeed, about 80% of the fractures in older humans are non-vertebral fractures that are mainly at the cortical bone (Riggs et al., 1981; Kanis et al., 2001). Thus, cortical bone loss, especially at the mid-shaft of the bone or diaphysis site, which is very important for weight bearing, should be a major concern in postmenopausal women.

Although BAP and OC are both secreted from bone-forming cells (osteoblasts), they act in a different manner. The serum level of BAP, which is secreted by osteoblasts during their differentiation and is found on their surfaces, has been shown to be a sensitive and reliable indicator of bone metabolism (Kress, 1998). Thus, the serum level of BAP is considered to indicate the average metabolic status of osteoblasts. OC is a noncollagenous, glutamate-rich polypeptide bone matrix protein that is incorporated into the bone matrix (Stein et al., 2004). OC is released into the circulation from the matrix during bone resorption and, therefore, is considered as a marker of bone turnover rather than a specific marker of bone formation (Delmas et al., 2000). Lastly, NTX molecules are mobilized from the bone by osteoclasts and subsequently excreted in the urine. Elevated levels of NTX indicate increased bone resorption. Interestingly, changes in the serum BAP and OC levels were observed to have different patterns after the monkeys entered into the perimenopausal period (Figure. 3.6), when no significant change in the BAP level, but an abrupt decrease in the OC level followed by a steady low level was observed. The paradoxical serum levels between BAP and OC have been proposed due to the temporal kinetic factor of the bone markers (Froberg et al., 1999). Likewise, in baboons, BAP and OC levels were positively correlated but accounted for only approximately 36% of the variance (Havill et al., 2006). Additionally, only the serum BAP and urine NTX levels were negatively correlated with the metaphysis trabecular BMCs (Figure. 3.7), which might indicate that an increased osteoblast differentiation and osteoclast resorption induced the bone loss in trabecular metaphysis. Because the serum OC level was negatively correlated with diaphysis in the cortical BMD (Figure. 3.7), this suggests that the increased bone turnover rate consequently led to a low cortical diaphysis.

From the above results, the mechanism of hormone (E_2 and FSH) action on the changes in trabecular and cortical bones is proposed. The lowered trabecular metaphysis occurred in parallel with the increased serum FSH levels, and increased FSH subsequently stimulated the release of NTX from bone (positive correlation between serum FSH and urine NTX levels in Figure. 3.8) indicating that FSH should be the main factor inducing bone resorption via NTX. Although the decreased cortical diaphysis occurred during the postmenopausal period when serum E_2 levels were low, no correlation in the serum E_2 levels with any bone markers was observed, and so the

detailed mechanism needs to be further investigated. However, from the negative correlations between serum BAP and urine NTX levels with the trabecular bone mass, and between the serum OC level and the cortical bone, it seems that serum BAP and urine NTX levels might be appropriate markers for the trabecular bone loss, and serum OC level might be an appropriate marker for the cortical bone loss, respectively, in the monkey model.

In conclusion, bone loss during the perimenopausal transition in naturally aged menopausal monkeys occurs at different bone compartments and bone sites at different time-courses after menopause, with more or less different underlying hormonal mechanisms and bone markers.

CHAPTER IV
PUERARIA MIRIFICA ALLEVIATES CORTICAL BONE LOSS IN NATURALLY MENOPAUSAL MONKEYS

Introduction

The increased life expectancy of humans alongside with the development of public health has led to a significant increase in the average life-expectancy of the population and age-associated diseases (Sweet et al., 2009). Osteoporosis is one such disease, of which the incidence is much higher in the elderly, and is often associated with bone fracture. It is reported that in the year 2000 there were some 9 million osteoporotic fractures in the world population of which 1.6, 1.7 and 1.4 million were hip, wrist and vertebral fractures, respectively, having significant impact on the quality of life and socioeconomic consequences (Johnell and Kanis, 2006; Woolf, 2006). Among the elderly, postmenopausal women are in the highest risk group for osteoporosis, which is attributed to the decreased estrogen level. Estrogen is a key hormonal regulator of bone metabolism, and regulates bone turnover directly via modulating the action of osteocytes, osteoblasts and osteoclasts (Khosla et al., 2012). Consequently, a low bone mass and quality, which account for the low bone composition and structure, occur during the estrogen-deficient postmenopausal stage.

In postmenopausal women, the BMD and BMC decrease by an average of 1.9 and 1.3% per year. This is mainly attributed to endosteal resorption. The endosteal resorption is associated with compensatory periosteal deposition (Bouxsein and Karasik, 2006). The medullary and periosteal diameters are increased by up to 1.1 and 0.7% per year, respectively, and the cortical thickness is increased by 0.4% per year. As a whole, this leads to an annual decrease in the strength index of about 0.7% (Ahlborg et al., 2003). Therefore, women in this postmenopausal period of life have 15% cortical bone loss (Khosla, 2012), with cortical bone fractures being the most frequent.

At present, many scientists have tried to search for new compounds to mitigate bone loss and improve bone quality. Some currently prescribed drugs can increase the

bone mass, but at the same time they lower the bone quality and increase the risk of bone fractures afterwards (Odvina et al., 2005). Although the positive effect of estrogen on bones is well recognized, estrogen replacement therapy (ERT) is no longer recommended due to the increased incidences of estrogen-dependent breast cancer, cardiovascular and venous thromboembolic events after the long-term use of ERT (Nelson et al., 2002). Thus, natural based products, such as plant-derived estrogens (or phytoestrogens), which have a similar structure and act in a similar manner with that of E_2, have attracted attention.

The tuberous roots of PM, contain at least 17 phytoestrogens (Malaivijitnond, 2012), and recently become a focal point of interest for its estrogenic activity. The estrogenic activity of PM powder (PMP) or extract (PME) has been widely tested *in vitro* and *in vivo* (Malaivijitnond, 2012), where it has also been shown to effectively prevent bone loss by increasing the BMC and BMD in OVX and ORX osteoporotic rats (Urasopon et al., 2007; 2008, Suthon et al., 2016a). Moreover, the underlying mechanism in rat osteoblast-like UMR106 cells has been investigated (Tiyasatkulkovit et al., 2012). Although the effects and mechanism of action of PM have been thoroughly verified in the rodent model, both *in vitro* and *in vivo*, based on the safety regulatory guideline of US-FDA (Thompson et al., 1995), the preclinical test of anti-osteoporotic agents needs to be performed in a second animal species which have similar bone structure and remodeling process to those of humans. Thus, the efficacy of PMP on bone structure modeling should be evaluated in monkeys because of its broadly similarly hormonal patterns (Goodman et al., 1977), reproductive functions (Weinbauer et al., 2008) and bone structures (Schaffler and Burr, 1984) to those of humans.

With respect to the previous reports indicating that OVX monkeys, animal models of choice for osteoporosis research, had different patterns of hormonal changes and bone loss from those of postmenopausal monkeys and women (Chen et al., 2013; Kittivanichkul et al., 2016b), in this study the effects of PMP on the bone quantity (BMD and BMC) and quality (geometry) were determined in aged, and so naturally menopausal cynomolgus monkeys.

Materials and Methods

Animals

Ten female cynomolgus monkeys were used in this study. They were reared at the Primate Research Unit, Faculty of Science, Chulalongkorn University. The selected postmenopausal monkeys were met the criteria of (i) being more than 20 years old, (ii) having a completed cessation of menstruation for at least 1 year, and (iii) having a total BMD at the radius and tibia of between -0.5 to -1 SD of those of premenopausal cynomolgus monkeys (Figure 4.1). The 10 osteoporotic monkeys selected by the above criteria were used in an attempt to mimic the osteoporosis that occurs in naturally postmenopausal aged women. Monkeys were housed in individual cages with a 12:12 h light: dark cycle at ambient temperature. They were fed daily with monkey chow diet (Perfect Companion Group. Co., Ltd, Samut Pakran, Thailand) in the morning (09:00–10:00 am) and supplemented with fresh fruits in the afternoon (01:00–02:00 pm). All animal procedures were approved by the Faculty of Science, Chulalongkorn University Animal Care and Use Committee (Protocol review no. 1123015). Clinical records for each animal were performed daily by veterinary staff and animal caretaker.

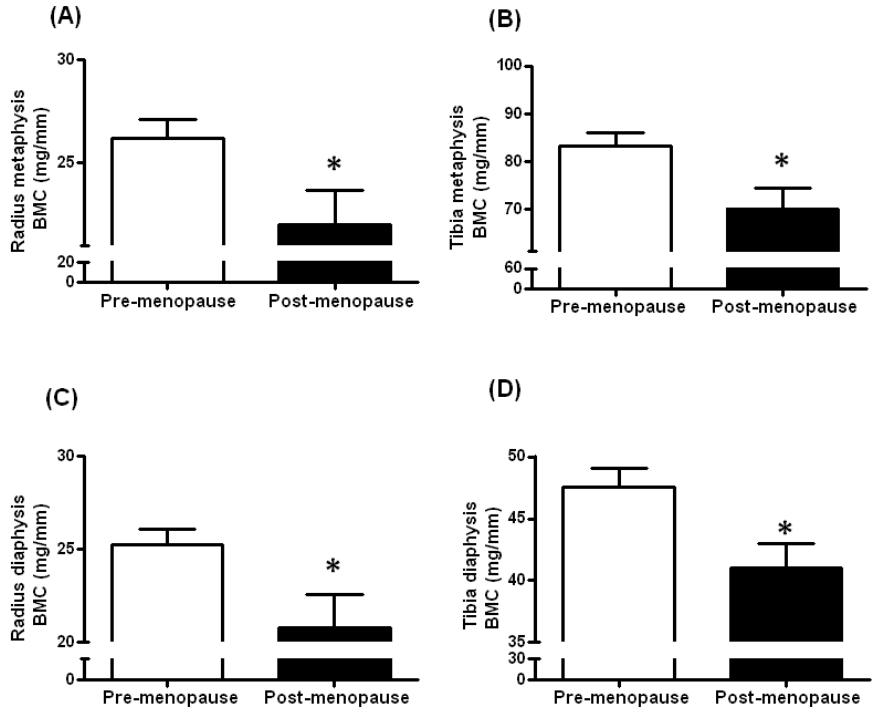

Figure 4.1 Bone mineral content (BMC) of the (A, C) radius and (B, D) tibia at the (A, B) metaphysis site and (C, D) diaphysis site of pre-menopausal monkeys (n = 33) and post-menopausal monkeys (n=10) that were selected for this study. Data are shown as the mean±SEM.and * represents $p < 0.05$ compared with the pre-menopausal monkeys.

Phytoestrogen analysis of PMP

Dried PMP (lot no. 141023), as a fine powder, was kindly provided by Dr. I. Sandford Schwartz, Smith Naturals Co., Ltd., Bangkok, Thailand. Liquid chromatography tandem mass-spectrometry (LC/MS/MS) was used for the analysis of puerarin and miroestrol levels in the PMP. Puerarin is the major phytoestrogen present in PM, while miroestrol shows a high estrogenic activity. Puerarin and miroestrol analytical standards were obtained from Sigma Aldrich Corp. (USA) and Professor Tsutomu Ishikawa (Chiba University, Japan), respectively. Glycyrrhetinic acid, used as an internal standard in the LC/MS/MS, was purchased from Wako Corp., Japan. All compounds were tested for quality control and had more than 95% of the active ingredient.

The puerarin and miroestrol standards were prepared by dissolving in dimethylsulfoxide (DMSO) and diluting with methanol. In brief, 100 mg of tested formulation of PMP was dissolved in 1 ml of DMSO, and then diluted 100-fold in methanol. The diluted samples were mixed with a 10-fold volume of methanol containing 10 ng of glycyrrhetinic acid as an internal standard for the LC/MS/MS analysis, performed using an Eksigent ekspert™ UHPLC 100 LC equipped with a QTRAP® 6500 MS, controlled by Analyst® software version 1.6 (AB Sciex, Framingham, MA, USA). The UHPLC system was equipped with a Synergi™ Fusion-RP C18 column as the stationary phase (Phenomenex Inc., Torrance, CA, USA), while the mobile phase was a methanol: water gradient starting at 10% (v/v) methanol for 0.5 min, increased linearly to 90% (v/v) methanol at 1.5–3.5 min, and then decreased linearly to 10% (v/v) methanol at 4–4.5 min. The retention times of puerarin, miroestrol and glycyrrhetinic acid were 1.56, 1.74 and 2.09 min, respectively (Figure 4.2A-C). The MS analysis was performed with negative mode ionization. The fragmentation of puerarin, miroestrol and glycyrrhetinic was showed in (Figure 4.3A-C). Calibration curves of puerarin and miroestrol showed good correlation coefficients ($r^2 > 0.99$) over the concentration range of 5 to 1,000 µg/l. The limit of detection of both compounds was estimated to be 1 µg/l with a signal to noise ratio of 5. The intra-assay accuracy and precision for analysis of both compounds were within ± 10%. The puerarin and miroestrol contents in the PMP (lot no. 141023) were 18.6 mg/100 g PMP and 233 µg/100 g PMP, respectively.

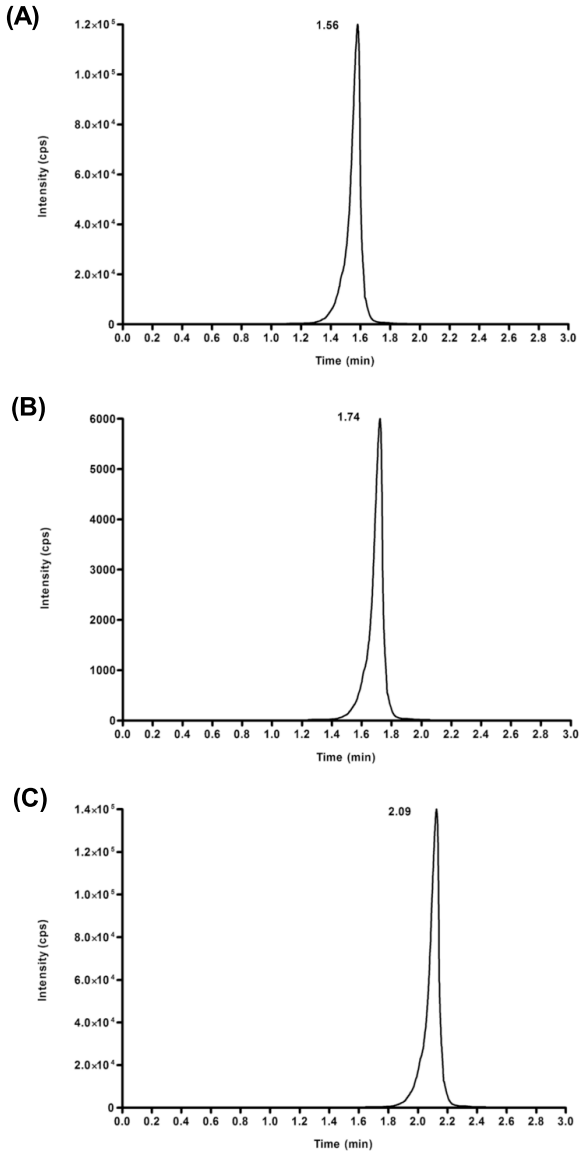

Figure 4.2 LC/MS/MS chromatogram for 100 μg/L of (A) puerarin, (B) miroestrol and (C) glycyrrhetinic acid.

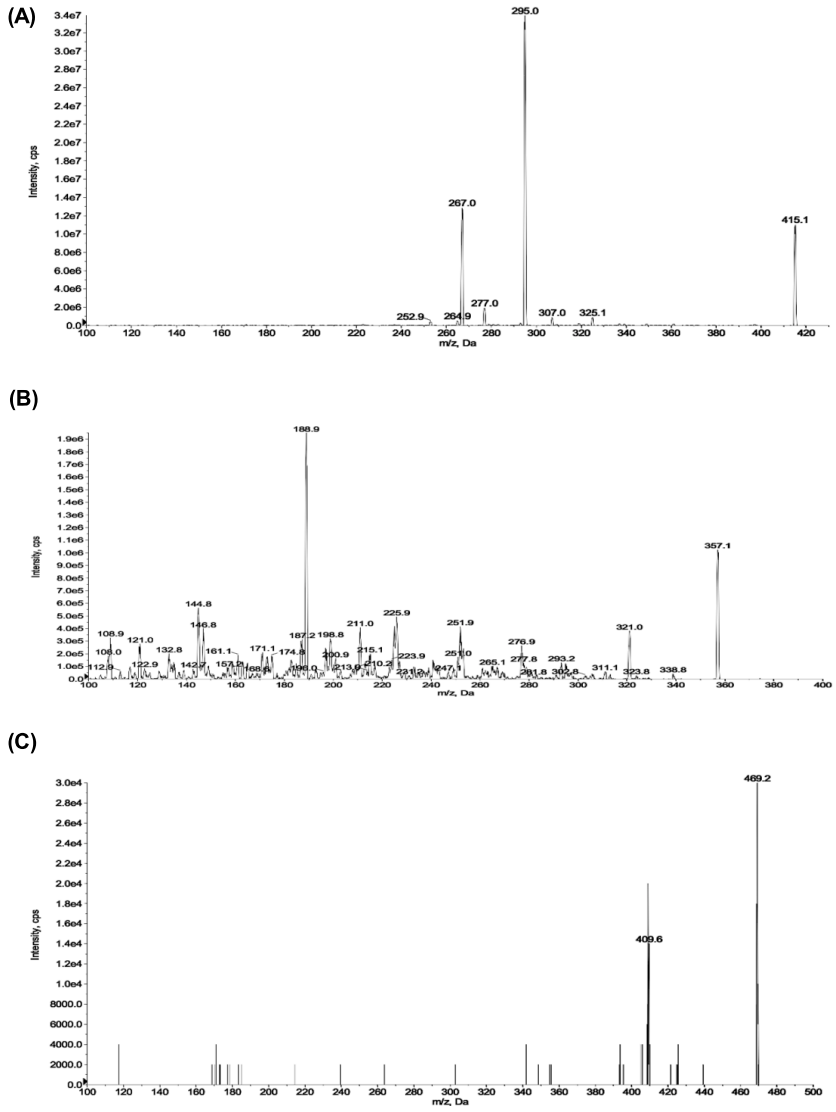

Figure 4.3 Fragmentation mode of (A) puerarin, (B) miroestrol and (C) glycyrrhetinic acid.

Experimental design

Prior to the onset of the study, the postmenopausal monkeys were randomly assigned into one of the two groups (five monkeys in each group), the control (PMP0) group and that treated with PMP (PMP1000 group). There was no significant difference between the PMP0 and PMP1000 groups in their age, body weight, menopause period and total BMD at both metaphysis and diaphysis at radius and tibia bone (Table 4.1). The PMP0 group was fed daily with standard diet alone and the PMP1000 group was fed with the same diet mixed with 1,000 mg/kg BW of PMP at 08:00–09:00 am for 16 months. A PMP dose of 1,000 mg/kg BW, equivalent to 0.18 mg/kg BW of puerarin and 2.33 μg/kg BW of miroestrol, was selected for this study because it was previously shown to significantly decrease the serum parathyroid hormone levels in aged female cynomolgus monkeys (Trisomboon et al., 2004a). To maintain the consistency of the dose treatment, monkeys were weighed in every two months and the amount of PMP fed to the monkeys was adjusted to their BW afterwards. To ensure that the same amount of phytoestrogen content was fed to the monkeys, the same batch of PMP was used throughout the experiment. Blood and urine were collected, and the BMD, BMC and bone geometry were measured every two months for 16 months (at month 0, 2, 4, 6, 8, 10, 12, 14 and 16, respectively).

Table 4.1 Body weight, age, menopause period, and total bone mineral density (BMD) of the monkeys in each treatment group.

Treatment	Body weight (kg)	Age (yrs)	Menopause period (yrs)	Total BMD (mg/cm^3)			
				Metaphysis		Diaphysis	
				Radius	Tibia	Radius	Tibia
PMP0 (n=5)	5.37±0.23 (4.8-5.9)	29.6±1.8 (24-33)	5.8±1.4 (2.5-10.9)	425.0±38.0 (317.7-541.7)	384.0±30.8 (292.6-459.5)	665.3±65.5 (439.2-837.8)	720.5±39.6 (620.1-825.5)
PMP1000 (n=5)	5.39±0.20 (5.1-6.1)	26.0 ±2.3 (20-33)	7.8±1.2 (4.3-10.6)	541.2±51.7 (406.1-670.2)	345.8±26.6 304.6-449.20	719.3±58.4 (571.4-835.3)	721.1±30.6 (646.8-822.7)

Urine and blood collection

For urine collection, monkeys were fasted from 06:00 pm on the day prior to collection and stainless steel trays covered with iron mesh were placed under each monkey cage. On the following day at 06:00 am, the trays were removed and the 12-h urine samples were collected by syringe. Urine samples were clarified by centrifugation at 1,700g, 4°C for 20 min and then the supernatants were harvested and kept at -20°C until analyzed for the levels of NTX and creatinine.

After the urine collection was performed, monkeys were anesthetized by intramuscular injection with a mixture of tiletamine/zolazepam, as a mixture of 3 mg/kg BW Zoletil 100 (Virbac, Nonthaburi, Thailand) and 40 µg/kg BW medetomidine hydrochloride (Vetcare, Inc, Jonesboro, AR, USA). Blood was withdrawn from the femoral vein between 08:00–11:00 am and immediately mixed with sodium heparin (Leo pharmaceutical, Ballerup, Denmark) at 0.1 IU/ml of whole blood, centrifuged (4°C, 1,700g for 20 min) and the blood plasma was harvested and kept at -80 °C until assayed for E_2, FSH, LH, calcium and bone turnover markers (see below). After the blood collection, the BMD, BMC and bone geometry were measured at the radius and tibia. Atipamazole (Vetcare, Inc, Jonesboro, AR, USA) at 40 µg/kg BW was administered by intramuscular injection to animals after all the procedures had been completed.

Plasma hormone level assays

Plasma E_2, FSH and LH levels were determined only at the month 0 to confirm the postmenopausal stage in monkeys. Plasma FSH and LH levels were determined using a heterologous radioimmunoassay as described previously (Trisomboon et al., 2004b, Kittivanichkul et al., 2016b). Plasma E_2 levels were determined by electrochemiluminescence immunoassay at the Department of Pathology, Faculty of Medicine, Ramathibodi Hospital, Mahidol University, Thailand. All samples were processed in a single run to minimize between-runs experimental variation in the data. The intra-assay coefficients of variation were 1.44%, 2.4% and 3.2% for the FSH, LH and E_2 assays, respectively.

Measurements of plasma calcium and biochemical markers levels

At month 0 and 16, the plasma levels of calcium, phosphorous, creatinine, blood urea nitrogen (BUN), ALP, alanine aminotransferase (ALT) and aspartate aminotransferase (AST) were determined by an automate clinical chemical analyzer (ILAB-650, Chema diagnostica, Monsano, Italy) at the Faculty of Veterinary Science, Chulalongkorn University, Bangkok, Thailand. All samples were assayed in a single run. The intra-assay coefficients of variation were lower than 5% for all parameters (calcium = 0.75%, phosphorous = 1.55%, creatinine = 3.15%, BUN = 1.35%, ALP = 2.00%, ALT = 1.90% and AST = 1.80%).

Measurement of the BMC, BMD and bone geometry

The BMC, BMD and bone geometry parameters, including the cortical area and thickness, and endosteal and periosteal circumferences (Figure 4.4), at the distal radius and proximal tibia, were determined using peripheral quantitative computed tomography (pQCT; Norland Startec XCT Research SA+ pQCT, Startec, Pforzheim, Germany) as reported previously (Kittivanichkul et al., 2016b). The BMD, BMC and bone geometry parameters of the total, trabecular and cortical bone regions were analyzed using the XCT-5.50E software (Startec, Pforzheim, Germany).

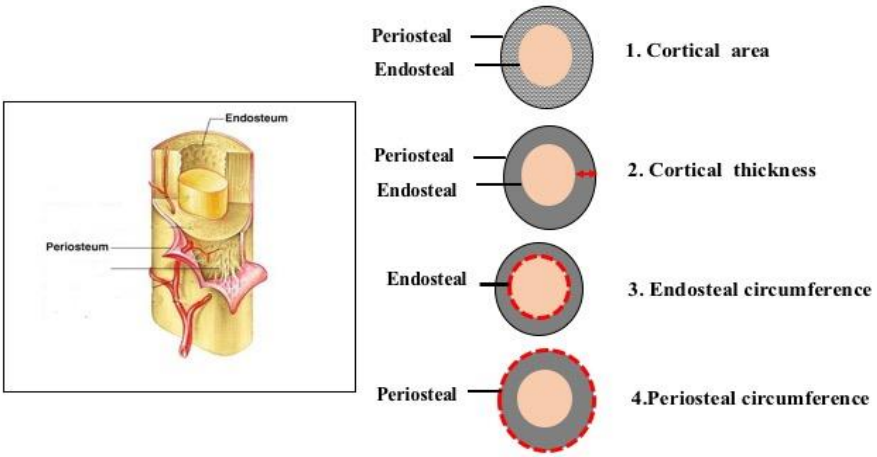

Figure 4.4 Cross-section of bone cortex demonstrated measurement of bone geometry which are cortical area, cortical thickness, endosteal and periosteal circumference.

Measurement of bone turnover markers

Dynamic changes in the bone turnover parameters were determined by measuring the plasma BAP (Quidel, San Diego, CA, USA, Catalog no. 8012) and OC (Quidel, San Diego, CA, USA, Catalog no. 8002) levels and urinary NTX levels (Wampole Labs, Princeton, NJ, USA, catalog no. OST0001) as markers. The BAP and OC were determined using by enzyme immunoassay assays, where the intra- and inter-assay coefficients of variation were 4.07% and 8.39% for BAP and 9.33% and 14.17% for OC, respectively. The urinary NTX levels were also measured by enzyme immunoassay, but normalized to the urinary creatinine levels that were determined by the Jaffe kinetic method (Legrand et al., 2003). The intra- and inter-assay coefficients of variation for NTX were 5.30% and 6.51%, respectively.

Statistical analysis

All data were transformed to percent changes according to the baseline (the month 0). Data are expressed as the mean±SEM. Since there was no significant interaction between the time and treatment when tested by two-way ANOVA (data not shown), then the changes in all the parameters were analyzed separately using a paired t-test (comparing between the values at month 0 and the other time points in the same group) or an unpaired t-test (comparing between groups at the same time point). Significance was accepted at the $p < 0.05$ level. Statistical analyses were performed using the IBM SPSS Statistics for windows, version 20.0 software (IBM Crop., Armonk, NY, USA). Pearson's correlations were performed using the R program (R Core Team, 2015). Similarity in the slope and intercept of each group regression line was tested using GraphPad Prism version 5.01 (GraphPad Software Inc., USA).

Results

Animal health and appearances

All monkeys remained in a good health condition throughout the 16 months of the study period. Monkeys showed regular food and water intake, normal behavior and movement. There were no signs of sickness involving in treatment condition. The blood chemical parameters are summarized in Table 4.2. Although some values tended to be high, they were still in the normal range (Fortman et al., 2002). It is of note that the ALT levels were high in both the control (PMP0) and PMP1000 treated group at month 16, while the AST and ALP levels were in the normal ranges. Thus, the increase in ALT serum levels might not be due to liver health problems from PMP treatment, but rather may be due to muscle or heart disease associated with old age in general.

Table 4.2 Blood chemical analysis of postmenopausal cynomolgus monkeys at 0 and 16 months after treatment with PMP0 or PMP1000

Blood chemical analysis	PMP0		PMP1000	
	Month 0	Month 16	Month 0	Month 16
Calcium (mg/dl)	7.76 ± 0.12	7.76 ± 0.10	7.78 ± 0.09	7.20 ± 0.17[a]*
Phosphorus (mg/dl)	5.02 ± 0.43	4.78 ± 0.28	4.73 ± 0.52	5.08 ± 0.77
Creatinine (mg/dl)	0.88 ± 0.06	0.78 ± 0.04[a]	0.92 ± 0.10	0.70 ± 0.10[a]
BUN (mg/dl)	14.94 ± 3.85	24.42 ± 5.35[a]	13.42 ± 3.21	20.53 ± 2.70
ALP (U/l)	133.80 ± 23.06	180 ± 71.55[a]	98.00 ± 99.27	163.25 ± 77.39
ALT (U/l)	3.4 ± 0.81	73.2 ± 20.11[a]	6.00 ± 1.83	127.75 ± 51.21
AST (U/l)	15.40 ± 1.21	34.40 ± 9.97	17.80 ± 2.24	35.75 ± 11.83

Data are shown as mean±S.E.M derived from five monkeys per group. a represent p <0.05 compare between month 0 and 16 in the same group. * represent p <0.05 compare between PMP0 and PMP1000 group at the same time point. BUN= Blood urea nitrogen; ALP= Alkaline phosphatase; ALT=Alanine aminotransferase; AST= Aspartate aminotransferase

Plasma E_2 levels

Plasma E_2 levels at month 0 did not significantly differ between the PMP0 and PMP1000 groups (73.93 ± 28.10 and 93.95 ± 26.84 pg/ml, respectively). Plasma FSH and LH levels were also not significantly different between the PMP0 and PMP1000 groups (FSH = 2.13 ± 0.14 and 1.82 ± 0.09 ng/ml, respectively, and LH = 2.82 ± 0.52 and 3.01 ± 0.23 ng/ml, respectively).

Advancing age gradually decreased cortical BMC and BMD

Since the experiment was performed for 16 months, an increase in the subject age might affect the bone, and so cause changes in the BMC and BMD. Thus, at each time point the respective values of the PMP0 group were also compared with the baseline (month 0) values. Increasing time (subject age) resulted in a gradual and continuous decrease in both the total BMC (Figure 4.5A, B, G and H) and BMD (Figure 4.6A, B, G and H) at the metaphysis and diaphysis of the radius and tibia in the PMP0 group. This decrease was significant from month 4 for the total metaphysis BMC of the radius (Figure. 4.5A), total diaphysis BMC of the tibia (Figure. 4.5H) and total metaphysis BMD of the tibia (Figure. 4.6B).

With respect to the different bone compartments at each bone site, metaphysis was comprised the trabecular and cortical bone while diaphysis contained mainly the cortical bone. Thus, the trabecular and cortical BMC and BMD were also analyzed separately. The trabecular BMC (Figure 4.5 C and D) and BMD (Figure 4.6C and D) at the metaphysis site fluctuated highly throughout the 16-month period in the PMP0 group. Conversely, changes in the cortical BMC (Figure 4.5E and F) and BMD (Figure 4.6E and F) at the metaphysis (Figure 4.5I and J) and diaphysis (Figure 4.6I and J) sites of the radius and tibia showed similar patterns with the total BMC (Figure 4.5A, B, G and H) and BMD (Figure 4.6A, B, G and H). This was especially the case for the cortical BMC at the diaphysis site of the radius and tibia (Figure 4.5I and J), where the significant decrease was greater than that of the total BMC (Figure 4.5G and H).

Generally, the changes in the BMC and BMD seen in the PMP1000 group at the metaphysis and diaphysis sites of both the radius and tibia resembled the patterns in the PMP0 group, but to a lesser extent.

Oral PMP administration ameliorates a decrease in cortical BMC and BMD

Comparing the values of BMC and BMD at the metaphysis site between the PMP0 and PMP1000 groups, significant differences were only detected at month 8 for the cortical BMC (Figure 4.5E) and total BMD (Figure 4.6A) of the radius and at month 2 for the trabecular BMD (Figure 4.6C). At the diaphysis, as a whole, significantly higher total and cortical BMC and BMD were detected in the PMP1000 group in both the radius and tibia (Figure 4.5I and J; 4.6G, H and J), except the total BMC at the radius (Figure 4.5G) and tibia (Figure 4.5H) diaphysis were not significantly different. Although the cortical BMD at the radius diaphysis in the PMP1000 group (Figure 4.6I) was numerically higher in month 16 than in the PMP0 group, this was not significantly different (p =0.054).

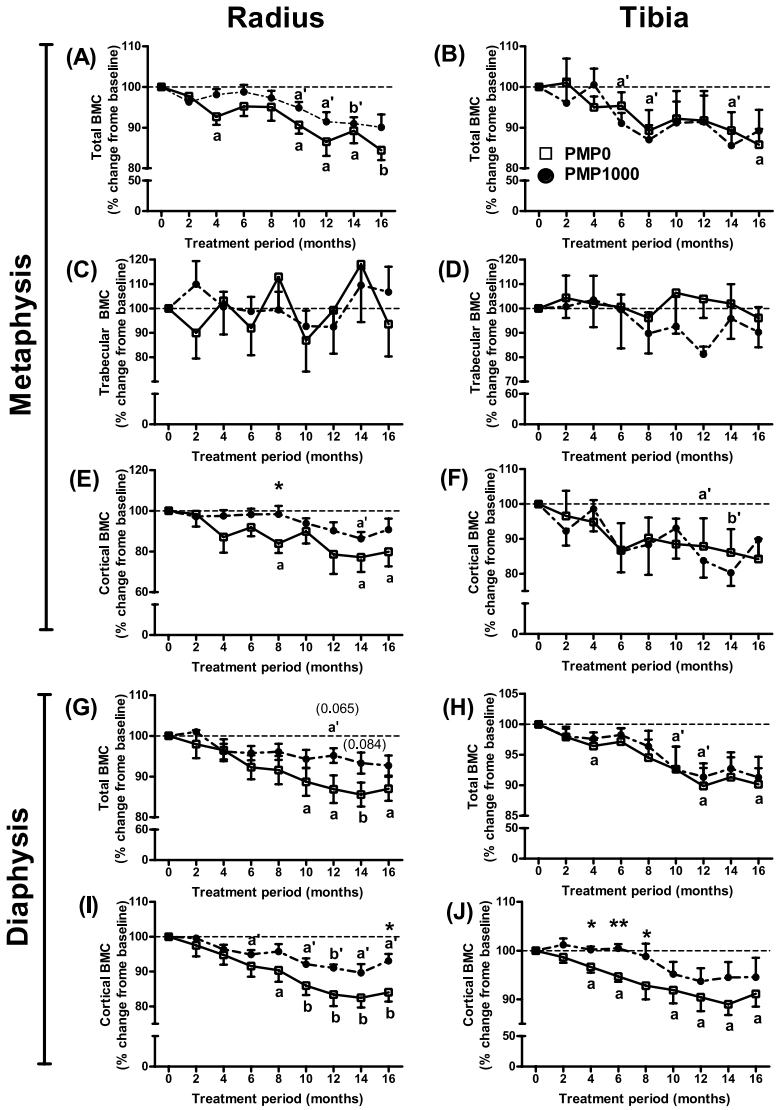

Figure 4.5 Total (A, B, G and H), trabecular (C and D) and cortical (E, F, I and J) bone mineral content (BMC) of the (A, C, E, G, I) radius and (B, D, F, H, J) tibia bone at (A–F) metaphysis and (G–J) diaphysis sites during the 16-month study period. The open square and closed circle indicate the PMP0 and PMP1000 groups, respectively. a, b and a', b' represent $p < 0.05$ and $p < 0.01$ compared between the baseline (month 0) and other time points of the PMP0 and PMP1000 groups, respectively. * represents $p < 0.05$ comparing the PMP0 and PMP1000 groups.

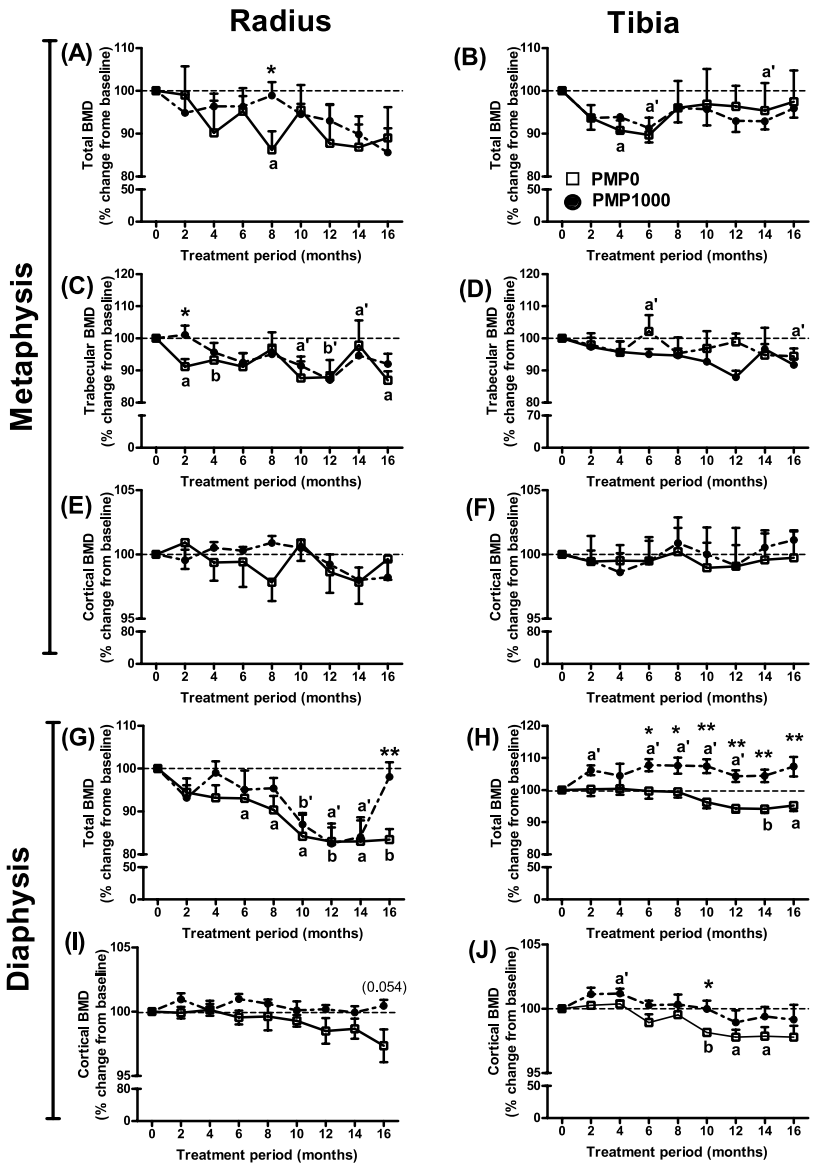

Figure 4.6 The (A, B, G and H) total, (C, D) trabecular and (E, F, I and J) cortical bone mineral density (BMD) of the (A, C, E, G, I) radius and (B, F, H, J) tibia bone at (A– F) metaphysis and (G– J) diaphysis sites during the 16-month study period. The open square and closed circle indicate the PMP0 and PMP1000 groups, respectively. a, b and a', b' represent $p < 0.05$ and $p < 0.01$ compared between the baseline (month 0) and other time points of the PMP0 and PMP1000 groups, respectively. * represents $p < 0.05$ comparing the PMP0 and PMP1000 groups.

Advancing age decreased radius and tibia cortical area and thickness

In agreement with the changes in the BMC and BMD, the cortical area and thickness of the PMP0 group gradually and continuously decreased at the metaphysis (Figure 4.7A–D) and diaphysis (Figure 4.8 A–D) of the radius and tibia compared to the baseline (month 0) values. However, the values fluctuated less and to a lower extent at the diaphysis. A significant decrease in the cortical area of the tibia diaphysis was first detected at month 4.

Conversely, as the PMP0 monkeys became older no significant longitudinal changes in the endosteal and periosteal circumferences of the radius and tibia metaphysis (Figure 4.7E–H) were observed, but rather the values fluctuated within the baseline range. However, they tended to be higher and lower than the baseline values for the radius and tibia diaphysis (Figure 4.8E–H), respectively. It is worth noting that the patterns of change in the endosteal and periosteal circumferences at the same diaphysis site were different between the radius and tibia.

Generally, the patterns of change in the bone geometry of the PMP1000 group at the metaphysis and diaphysis sites in both the radius and tibia resembled those of the PMP0 group, except at the tibia diaphysis where the endosteal and periosteal circumferences (Figure 4.8F and H) decreased to a greater extent.

Oral PMP administration extenuated a decrease in cortical thickness

In the same line with changes in the BMC and BMD, PMP treatment improved the bone quality by alleviating the decreased cortical thickness and area that occurred during estrogen deprivation and increasing age (Figure 4.7 and 4.8A–D). However, significant differences between the PMP0 and PMP1000 groups could only be detected for the cortical thickness at the diaphysis site of both the radius (only at month 16; Figure 4.8C) and tibia (Figure 4.8D), especially at the tibia diaphysis where PMP1000 treatment significantly increased the cortical thickness to a higher level than the baseline value. In agreement with the increased cortical area and thickness, only the endosteal circumference at the diaphysis site of the tibia of the PMP1000 group was significantly smaller than the PMP0 group (Figure 4.8F).

The patterns of change in the endosteal and periosteal circumferences were also different in the radius and tibia diaphysis in response to PMP treatment. While the values in the PMP0 group fluctuated near the baseline values in both bone types, the endosteal and periosteal circumferences at the diaphysis site were significantly lower than the baseline values for the tibia bone of the PMP1000 group, but not significantly different from the PMP0 group for the radius bone (Figure 4.8E–H).

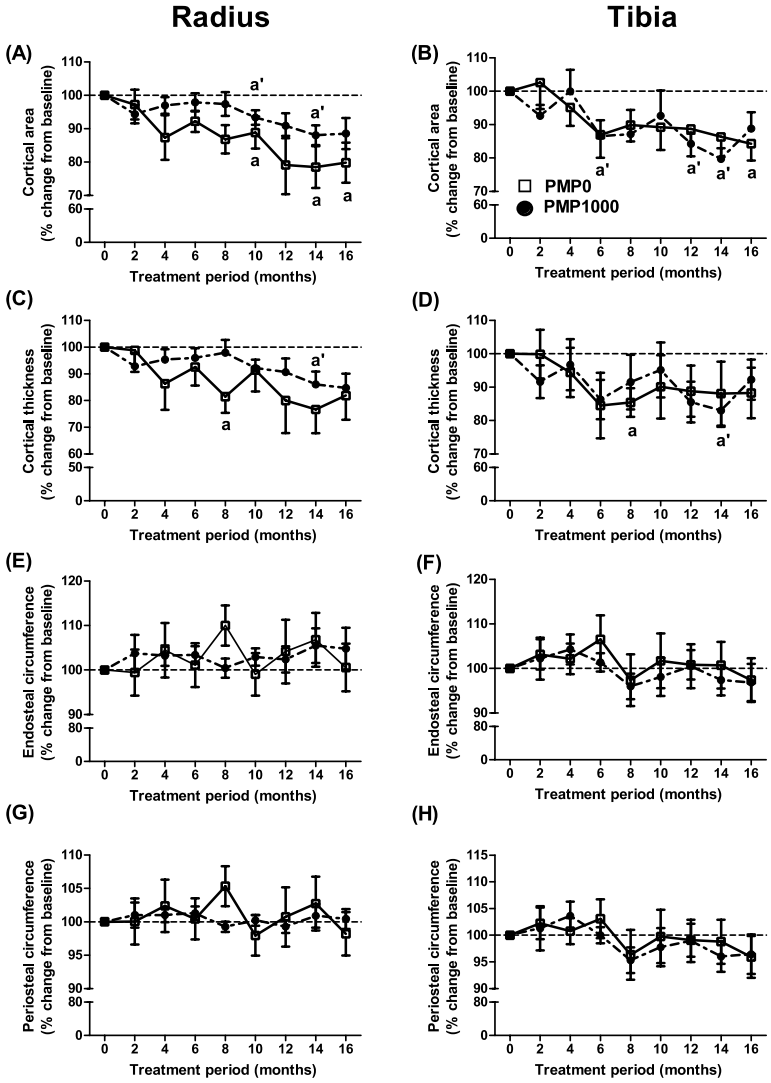

Figure 4.7 Bone geometry, in terms of the cortical area, thickness, endosteal and periosteal circumference, at the metaphysis of the (A, C, E, G) radius and (B, D, F, H) tibia during the 16-month study period. The open square and closed circle indicate the PMP0 and PMP1000 groups, respectively. a, b and a', b' represent $p < 0.05$ and $p < 0.01$ compared between the baseline (month 0) and other time points of the PMP0 and PMP1000 groups, respectively. * represents $p < 0.05$ comparing the PMP0 and PMP1000 groups.

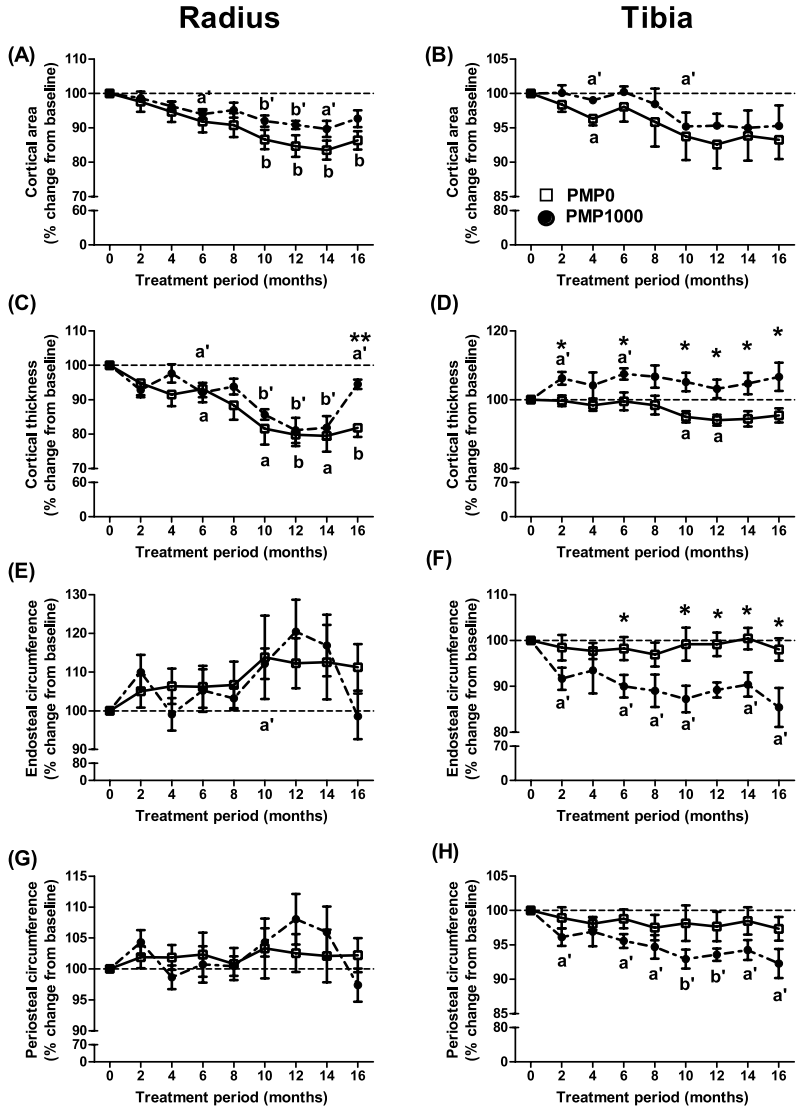

Figure 4.8 Bone geometry, in terms of the cortical area, thickness, endosteal and periosteal circumference, at the diaphysis site of the (A, C, E, G) radius and (B, D, F, H) tibia bone during the 16-month study period. The open square and closed circle indicate the PMP0 and PMP1000 groups, respectively. a, b and a', b' represent $p < 0.05$ and $p < 0.01$ compared between the baseline (month 0) and other time points of the PMP0 and PMP1000 groups, respectively. * represents $p < 0.05$ comparing the PMP0 and PMP1000 groups.

Changes of plasma and urinary bone turnover markers in response to age and PMP treatment

The increasing age of the postmenopausal monkeys during the 16-month study period in the PMP0 group resulted in a significant decrease in plasma BAP (at months 2 and 8) and OC levels (starting from month 10), while no significant changes were detected in the NTX levels (Figure 4.9A–C).

Treatment of the PMP1000 decreased the plasma BAP and OC levels to a greater degree than those observed in the PMP0 group (Figure 4.9A and B), and this was significant from month 4 ($p < 0.05$ or 0.01) compared to the baseline values. Moreover, the NTX level was also significantly lower than the baseline value at month 16 ($p < 0.01$) in the PMP1000 group (Figure 4.9C). Thus, the levels of BAP and OC in the PMP1000 group were significantly lower than those in the PMP0 group starting from month 4 and 6, respectively.

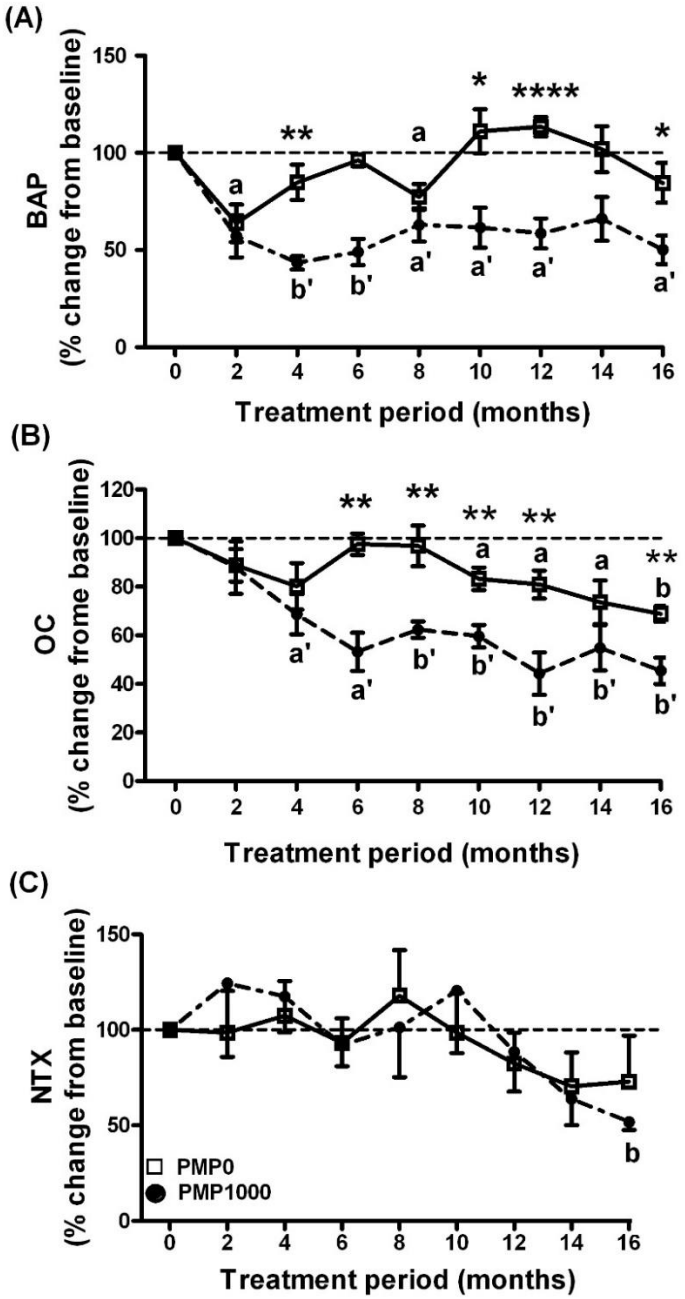

Figure 4.9 Level of bone turnover markers. The (A, B) plasma (A) bone-specific alkaline phosphatase (BAP) and (B) osteocalcin plus the (C) urinary cross-linked N-telopeptide of type I collagen (NTX) levels during the 16-month study period. The open square and closed circle indicate the PMP0 and PMP1000 groups, respectively. a, b and a', b' represent $p < 0.05$ and $p < 0.01$ compared between the baseline (month 0) and other time points of the PMP0 and PMP1000 groups, respectively. * represents $p < 0.05$ comparing the PMP0 and PMP1000 groups.

Correlation between bone mass/geometry and bone turnover markers

Correlations between the bone mass (total, cortical and trabecular BMC and BMD) and the geometry (cortical area and thickness, endosteal and periosteal circumferences) at the metaphysis and diaphysis sites of the radius and tibia with the bone turnover markers (BAP, OC and NTX levels) were analyzed (Table 4.3). In the PMP0 group, 15 pairs of parameters were significantly correlated (nine positive and six negative pairs), while in the PMP1000 group, 23 pairs of parameters were significantly correlated (16 positive and seven negative pairs). Interestingly, four out of the six pairs of negative correlations in the PMP0 group were found between NTX and the bone mass/geometry parameters, while only one each between BAP and the bone mass (trabecular BMC at the radius metaphysis), and between OC and the bone geometry (endosteal circumference at the radius diaphysis) were found. Conversely, six out of the seven pairs of negative correlations in the PMP1000 group were found between BAP and the bone mass/geometry parameters, while only one was detected between NTX and the bone mass (cortical BMD at radius diaphysis). As such, different direction (positive or negative) correlations of BAP or NTX and the bone mass/geometry parameters were observed between the PMP0 and PMP1000 groups for five pairs (Table 4.3). Considering carefully those five pairs of correlations, the PMP0 group showed positive correlations between the total or cortical BMD of diaphysis with either BAP (two pairs) or NTX (one pair) and *vice versa* for the PMP1000 group. On the other hand, the PMP1000 group showed positive correlations between the periosteal circumference or cortical area of diaphysis with NTX (two pairs), but was negative for the PMP0 (Table 4.3).

Table 4.3 Correlations between the bone turnover markers (plasma BAP, OC and urinary NTX levels) and bone mass (BMD and BMC) or geometry (cortical area and thickness, endosteal and periosteal circumference) parameter. ns = non-significant difference of correlation. *, ** and *** = p<0.05, 0.005 and 0.001, respectively. Bold numbers indicate the opposite directions of correlations between the PMP0 and PMP1000 groups.

Bone markers	**Bone mass or geometry**				**PMP0**	**PMP1000**
BAP	Radius	Metaphysis	BMD	Total	ns	-0.578***
				Cortical	0.360*	ns
			BMC	Trabecular	-0.324*	ns
		Diaphysis	BMD	Total	ns	-0.688***
				Cortical	**0.313***	**-0.811*****
			BMC	Total	0.503***	0.696***
				Cortical	0.305*	ns
	Tibia	Metaphysis	BMD	Total	ns	-0.334*
			BMC	Trabecular	ns	0.518**
		Diaphysis	BMD	**Total**	**0.351***	**-0.618*****
				Cortical	ns	-0.769***
			BMC	Cortical	0.471**	0.583***
			Thickness	Cortical	0.463**	ns
OC	Radius	Metaphysis	BMC	Total	ns	0.371*
				Cortical	ns	0.467**
		Diaphysis	BMC	Total	ns	0.552***
				Cortical	ns	0.552***
			Circumference	Endosteal	-0.306*	ns
	Tibia	Metaphysis	BMD	Cortical	ns	0.400*
		Diaphysis	BMC	Total	ns	0.381*
				Cortical	ns	0.579***
NTX	Radius	Diaphysis	BMD	Total	0.351*	ns
				Cortical	**0.363***	**-0.364***
			Circumference	**Periosteal**	**-0.489****	**0.348***
				Endosteal	ns	0.328**
	Tibia	Metaphysis	BMD	Total	-0.362*	ns
				Trabecular	-0.320*	ns
			Circumference	Periosteal	ns	0.365*
				Endosteal	ns	0.318*
		Diaphysis	BMC	Total	ns	0.374*
			Area	**Cortical**	**-0.560*****	**0.344***

BMC, BMD, BAP, OC and NTX stand for bone mineral content and density, bone-specific alkaline phosphatase, osteocalcin and cross-linked N-telopeptide of type I collagen, respectively.

Discussion

Theoretically, the development of anti-osteoporotic agents should first be tested at the preclinical level in laboratory animals, mostly rodents, before moving on to humans (Thompson et al., 1995). However, the bone structure and remodeling in rodents are different from those in humans, challenging or restricting the validity of rodent models for humans. Generally, ovariectomy-induced estrogen deficiency in rats causes a significant trabecular bone loss without any significant changes in the cortical bone (Urasopon et al., 2007; 2008, Suthon et al., 2016a). However, in humans, estrogen deficiency during postmenopausal period leads to the loss of both trabecular and cortical bones (Chen et al., 2013). As a result, the FDA requires anti-osteoporotic drugs to be tested in at least two species of laboratory animals before clinical tests in humans, with the recommended second species is monkeys (Thompson et al., 1995). It is of particularly importance to note that OVX monkeys do not experience the perimenopausal transition period, which is critical for the occurrence of osteoporosis (Kittivanichkul et al., 2016b). Thus, naturally postmenopausal monkeys were selected for this study. The postmenopausal stage was confirmed by the low plasma E_2 level, and high plasma FSH and LH levels of the 10 selected subject monkeys (Kittivanichkul et al., 2016b).

During the longitudinal 16-month study period, changes in bone quantity (decreased BMC and BMD) and quality (decreased cortical area and thickness) in postmenopausal monkeys could be detected. After the PMP treatment for 16 months, the deterioration of both bone quality and quantity, especially at cortical diaphysis, was alleviated. One of the possible explanations for this is that PM was slower the bone turnover process because a greater degree of reduction in BAP and OC levels were observed in the PMP1000 group. Furthermore, these changes could lead to a more number of correlations between bone turnover markers and bone mass/geometry parameters in the PMP1000 group comparing to the PMP0 group.

It has previously been proposed that the pathogenesis of osteoporosis in humans can be divided into the three different stages of early, accelerated and late slow phase of bone loss (Riggs et al., 1998, Khosla et al., 2011). A recent unitary model indicated that the late slow phase involved the loss of both trabecular and cortical bone. This is

consistent with a previous study in aged cynomolgus monkeys, where the trabecular bone abruptly declined during the peri-menopause period whereas the cortical bone loss was gradual, continuous and negatively correlated with the menopause period (Kittivanichkul et al., 2016b). However, in the present study the trabecular BMCs fluctuated to a large magnitude with no significant difference compared to the baseline (month 0) values. The cross-sectional images of bone, as determined by pQCT analysis, revealed that the trabecular bone at the metaphysis sites was minimal and barely seen in some individual monkeys. On the other hand, the total or cortical BMCs and BMDs of the diaphysis sites and the cortical BMCs of the metaphysis sites at both the radius and tibia gradually and continuously decreased. Taking the data for the BMDs and BMCs together with the average age and menopausal periods, it indicated that all 10 monkeys used in this experiment were in the late slow phase of bone loss.

In this study, the effects of oral administration of PMP on the bone mass in postmenopausal cynomolgus monkeys were investigated because of the established positive effects of PMP on the BMD and BMC in rat models (Urasopon et al., 2007; 2008, Suthon et al., 2016a). With regard to the *in vitro* study in rat osteoblast-like UMR 106 cells, the PME could enhance expression of gene associated with osteoblast differentiation (i.e., *Alp*) and suppress expression of gene associated with osteoclast differentiation (i.e., *Rankl*). Besides, PME also increased the expression of *Opg*, a decoy protein receptor of RANKL, mRNA level (Tiyasatkulkovit et al., 2012). Although it was reported that PME could enhance the *OPG*/*RANKL* ratio in baboon primary osteoblast (Tiyasatkulkovit et al., 2014), and could also decrease the serum parathyroid hormone levels in postmenopausal monkeys (Trisomboon et al., 2004), it was still required to test if PMP or PME can ameliorate bone loss in naturally postmenopausal monkeys.

With respect to this relatively long-term study (16 months) in postmenopausal monkeys, the two parameters of age and estrogen deficiency, although not related, were evaluated for changes in the bone mass. Interestingly, either the age or PMP-treatment induced or extenuated the loss of BMD and BMC, principally at the diaphysis sites and especially in the cortical bone. The cortical, but not the trabecular, region is the predominant site of bone fractures in age-related osteoporotic patients (Zebaze et al.,

2010). Several studies have reported that the cortical bone becomes more brittle and weaker with advancing age (McCalden et al., 1993). Generally, most bone fractures occur in the long bones that mainly consist of cortical bone tissue (Li et al., 2013), and so drug targeting to cortical bone should be prescribed for age-related bone loss late in life (Zebaze et al., 2010). Indeed, bone cells are comprised of both ERα and ERβ positive cells (Bord et al., 2001), and the phytoestrogens in PMP can bind with either ERβ or ERα (Setchell, 1998). Thus, PMP should have the potential to increase the trabecular as well as the cortical bone. However, changes in the trabecular bone of the PMP-treated monkeys were minimal and so PMP might affect the cortical bone to a greater extent in these postmenopausal aged monkeys. Thus, PMP could be a candidate for therapeutic intervention to reduce age-related bone fractures in osteoporotic menopausal women.

To prevent bone fractures, the skeletal structure or bone geometry also need to concern in addition to the bone mass, since to predict the risk of osteoporotic fracture requires consideration of both the bone density and its size/shape. These results of post-menopausal monkeys are consistent with a previous report in menopausal women, where expansions in the medullary cavity and periosteal diameter were observed in the radius (diaphysis) bone after menopause (Ahlborg et al., 2003). It is worth noting that the response in the tibia bone geometry to estrogen deprivation and increasing age (PMP0 group) was different from that in the radius. Both the endosteal and periosteal circumferences of the tibia bone fluctuated within the baseline values throughout the 16-month period, but they tended to increase in the radius. This significant difference might be because of the effect of the weight-bearing load on the tibia bone. The monkeys were kept in individual cages in captivity and so rarely walked in a quadrupedal pattern resulting in a lower weight-bearing load on the radius than on the tibia. Loading is known to directly regulate osteogenesis by increasing bone formation via mechano-responsive cells (Ehrlich and Lanyon, 2002). Moreover, estrogen deficiency has been proposed to reduce the sensitivity of bone cells to mechanical force resulting in a reduced bone mass (Frost, 1992). Indeed, a synergistic relationship between estrogen and mechanical loading on bone metabolism has been described (Kohrt et al., 1995). Therefore, any compound that can stimulate ERs, like PMP, would be expected to increase the machanostat and improve the mechanical properties of the

tibia bone. It was found that the radius and tibia responded to PMP treatment differently, where in the radius PMP predominantly increased the bone mass, while in the tibia it mainly affected the bone structure. After 16 months of PMP treatment, the increased cortical BMD and BMC were more evident at the diaphysis site of the radius bone. However, PMP treatment decreased endosteal resorption (significantly decreased endosteal circumferences comparing to the PMP0 group in Figure 4.8F) and periosteal deposition (marginally decreased periosteal circumferences comparing to the PMP0 group in Figure 4.8H) of the tibia bone. This correlated with the effect of estrogen that promoted endosteal formation and inhibited periosteal apposition in humans (Vanderschueren et al., 2006). It has previously been reported that ERβ is responsible for the effect of estrogen on the periosteal and endosteal surface (Bellido and Gallant, 2014). Thus, the cooperative actions of PMP treatment and weight bearing support the different results between the radius and tibia observed in this study.

Together with the reduction in cortical bone mass, area and thickness during the 16-month study period in the PMP0 monkeys, the plasma BAP and OC levels decreased (although they transiently fluctuated to a high degree) with time. Generally, BAP and OC are counted as bone formation and bone turnover marker, respectively. Thus, the decrease in both bone markers indicates a lower rate of bone remodeling when the animals enter aging period. This is consistent with a previous cross-sectional study in baboon monkeys, which revealed that the plasma BAP level was lowest among the oldest individuals (Havill et al., 2006). Moreover, it has previously been reported that serum OC levels were negatively correlated with the cortical diaphysis BMDs in postmenopausal monkeys (Kittivanichkul et al., 2016b). Together with the lower plasma OC level in the PMP1000 group compared to the PMP0 group, the data also indicated the reduction of plasma calcium level in the PMP1000 group. Previously, it was reported that PMP could reduce serum parathyroid hormone and calcium levels in aged menopausal monkeys (Trisomboon et al., 2004a). Thus, it might be hypothesized that PMP can play a part in reducing bone turnover rate through the parathyroid hormone and OC action, and might indirectly increase the cortical diaphysis BMD. Based upon on the fact that the rate of bone resorption (ca. 3 weeks) and bone formation (ca. 3–4 months) are not equal (Sims and Martin, 2014), then the reduced bone turnover

might alleviate the cortical bone loss by uncoupling the osteoblast and osteoclast activity.

As the correlations between bone markers and bone mass/geometry are higher in the PMP1000 group comparing to the PMP0 group (23 and 13 pairs, respectively), it suggests that PMP treatment decreased the bone turnover rate beyond the decrease that was caused by an increasing age only (as indicated by significantly lowered BAP and OC levels comparing to the PMP0 group). Besides, changes of bone turnover markers by increasing age are also depended on other various factors such as animal health, duration of menopause or senile in other endocrine organs. However, as bone markers are dynamic parameters, some changes might be missed during a point of time when the blood sample was collected.

Although PMP treatment reduced in the plasma OC levels, seven positive correlations between the OC levels and bone mass/geometry parameters was found (Table 4.3). The positive correlations between the urinary NTX levels and bone geometry parameters (diaphysis periosteal circumference and cortical area) and negative correlations between the urinary NTX and plasma BAP levels with the bone mass parameters (diaphysis cortical and total BMDs) were also observed following PMP1000 treatment. Taking these results of bone markers and bone mass/geometry parameters together, it can conclude that if the bone turnover (accounting for the BAP and NTX levels) increased in the PMP1000 group, the changes in bone geometry were in the opposite direction to the changes in the bone mass.

Although naturally menopausal cynomolgus monkeys are a more valuable animal model than OVX animals to mimic the changes in the slow phase of bone loss in postmenopausal aged women, it is very difficult to obtain a large enough sample size of old animals in most primate facilities, which is then a limitation of their use for many researchers.

CHAPTER V
A POTENTIAL USE OF *PUERARIA MIRIFICA* FOR BONE HEALING IN OSTEOPOROTIC MONKEYS

Introduction

Bone fracture is a medical condition in which the respective bone is completely or partially discontinuity. Indeed, almost half of all fractures are related to osteoporosis, which is characterized by a low bone mass and deterioration of the bone microarchitecture (Kanis et al., 2013). It has been reported that osteoporotic fractures cause a higher mortality and morbidity than cancers (except lung cancer), particularly for hip fractures that cause 10–20% increased mortality in age-matched women (Pisani et al., 2016). Currently, osteoporotic fractures are an increasing public health and socioeconomic problem and cost about $20 billion per year in the United States (Cummings and Melton, 2002) and €30.7 billion in Europe (Johnell and Kanis, 2006). The incidence of osteoporotic related bone fractures is growing significantly according to the global demographic trend. The number of osteoporosis hip fractures reached 1.7 million in 1990 and it has been projected to reach 21 million in 2050 (Cummings and Melton, 2002).

It is well known that estrogen deficiency is a major risk factor of osteoporosis (Ettinger, 2003), while it also directly affects the bone healing process (Beil et al., 2010). Thus, estrogen or estrogen-like compounds are widely used for the prevention and therapeutics of osteoporosis in postmenopausal women (Tella and Gallagher, 2014). Estrogen deficiency or supplementation has been shown to effect bone healing. For example, estrogen deficient mice showed an impaired periosteal callus formation, diminished chondrocytes, less mineralization, and a thinner and more porous bone cortex compared to the control mice. However, when they were treated with estrogen, the fracture healing was progressed by increasing the chondrocyte area, stimulating mineralization and giving a thicker cortex (Beil et al., 2010). The identification of estrogen-regulated genes in the fractured callus revealed that four important bone-related genes (collagen type 2, extracellular superoxide dismutase, urokinase-type plasminogen activator and ptk-3) were down-regulated in OVX rats but restored to

normal levels after estrogen treatment (Hatano et al., 2004). This is supported by a study in humans that noted that the lack of E_2 in menopausal women promoted the development of fat tissue from bone marrow cells rather than the osteogenic lineage (Justesen et al., 2001). Although estrogen seems to be beneficial for the treatment of both bone healing and osteoporosis, it also has adverse side effects, such as the promotion of estrogen-dependent cancers and diseases (Gambacciani et al., 2003).

PM, which contains at least 17 phytoestrogenic substances (Malaivijitnond, 2012) and has been widely tested, established that its phytoestrogen content stimulated bone formation and suppressed bone resorption both *in vitro* (Tiyasatkulkovit et al., 2012) and *in vivo* (Suthon et al., 2016a; Urasopon et al., 2007; 2008) in rodent models. Recently, the therapeutic effects of PMP or PME have been confirmed in non-human primate models (Kittivanichkul et al., 2016a; Tiyasatkulkovit et al., 2014), where PMP could ameliorate the loss of cortical bone mass in naturally postmenopausal cynomolgus monkeys (Kittivanichkul et al., 2016a), especially at the diaphysis site. Apart from the effect on bone mass, PMP also improved the bone structure by decreasing the endosteal circumferences and increasing the cortical thickness at the diaphysis site of both the radius and tibia.

With respect to the positive effect of PM on osteoporosis in rodents and in non-human primates, its efficacy on bone fracture healing has been raised. Although the US-FDA has approved many anti-osteoporotic drugs for osteoporotic patients, they have undesirable side effects on bone healing. For example, alendronate, an anti-bone resorptive agent that has been widely used for osteoporosis since it can increase bone density, has been reported to have a negative impact on bone healing (Kates and Ackert-Bicknell, 2016). Moreover, in osteoporotic or osteopenia patients who had spontaneous nonspinal fractures, alendronate, the bone resorption inhibitor, therapy resulted in the delayed or prevention of bone fracture healing due to the severe suppression of bone turnover which is a crucial process of bone healing (Odvina et al., 2005). Thus, this study aimed to test whether PMP, which had positive effects on osteoporosis, could accelerate bone fracture healing process in osteoporotic monkeys.

Materials and Methods

Experimental design

Prior to the experiment, all 10 postmenopausal monkeys were subject to an iliac crest biopsy. Two bone fracture defects were created by cut 1x1 cm of bone at the right ilium wing (Figure 5.1). Three days after the surgery procedure, monkeys were randomly divided into two groups (n = 5 per group) and treated with standard monkey diet either alone (PMP0) or mixed with PMP at a dose of 1,000 mg/kg body weight (BW)/day (PMP1000) at 08:00–09:00 am for 16 months. The age (29.6 ± 1.8 years and 26.0 ± 2.3 years, respectively) and menopause period (5.8 ± 1.4 years and 7.8 ± 1.2 years, respectively) were not significantly different between the PMP0 and PMP1000 groups.

Progression of bone healing was accessed by radiography (X-ray) and the determination was performed immediately after the biopsy procedure (month 0) and then at 1, 2, 3, 4, 6, 8, 12 and 16 months afterwards. Three individuals from each group were randomly selected and subjected to CT at month 0, 8 and 16. Based upon the 3D reconstructed CT images, the individual from each group that showed the greatest progression of bone healing was selected for a right ilium biopsy after 16 months of the PMP0 or PMP1000 treatment and histological changes were determined.

Figure 5.1 Bone defects were created by a 1 x 1 cm cut from the lateral ilium wing in each monkey. In the magnified insert image, the dashed line and shaded area indicate the perimeter and area measurement of the radiography, respectively. (Drawn by Mr. Ronnakrit Rojyindeelert)

Bone biopsy procedure

The monkeys were subcutaneously premedicated with tramadol (4 mg/kg BW; T.P. Laboratories (1969), Bangkok, Thailand) and cefazolin (25 mg/kg BW; Biolab Co., Ltd., Samutprakarn, Thailand). After that monkeys were anesthetized by intramuscular injection of tiletamine/zolazepam (3 mg/kg BW; Zoletil 100, Virbac, Nonthaburi, Thailand) and medetomidine hydrochloride (40 μg/kg BW; Vetcare, Joneboro, AR, USA). During surgical procedure, 4 mg/kg BW carprofen (Zoetis, Pasippany, New Jersey, USA) was subcutaneously injected as an analgesic. Operation was performed under strict aseptic techniques to avoid any complications. The ilium wing was palpated and the biopsied position was marked. Each bone defect was created by a 1 x 1 cm cut from the lateral ilium wing (Figure 5.1). The monkeys were intramuscularly injected with tramadol (3 mg/kg BW) and cefazolin (20 mg/kg BW) immediately after surgery and continued twice a day for 4 days. Monkey's health was checked twice daily for any sign of sickness or complications. Moreover, blood samples were collected at month 0 and 16, for determination of plasma biochemical markers (see below).

Assessment of bone repair by radiography

Monkeys were anesthetized by intramuscular injection with a mixture of 3 mg/kg BW tiletamine/zolazepam (Zoletil 100, Virbac, Nonthaburi, Thailand) and 40 μg/kg BW medetomidine hydrochloride (Vetcare, Joneboro, AR, USA). They were placed ventrodorsally, and the ilium wing was palpated and aligned parallel to the cassette. A 2-cm calibration scale was also placed on the cassette in every exposure. A portable X-ray machine (Poskom model PXP-60HF, Goyang, Korea) was used with a constant source to image distance of 70 cm while the kilovoltage peak (kVp) and milliampere seconds (mAs) was adjusted to acquire a proper image. After exposure, the X-ray cassette was developed with a digital X-ray reader (Fujifilm FCR Capsula, Tokyo, Japan) and the resulting of each bone defect was used to measure the perimeter and area of the damage by a specialist using the Osirix Lite (Version V.7.0.2, Bernex, Switzerland), as a blind assay, and the average value of two bone defects in each monkey was used for further analysis.

Assessment of bone repair by 3D-CT scans

The scan was performed to unveil the anatomical lesion of the ilium at 0, 8 and 16 months after the biopsy using a 64 slice multidetector CT scanner (Optima CT660, GE, Bangkok, Thailand). All monkeys were immobilized by intramuscular injection of a mixture of 3 mg/kg BW tiletamine/zolazepam (Zoletil 100, Virbac, Nonthaburi, Thailand) and 40 µg/kg BW medetomidine hydrochloride (Vetcare, Joneboro, AR, USA), and then were scanned in a supine position on the radiolucent V-pad positioning device. After the pre-scan phase, the region of interest was set to cover the whole area of the pelvic girdle, and helical CT images were acquired at 120 kVp, 250 mAs, pitch speed of 0.531 and a slice thickness of 1.25 mm. Subsequently, the CT images were analyzed in the digital imaging and communication in medicine (DICOM) format using the open source workstation viewer (Osirix Lite Version V.7.0.2, Bernex, Switzerland). To measure the bone structure parameters of both the post-operative ilium defects at different time points, the CT images were subjected to 3D multiplanar reconstruction and were revealed under the bone window (WL = 300, WW = 1500). For each ilium defect, the depth was repeatedly measured at the top (0%), center (50%) and lower (100%) position of the lateral height of the defect (see later; Figure 5.3). Moreover, the perimeter and area of each bone defect were also measured.

Bone histology

The biopsy of the post-treatment right ilium was performed at the end of the treatment period (month 16). The specimens were trimmed, washed in sterile normal saline solution and fixed in 10% neutral buffer formalin at room temperature. The specimens were decalcified, dehydrated, paraffin embedded, sectioned and stained with hematoxylin and eosin (H&E) by the Vet & Vitro Central Lab, Bangkok, Thailand.

Statistical analysis

The radiography and CT data are presented as the mean±SEM. As there was no significant interaction between the time and treatment when tested by two-way repeated measures ANOVA, the effects of time on bone healing in each monkey group, comparing values between month 0 and other time points, were analyzed using a paired t-test. Moreover, the effects of PM treatment compared between the PMP0 and PMP1000 groups at the same time point were analyzed using an unpaired t-test. The level of $p < 0.05$ was accepted as significantly different. Statistical analyses were performed using the IBM SPSS Statistics for windows, version 20.0 software (IBM Crop., Armonk, NY, USA).

Results

Clinical and physical examinations

All monkeys recovered rapidly after surgery without any sign of infection or complication. Moreover, the animals remained in a good health throughout the 16-month post-biopsy study period.

Decreased size of the bone defect under PMP treatment

Compared to the baseline value (month 0), the perimeter of the bone defect in the PMP0 group was significantly decreased at month 8 ($p = 0.006$) and 12 ($p = 0.012$) of treatment, while a significant decrease was detected earlier (since month 4; $p = 0.026$) in the PMP1000 group (Figure 5.2A). In concordance with the perimeter, the area of the bone defect was significantly decreased at month 8 ($p = 0.024$) and 12 ($p = 0.023$) in the PMP0 group, and from month 4 ($p = 0.020$) in the PMP1000 group (Figure 5.2B). Interestingly, no significant differences between the PMP0 and PMP1000 groups were detected in either the perimeter or the area throughout the 16-month post-biopsy study period.

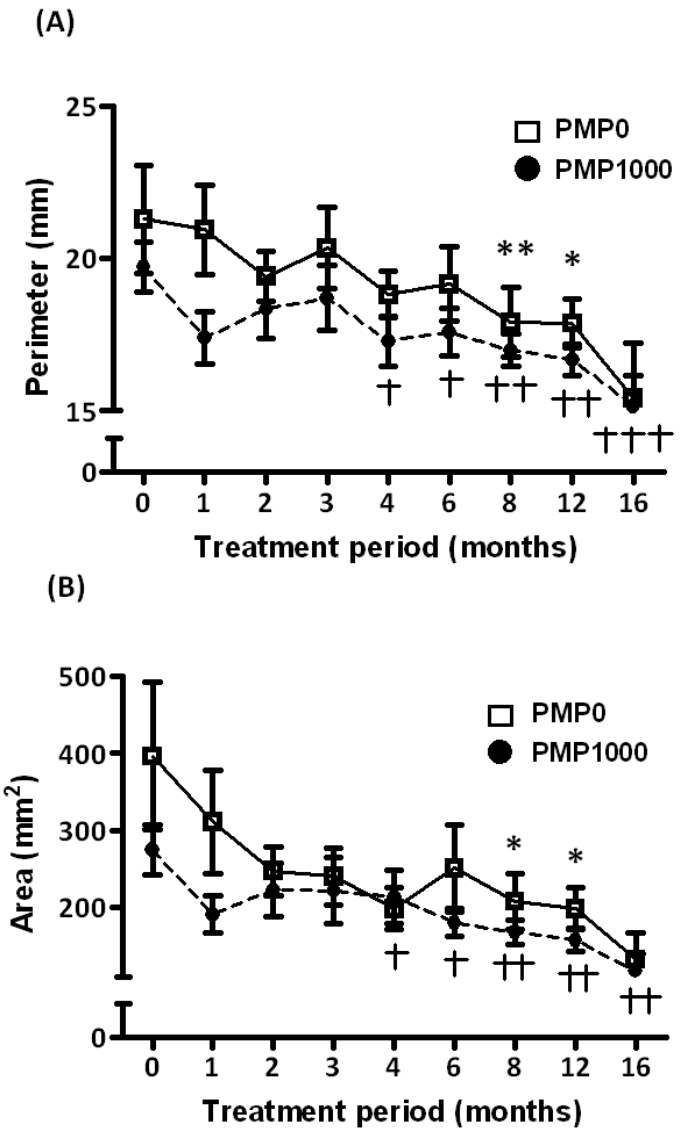

Figure 5.2 The (A) perimeter and (B) area of bone defect, as determined by X-ray radiography, during the 16-month experimental period. Open square and closed circle indicate the PMP0 and PMP1000 groups, respectively. *, ** and ***, and †, †† and ††† represent $p < 0.05$, 0.01, and 0.001 for month 0 and the other time points of the PMP0 and PMP1000 groups, respectively.

The area (Figure 5.3A), perimeter (Figure 5.3B) and depth (Figure 5.3C) of the 3D reconstructed CT images of the bone defect in the PMP0 and PMP1000 groups were not significantly different, considering either the comparison between month 0, 8 and 16 of both monkey groups or between the PMP0 and PMP1000 groups at the same time point. However, the CT image clearly revealed the progression of bone healing in one monkey of the PMP1000 group where the bone defects were evidently shallower at month 8 and 16 compared to those in the PMP0 group (Figure 5.4).

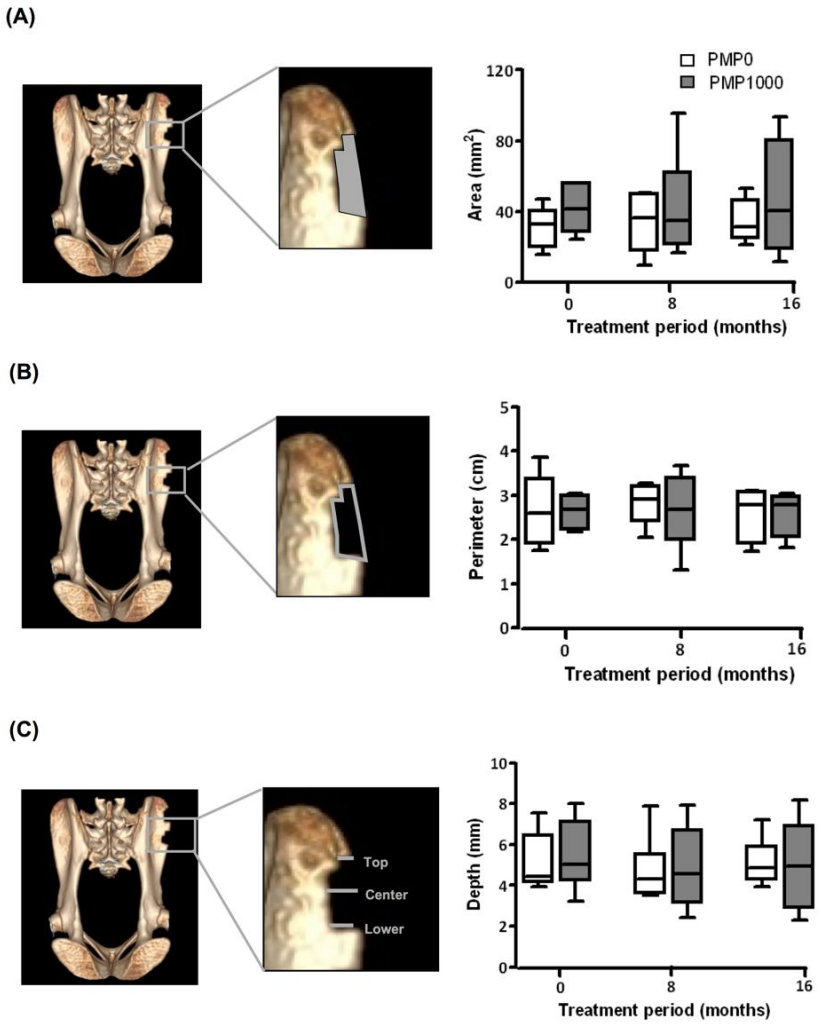

Figure 5.3 The (A) area, (B) perimeter and (C) depth of the bone defect, as determined by 3D-CT scans at month 0, 8 and 16. Open square indicates the area of magnification. Open and closed box indicate the PMP0 and PMP1000 groups, respectively. Box plot indicates the median and 25th and 75th percentiles.

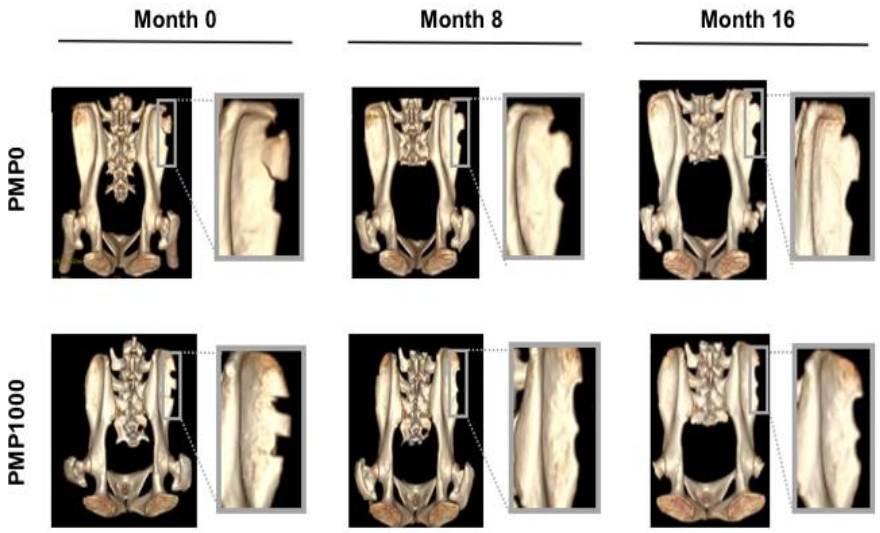

Figure 5.4 Reconstructed 3D-CT scans at month 0, 8 and 16 of the representative PMP0 (upper panel) and PMP1000 (lower panel) monkeys.

Bone histology

Since the measurements of area, perimeter and depth of bone defect did not indicate the bone healing process, the bone histology was examined. As expected, the PMP0 group showed a thick layer of fibrocartilage cells. In contrast, the PMP1000 group showed a lower number of fibrocartilage cells but a region of new bone formation, as indicating by the presence of chrondrocyte cells, was clearly observed (Figure 5.5).

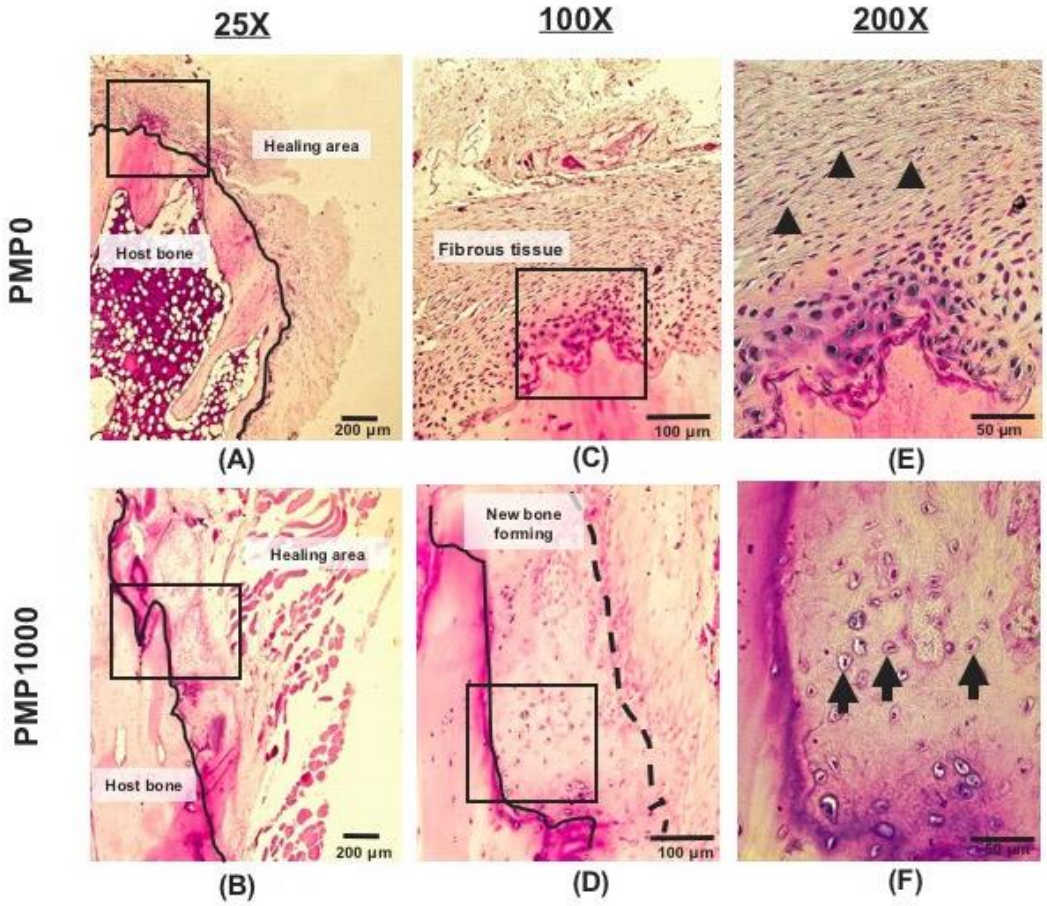

Figure 5.5 Longitudinal plane histology section (stained with H&E) of the ilium biopsy at month 16 of the (A, C, E) PMP0 and (B, D, F) PMP1000 treated monkeys at (A, B) 25X, (C, D) 100X and (E, F) 200X magnification. Open square indicates the area of magnification. The arrow head and arrow indicate fibrocartilage and chrondrocyte cells, respectively.

Discussion

In this study, the effects of PMP on bone healing in naturally menopausal osteoporotic monkeys was tested as a model to assess the benefit for fracture healing in postmenopausal osteoporotic women. This is because monkeys have a similar reproductive pattern (Weinbauer et al., 2008), bone biology and remodeling (Schaffler and Burr, 1984) as that of the humans. The PMP treatment at a dose of 1,000 mg/kg BW, which could alleviate cortical bone loss in naturally postmenopausal cynomolgus monkeys (Kittivanichkul et al., 2016a), potentially stimulated the bone healing process as seen in the earlier significant decrease in the perimeter and area of bone defect in the PMP1000 group (since month 4) compared to in the PMP0 group (since month 8) and a faster progressive bone healing process in the PMP1000 treated monkey confirming by 3D-CT scan and histological data. These results are in agreement with previous reports on the effect of the phytoestrogens puerarin (Wong and Rabie, 2007), genistein (Wong and Rabie, 2010) and daidzein (Wong and Rabie, 2009) on bone defects in rabbits. These rabbit bone defects were grafted with collagen matrix alone (control) or the same mixed with phytoestrogens. By the early healing stage (day 14) the presence of puerarin, genistein or daidzein in the collagen matrix had significantly increased new bone regeneration by 554%, 520% or 620%, respectively.

Previously, puerarin at concentrations of 0.1 nM to 1 μM stimulated differentiation of mesenchymal stem cells (ST2/Rx2^{dox}) indicating by ALP activity in dose dependent manner (Ji et al., unpublished manuscript). Moreover, it was reported that genistein and daidzein enhanced osteogenesis while depressing adipogenic differentiation of mesenchymal progenitor cells (Heim et al., 2004; Schilling et al., 2014). Likewise, it was shown that genistein and daidzein enhanced the osteogenic activity in mesenchymal and adipocyte stem cells (Strong et al., 2014). Moreover, *in vitro* studies on the effects of PME on osteoblasts and osteoclasts (Tiyasatkulkovit et al., 2012; 2014; Suthon et al., 2016b) support the results of this study on bone repair in osteoporotic monkeys. The administration of PME or puerarin increased the mRNA expression level of *Alp* and *Opg* and decreased the *Rankl*/*Opg* mRNA ratio in rat osteoblast-like UMR 106 cells (Tiyasatkulkovit et al., 2012) and primary baboon osteoblasts (Tiyasatkulkovit et al., 2014). In primary baboon osteoblasts, PME also

increased *COL1A1* mRNA expression (Tiyasatkulkovit et al., 2014). The mechanism of action was shown to initially depend on the ER, since the upregulation of *Alp* mRNA levels was abolished by pre-treatment with the ER antagonist, ICI182780 (Tiyasatkulkovit et al., 2012). However, the subsequent underlying mechanisms of actions of PME or other phytoestrogens on bone healing in monkeys are still unknown and need to be elucidated in the future.

The iliac crest was selected for bone biopsy in this study because it was easily accessible and did not require extensive surgery (Malluche et al., 2007). From 99 iliac crest biopsies of osteoporotic patients, complications were observed in only eight (8.1%) cases (Hodgson et al., 1986). Furthermore, the progression of the iliac crest biopsies correlated with the pattern seen for bone repair in the vertebrae (Meunier et al., 1973), tibiae (Dorr et al., 1990) and femur (Dorr et al., 1993). Another reason for performing an iliac crest biopsy in this study rather than the usual transiliac crest biopsy was that the transiliac crest biopsy might lead to immobility in the aged osteoporotic monkeys used this study. Therefore, the bone defect was created by cutting the lateral site of iliac crest, where the weight bearing or tension is minimal (Malluche et al., 2007).

One serious limitation of this study was the number of animals used, especially for the CT scan. It is difficult to acquire postmenopausal monkeys and it is much more difficult to obtain sufficient osteoporotic postmenopausal animals at the same time. Since the progress of bone healing has a high variation between individuals, the 3D-CT images of just three monkeys per group could not reach a statistically significant difference. However, the qualitative data from one monkey in the PMP1000 group evidently showed a greater progression of bone healing compared to the PMP0 monkeys. Close examination of the 3D-CT image of this monkey revealed that during the reduction in depth and area of the bone defect, the perimeter was actually increased. Combining the CT data and CT image together, the shallower depth and wider perimeter of the bone defect at month 16 of the PMP1000 treatment might due to the initiation of the remodeling process (bone resorption followed by its formation) at the site of the iliac crest biopsy occurring from the bottom before moving to the edge which has a high bone surface area.

With respect to the bone histology, PMP0 monkeys showed a thick layer of fibrocartilage cells while the PMP1000 monkeys had less fibrocartilage cells but a higher level of new bone formation. This indicates that bone healing in the PMP0 individuals was at the early stage of fibrocartilaginous callus formation because the fibrocartilage cells were not yet differentiated into a soft callus, while in the PMP1000 monkeys it was in the late stage of fibrocartilaginous formation up to the early stage of bony callus formation since chondrocytes or osteocytes could be observed together with the existence of woven bone. This leads to the conclusion that bone healing can occur, in general, in the non-treated PMP0 monkeys, but the PMP1000 treatment accelerated the bone healing process.

Even though the progression of bone healing gradually occurred throughout 16 months of the experiment, it should be noted that the bone defect of both the PMP1000 and PMP0 groups was still not completely connected at month 16 of the study period. Based on the fact that the age of monkeys in this study was over 20 years old, cellular senescence and alteration of the microenvironment surrounding the bone cells might be the cause of the incomplete bone healing. It has been reported that aging affects the proliferation and functional ability of osteal macrophages (Gibon et al., 2016), which are crucial in bone repair for coordinating the crosstalk between osteoclasts and osteoblasts (Cho, 2015). Moreover, a decrease in the number of mesenchymal stem cells with increasing age has also been observed in rats (Quarto et al., 1995) and humans (Muschler et al., 2001). The impairment in aged mesenchymal stem cell proliferation and differentiation has been linked to a shortening in telomere length and to changes in the microenvironment (Gibon et al., 2016). A comparison between juvenile (4-week-old), middle aged (6 month), and aged (18 month) mice found a decrease in the vascularization of a fracture callus, together with a decreased expression of hypoxia-inducible factor-1 alpha protein and transcripts of vascular endothelial growth factor, with age (Lu et al., 2008). Furthermore, the process of bone remodeling by osteoblasts and osteoclasts also decreases with age (Szulc and Seeman, 2009), potentially due to a reduction in osteoblast precursors, mesenchymal stem cells and osteoblast life span (Boskey and Coleman, 2010). A study in non-human primates also showed a similar trend in that the osteoclast precursor, hematopoietic cells, declined with age (Lee et al., 2005).

It has been reported that osteoporosis can cause irregular bone healing and affect different stages in the bone healing process depending on the species of animals used. In rats, osteoporosis affects callus formation and mineralization in the early and late stages of bone healing, respectively (Egermann et al., 2005). In osteoporotic sheep, a delay in the tibiae bone healing at callus formation and mineralization was observed as well as altered mechanical properties (Lill et al., 2003). Although no study of bone healing in osteoporotic monkeys has been performed, the progression and mechanism of action of bone remodeling and osteoporosis occurrence in monkeys resembles that in humans (Turner, 2001). Thus, naturally osteoporotic monkeys are an ideal animal model for research on bone fracture healing.

In conclusion, the present study demonstrates that PMP treatment could accelerate the progression of bone fracture healing in naturally postmenopausal osteoporotic monkeys, in addition to the previously reported amelioration of bone loss (Kittivanichkul et al., 2016a). Therefore, PMP has a high potential to be developed as anti-osteoporotic agent and also for bone fracture healing for human use in the future.

CHAPTER VI

PUERARIA MIRIFICA REGULATES BONE RESORPTION AND FORMATION IN MONKEY BONE CELLS PARTIALLY THROUGH RANKL/RANK/OPG SYSTEM

Introduction

Osteoporotic patients are at risk for bone fracture. In humans, about one of three menopausal women and one of five men at over 50 have a potential to encounter an osteoporotic fracture (Melton et al., 1998) (Melton et al. 1992). It is well known that estrogen is a key hormonal regulator on bone because it can bind with ERs located in osteoblasts, osteoclasts and osteocytes (Khosla et al., 2012). However, ERT is no longer recommended to osteoporotic patients because of its undesirable side effects. The Women's Health Initiative (WHI) reported that use of estrogen plus progestin increased the incidence of breast cancer, cardiovascular disease and dementia (Rossouw et al., 2002). Therefore, the alternative approaches of using chemicals that deliver estrogenic activity on bone but no adverse side effects to other tissues such as SERMs attract much attention.

PM contains at least 17 phytoestrogens, including 10 isoflavonoids, four coumetrans and three chromenes. Puerarin is a major phytoestrogen found in PM while miroestrol exhibits highest estrogenic activity (Malaivijitnond et al., 2012). During the past 10 years, the estrogenic activity of PM on bone has been tested both *in vitro* and *in vivo*, either in rodents or in monkeys. In rodents, *in vitro study*, PME decreased cell proliferation while increased *Alp* and *Opg* mRNA expression in osteoblast-like UMR 106 cells. Besides, PME suppressed osteoblast-induced osteoclastogenesis by decreasing *Rankl*/*Opg* mRNA ratio (Tiyasatkulkovit et al., 2012). RANKL expresses on the membrane of osteoblast lineages and binds to its RANK receptor located on hematopoietic precursor cells. When RANKL presents to the hematopoietic precursor cells together with M-CSF, it stimulates osteoclastogenesis, attachment of osteoclast to bone surface (O'Brien et al., 2000), and activation (Burgess et al., 1999) and survival (Lacey et al., 2000) of osteoclasts. OPG is a decoy receptor protein for RANKL secreted

by osteoblasts or osteogenic stromal cells which prevents osteoclast differentiation and function. In primary baboon osteoblast culture, PME stimulated cell proliferation and *ALP* and *COL1A1* mRNA expression, but decrease *RANKL*/*OPG* mRNA ratio (Tiyasatkulkovit et al., 2014). *In vivo* rat study, 90-day PMP treatment in OVX and ORX rats dose-dependently increased trabecular and cortical BMDs and BMCs (Urasopon et al., 2007; 2008). When the rats were induced bone loss by ovariectomy, treatment of 50 mg/kg BW/day of PMP for 12 weeks could retain trabecular BMDs at tibia metaphysis as well as total and trabecular BMDs of the 4th lumbar vertebra (L4) (Suthon et al., 2016a). Later, the anti-osteoporotic effect of PMP was confirmed in postmenopausal cynomolgus monkeys (Kittivanichkul et al., 2016a). Although it is undoubted, at this point, that PMP acquired the anti-osteoporotic effects both in rodents and non-human primates, and it mechanism of actions were progressively verified both in osteoblast and osteoclast cells, the real-time changes of mRNA expression in osteoblast cells collected from PMP-treated animals have not done yet. Here, the expression of genes associated with bone turnover markers in osteoblast cells isolated from menopausal cynomolgus monkeys after 16-month PMP treatment have been performed.

Materials and Methods

Experiment design

The 10 postmenopausal monkeys which were subjected to the experiments in CHAPTER IV and V were analyzed further in this study. The monkeys were previously divided into two groups (n = 5 per group) and treated with standard monkey diet either alone (PMP0) or mixed with PMP at a dose of 1,000 mg/kg body weight (BW)/day (PMP1000) at 08:00–09:00 am for 16 months. Before (month 0) and after (month 16) the treatment, the monkeys were subjected to an iliac crest biopsy as mentioned in CHAPTER VI. Pieces of 1x1 cm cut of bone samples were trimmed and clean in sterile 0.85% sodium chloride and immediately kept in dry ice before snap freezing in liquid nitrogen.

RNA extraction and cDNA synthesis

The bone samples were homogenized by sterile mortar and pestle under cooled temperature in a liquid nitrogen bath. The total RNA was extracted with the guanidium thiocyanate-phenol-chloroform method (Hughes et al., 2012). The homogenized samples were dissolved in 1 ml of TRIZOL reagent (Invitrogen, Carlsbad, CA, USA) and transferred into 1.5-ml microcentrifuge tube. Then, 200 μl of chloroform was added for RNA phase separation. The 500 μl of isopropanol was used for total RNA precipitation. The RNA was washed and recompensed in 75% ethanol and diethylpyrocarbonate (DEPC) water, respectively. The RNA quantity and purity were checked by NanoDrop-2000c spectrometer (Thermo Scientific, Waltham, MA, USA) of which the A_{260}/A_{280} ratio ranging by 1.8-2.0 was accepted. After the mRNA extraction, the mRNA was used to synthesize the cDNA. One μg of total RNA was reversed transcriped (iScript Select CDNA Synthesis Kit; Catalog no**.** 170**-**8896, BIO**-**RAD, Hercules, CA, USA**)** at 42^{o}C for 60 min and 85^{o}C for 5 min by a conventional thermal cycler (model MyCycler, Bio**-**RAD).

Gene expression analysis

The expression of genes associated with bone turnover markers in osteoblast cells which are *ALP*, *RANKL* and *OPG* were investigated by qRT-PCR technique

(Table 6.1). The *β-ACTIN* was used as a house keeping gene. The *ALP*, *OPG* and *β-ACTIN* primers were followed the previous report in baboon monkeys (Tiyasatkulkovit et al., 2014). The *RANKL* primer was designed using Primer 3 program based on *Macaca fascicularis* genome sequence (Accession no. XM_005585744.2). The specificity of all primers was confirmed by conventional PCR **(**Gotaq DNA Polymerase Promega, Madison, WI, USA, catalog no**.**M3001**).** The PCR amplicons were checked by 1**.**5*%* agarose gel stained with 1μg*/*L ethidium bromide **(**Sigma**)** under a UV transilluminator **(**Alpha Innotech, San Leandro, USA**).** The sequence homologies of the PCR product identity comparing to reference sequences were 97*%*, 99*%*, 99*%* and 91*%* for *β-ACTIN*, *ALP*, *RANKL* and *OPG*, respectively. The qRT-PCR was performed using the StepOne^{TM} Plus Real-Time PCR System (Applied Biosystems, Foster city, CA, USA) in a 20 μL reaction mixture containing 1x SensiFAST SYBR Hi-ROX Mix (Bio Line, London, UK, catalog no. BIO-92005) 200 nM each of the respective forward and reverse primers, and 40 ng of the cDNA sample. The reaction was performed at 95 °C for 2 min followed by 35 cycles of 95 ºC 5 sec, 56**-**59 °C for 30 sec and 72 °C for 30 sec, respectively and then a dissociation curve step (StepOne Plus Real**-**Time PCR System, Applied Biosystems, USA)**.** The relative expression levels of the target genes were calculated by the $2^{-\Delta\Delta Ct}$ method.

Table 6.1 *Macaca fasciscularis* primers used in qRT-PCR analysis

Genes	Primers (forward/reverse)	Product length (bp)	Annealing temperature (^{o}C)
β-ACTIN	5′-CACACGCAGCTCATTGTAGA-3′ 5′-GGCATGGGTCAGAAGGATT-3′	153	56
ALP	5′-AACCACCACGAGAGTGAACC-3′ 5′-TCCCTGATGTTATGCACGAG-3′	150	56
RANKL	5'-TTCAGCTAATGGTGTACGTCA-3' 5'-AGTACGTTGCATCCTGATCC-3'	216	59
OPG	5′-TGTATTTCGCTCTGGGGTTC-3′ 5′-CTGCAGTACGTCAAGCAGGA-3′	153	56

Statistical analysis

The fold change of mRNA levels was presented as the mean±SEM. The effects of increasing age on mRNA expression in each monkey group (PMP0 or PMP1000), comparing values between month 0 and other time points, were analyzed using a paired t-test. Moreover, the effects of PMP treatment compared between the PMP0 and PMP1000 groups at the same time point were analyzed using an unpaired t-test. The level of $p < 0.05$ was accepted as significantly different. Statistical analyses were performed using the IBM SPSS Statistics for windows, version 20.0 software (IBM Crop., Armonk, NY, USA).

Results

Effect of aging on bone markers gene expression

Considering the increasing in age of the monkeys for 16 months of the study period, the PMP0 postmenopausal monkeys had no changes of mRNA expression of any genes determined (*ALP*, *RANKL* and *OPG*) comparing between month 0 and month 16 (Figure 6.1). The similar patterns were seen in the PMP1000 monkeys. However, the ratios of *RANKL*/*OPG* were significantly decreased in both PMP0 and PMP1000 groups (p=0.0434 and 0.0188 for PMP0 and PMP1000 group, respectively).

Effect of PMP treatment on bone marker gene expression

Before the treatment (month 0), the mRNA expression of *ALP*, *RANKL* and *OPG* was not significantly different between the PMP0 and PMP1000 group (Figure 6.1 A-C). However, the *RANKL/OPG* ratio of the PMP1000 group significantly higher than the PMP0 group (Figure 6.1D). At the end of experiment (month 16), the mRNA expression of all three genes, *ALP*, *RANKL* and *OPG*, was not significant difference including the *RANKL/OPG* ratio, between the PMP0 and PMP1000 groups.

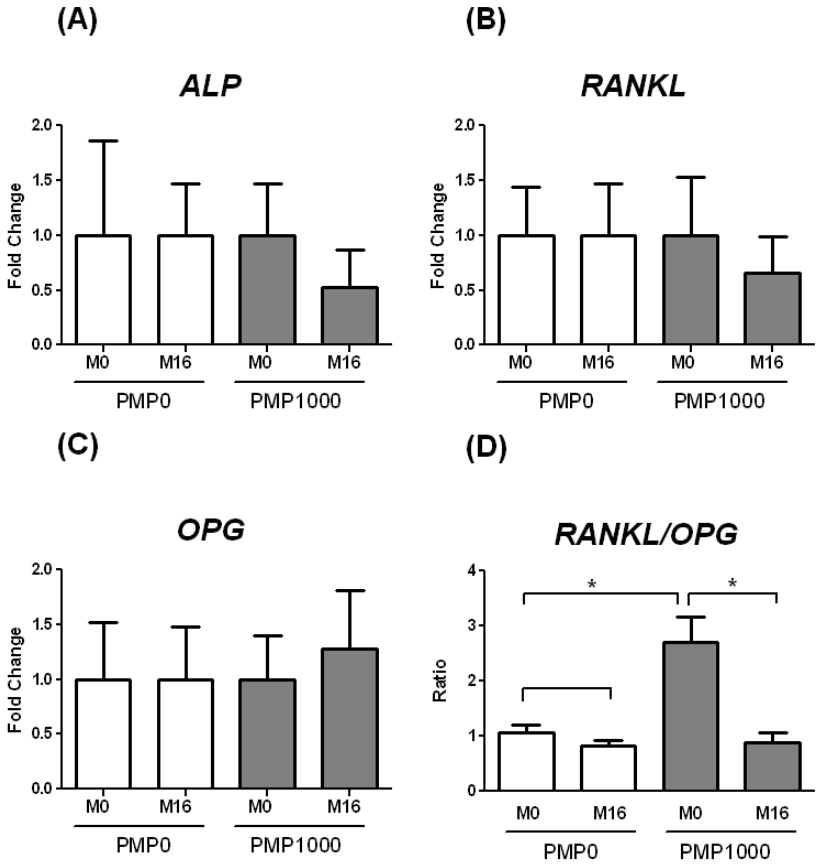

Figure 6.1 The mRNA expression of (A) alkaline phosphatase (ALP) , (B) nuclear factor κ-B ligand (RANKL), (C) osteoprotegerin (OPG) and (D) RANKL/OPG ratio at month 0 and moth 16 of the monkeys in PMP0 and PMP1000 group. Data are shown as the mean ± SEM., respectively. * represents $p < 0.05$.

Discussion

The mRNA expression of *ALP*, *RANKL* and *OPG* was not changed according to both increasing aging (comparing between month 0 and month 16 of the PMP0 group) and treatment effect (comparing between PMP0 and PMP1000 groups), however, the protein expression measured by ELISA showed a significant decrease in ALP level in PMP1000 group, comparing between month 0 and 16 (Kittivanichkul et al., 2016a). Moreover, the significant differences between the PMP0 and PMP1000 groups were detected at month 4, 10, 12 and 16 of the treatment. Therefore, it might be possible that changes at the protein levels, without any changes at the mRNA levels, occurred at the translation or post-translation level. Another possibility is that changes in mRNA expression could occur at other time points of the treatment which were not analyzed in this study. It should be noted that, besides bone, ALP also synthesized and secreted from liver and kidney, thus the changes of plasma ALP might also come from liver or kidney function.

Based on the fact that the balance between levels of RANKL and OPG is crucial for maintenance of bone homeostasis, the RANKL/OPG ratio was therefore calculated. Unexpectedly, the *RANKL/OPG* mRNA ratio significantly decreased in both of PMP0 and PMP1000 group at month 16 of the study period. In concordance with the previous study reported that old mice (aged 2.5 years old) tended to decrease in *Rankl* and *Opg* mRNA expression comparing to the young mice (aged 8 weeks old) (Ikeda et al., 2001). Moreover, the serum RANKL/OPG protein ratio in 504 Chinese women was decreased during post-menopausal period, and the increasing age was positively and negatively correlated with serum OPG and RANKL levels, respectively (Liu et al., 2005). However, in this study the significant increase or decrease in *OPG* and *RANKL* mRNA expression was not detected. Generally, the levels of mRNA *RANKL/OPG* ratio were positively correlated with eroded bone surface (Fazzalari et al., 2001), hip fracture (Abdallah et al., 2005) and osteolysis (Grimaud et al. 2003), thus the decrease in *RANKL/OPG* mRNA ratio observed here was hypothesize to be the compensate mechanism of the skeleton to protect further bone loss in aging.

Since the *RANKL/OPG* mRNA ratio of the PMP1000 monkeys was higher than the PMP0 monkeys at month 0, it is not surprise to see the greater reduction of

RANKL/OPG mRNA ratio in the PMP1000 monkeys after 16 months of the treatment (~3 and 1.3 folds reduction in the PMP1000 and PMP0 group). Therefore, other than the aging effect, PMP might partially play a role to reduce *RANKL/OPG* mRNA ratio. Previously, the *in vivo* study in rat osteoblast-like UMR106 indicated that the PM extract decreased *Rankl*/*Opg* ratio by increasing *Opg* mRNA expression (Tiyastatkulkovit et al., 2012), however, in baboon primary osteoblast, the decreased *RANKL/OPG* mRNA ratio was caused by a decreased *RANKL* mRNA level (Tiyastatkulkovit et al., 2014). Thus, the underlying mechanisms of actions of how and why aging and PM affect *RANKL*, *OPG* and *RANKL*/*OPG* mRNA ratio need to be investigated further.

It is worth noting that the limitation of this study is a few numbers of bone specimens obtained for determination of mRNA expression. Thus, the longitudinal (16 months) changes of gene expression could not reach the statistical significant level. As seen, the mRNA expression highly varied between individuals. Another point to which need to be kept in mind is the measurement of RANKL and OPG protein level in bone microenvironment should be conducted.

CHAPTER VII
GENERAL DISCUSSION AND CONCLUSIONS

Cynomolgus monkey (*M. fascicularis*) is an animal model of choice recommended by US-FDA for postmenopausal osteoporotic research based on the similarity of their physiology and anatomy to those of humans (Thompson et al., 1995). The naturally menopausal monkeys in this study showed difference patterns of trabecular and cortical bone loss with respect to the menopause status (seen in Chapter III). The trabecular metaphyseal bone was abruptly decreased during perimenopausal period. In contrast, the cortical bone mass at the diaphysis gradually and continuously decreased in the postmenopausal period. Thus, the negative correlation between cortical bone loss at diaphysis site and menopause period was detected. These results are similar to the clinical observations with humans showing that trabecular bone loss in women started in a younger age (about 30 years old) and the loss was accelerated at the perimenopausal phase, whereas the cortical bone loss was minimal during the transition from the premenopausal to perimenopausal period (Khosla et al., 2011).

Further investigation is needed to understand the difference between the patterns of trabecular versus cortical bone loss during naturally occurring menopause. A study in C57/BL6 mice comparing between young control, aged/sham, age/OVX and age/OVX plus ERT showed that latter group had an increase in cortical bone in the identical level to those of the young control, but the increase in trabecular bone was similar to the age/sham group and lower than the young control group (Syed et al., 2010). This suggests that, at least in part, cortical bone loss depends on estrogen level while trabecular bone loss might be affected by other factors such as increasing age although estrogen deficiency is an important acceleration factor (Khosla et al., 2011; Ucer et al., 2017). The development of target deletion of ER in specific cell types by using Cre/LoxP system provided a novel underlying mechanism of estrogen in bone cells. Recently, it was revealed that estrogen protect the trabecular and cortical bone in difference mechanism (Almeida et al., 2017). Targeted deletion of ERα in osteoclast or myeloid lineage resulting in increased osteoclast number in bone marrow along with

decrease trabecular but not cortical bone (Martin-Millan et al., 2010). On the other hand, targeted deletion of ERα in mesenchymal stem cells exhibited decrease in periosteal apposition and cortical bone mass (Almeida et al., 2013). Consistence with the study in the *in vivo* mice model showed that the effect of aging and sex steroid deficiency on the skeleton are independent and distinct mechanism (Ucer et al., 2017). Estrogen deficiency driven cortical bone loss by increasing osteoclastogenesis at least in part, through stromal cell –derived factor 1(SDF1). On the other hand, aging resulting in increased H_2O_2 in mesenchymal lineage combined with increase osteoclastogenesis are causes of cortical bone loss (Ucer et al., 2017). However, the underlying mechanism and relation of trabecular bone in response to aging still elusive. Thus, use of the naturally menopausal monkeys here in an attempt to mimic the symptom of menopausal bone loss in women, especially the perimenopausal bone loss, has the advantages far beyond the use of OVX rodent and monkey model. Bone loss occurring at the perimenopausal period should be seriously taken because it could be a critical period for bone loss protection (Appt and Ethun, 2010). Besides, 80% of the fractures in older humans are nonvertebral fractures, mainly at the cortical bone (Riggs et al., 1981; Kanis et al., 2001). Thus, the protection against cortical bone loss is highly significant for management of postmenopausal osteoporosis. Other than estrogen, the cortical bone loss occurring in postmenopausal period might be affected by other factors such as FSH because a significant increase in serum FSH levels was detected earlier during early- and mid-postmenopausal periods while a significant decrease in serum E_2 level was detected later in the late postmenopausal stages in this study. Recent study indicated that FSH potentially directly stimulated osteoclast bone resorption (Sun et al., 2006). Moreover, treatment with anti-FSH antibody could stimulate bone formation both *in vivo* and *in vitro* in mice (Zhu et al., 2012). Moreover, the levels of FSH were positively correlated with bone resorption marker NTX. Therefore, this suggests that bone loss occurring in early- and mid-menopausal monkeys is affected partly by an increased FSH concentration, whereas that in the late-menopausal monkeys is mainly caused by the decrease in E_2 concentration. Furthermore, as the negative correlations between serum BAP and urinary NTX levels with the trabecular bone mass, and between the serum OC level and cortical bone mass were detected, it suggests that serum BAP and

urinary NTX levels should be used as biochemical markers for the trabecular bone loss, and serum OC level should be a marker for the cortical bone loss in the monkey model.

In consistence with cross-sectional study in elderly women (Riggs et al., 2008), the longitudinal 16-month study in naturally postmenopausal monkeys revealed that the cortical bone either metaphysis (total and cortical BMC) or diaphysis (total and cortical BMC/BMD) continuously decreased in both radius and tibia, while the trabecular bone fluctuated with barely significant change (seen in Chapter IV). This is because trabecular bone mass was minimal in old aged monkeys and women (Riggs et al., 2008). Together with changes in cortical bone at the diaphysis, the changes of bone structure or bone geometry was also found during 16-month study period. Although the cortical area and thickness in both radius and tibia continuously decreased, the endosteal and periosteal circumference of the tibia bone fluctuated within the baseline values, but they tended to increase in the radius bone. The human population based cross-sectional study found the site-specific of cortical bone loss between distal radius (non-weight bearing site) and tibia (weight bearing site). In women, the loss of cortical thickness at the radius was attributable to the insufficient periosteal apposition while in increased endocortical expansion was implicated in the tibia (Macdonald et al., 2011).

Although the positive effect of PMP and PME treatments on bone *in vitro* (Tiyasatkulkovit et al., 2012; 2014) and *in vivo* rodent model (Urasopon et al., 2007; 2008; Suthon et al., 2016) has been clarified, the therapeutic effects of PMP on bone loss in osteoporotic naturally menopausal cynomolgus monkeys was conducted in an attempt to mimic the condition in osteoporotic postmenopausal women (seen in Chapter IV). Treatment of PMP at a dose of 1,000 mg/kg BW/day for 16 months significantly increased cortical BMD and BMC at diaphysis site of radius and tibia bone of osteoporotic postmenopausal monkeys, although it was lower than those of the premenopausal monkeys. The PMP treatment also showed beneficial effect on bone geometry of which the decreased endosteal resorption and periosteal deposition was more evident in the tibia bone. Moreover, the PMP treatment could lower the bone turnover in postmenopausal monkeys indicating by lowering serum BAP and OC and urinary NTX levels. In the same line with changes of those biochemical markers, the *RANKL*/*OPG* mRNA expression was decreased greater in the PMP1000 monkeys

comparing to the PMP0 monkeys. (seen in Chapter VI) Based upon on the fact that the rate of bone resorption (~ 3 weeks) and bone formation (~ 3–4 months) are not equal (Sims and Martin, 2014), then the reduced bone turnover in postmenopausal monkeys after the PMP treatment might alleviate the cortical bone loss by uncoupling the osteoblast and osteoclast activity.

The loss of cortical bone mass and changes in bone geometry observed in postmenopausal monkeys are a major predisposing cause of osteoporotic fracture. Unfortunately, osteoporotic patients showed a delay in bone fracture healing because of the poor bone quantity and quality while entering the menopausal period. In the present study, PMP not only had anti-osteoporotic effects (Chapter V) but also accelerated bone fracture healing (Chapter VI). For the latter study, the perimeter and area of iliac crest defect was significantly decreased earlier in the PMP1000 monkeys (since month 4) compared to the PMP0 monkeys (since month 8). The histological examination showed that that bone healing in PMP1000 monkeys were in the late stage of fibrocartilaginous formation up to the early stage of bony callus formation while the PMP0 individuals were only at the early stage of fibrocartilaginous callus formation. These results are in agreement with the previous studies in rabbits treated with puerarin (Wong and Rabie, 2007), genistein (Wong and Rabie, 2010) and daidzein (Wong and Rabie, 2009). However, it should be noted that at the end of 16-month experiment, the bone healing process in these postmenopausal osteoporotic monkeys was incomplete. Possibly, PM may be more beneficial for the acceleration of bone healing in younger individuals.

In conclusion, this study demonstrated the high potential of use of naturally postmenopausal cynomolgus monkeys as a suitable animal model for osteoporotic research. Longitudinal 16-month treatment of PMP to osteoporotic postmenopausal monkeys showed no adverse side effects, but the beneficial effects on bone loss and bone healing. Thus, PMP or its phytoestrogen component has a high potential to be developed as a drug for anti-osteoporosis and bone healing aspect for human use in the future.

REFERENCES

Abdallah, B. M., Stilgren, L. S., Nissen, N., Kassem, M., Jorgensen, H. R., & Abrahamsen, B. Increased *RANKL/OPG* mRNA ratio in iliac bone biopsies from women with hip fractures. Calcif Tissue Int, *76*(2) (2005): 90-97.

Ahlborg, H. G., Johnell, O., Turner, C. H., Rannevik, G., & Karlsson, M. K. Bone loss and bone size after menopause. N Engl J Med, *349*(4) (2003): 327-334.

Almeida, M., Iyer, S., Martin-Millan, M., Bartell, S. M., Han, L., Ambrogini, E., et al. Estrogen receptor-alpha signaling in osteoblast progenitors stimulates cortical bone accrual. J Clin Invest, *123*(1) (2013): 394-404.

Almeida, M., Laurent, M. R., Dubois, V., Claessens, F., O'Brien, C. A., Bouillon, R., et al. Estrogens and Androgens in Skeletal Physiology and Pathophysiology. Physiol Rev, *97*(1) (2017): 135-187.

Appt, S. E., & Ethun, K. F. Reproductive aging and risk for chronic disease: Insights from studies of nonhuman primates. Maturitas, *67*(1) (2010): 7-14.

Augat, P., & Schorlemmer, S. The role of cortical bone and its microstructure in bone strength. Age Ageing, *35 Suppl 2* (2006): ii27-ii31.

Bahar, S., Abali, R., Guzel, S., Bozkurt, S., Guzel, E. C., Aral, H., et al. Comparison of the acute alterations in serum bone turnover markers and bone mineral density among women with surgical menopause. Eur J Obstet Gynecol Reprod Biol, *159*(1) (2011): 194-197.

Beil, F. T., Barvencik, F., Gebauer, M., Seitz, S., Rueger, J. M., Ignatius, A., et al. Effects of estrogen on fracture healing in mice. J Trauma, *69*(5) (2010): 1259-1265.

Bellido, T., & Gallant, K. H. (2014). Hormonal effect on bone cells. In Burr, D., & Allen, M. (Eds.), *Basic and applied bone biology* (pp. 300-313). London: Academic Press.

Bellido, T., Plotkin, L.., & Bruzzaniti, A. (2014). Bone cells. In Burr, D., & Allen, M. (Eds.), *Basic and Applied Biology* (pp. 27-45). London: Academic press.

Bellino, F. L., & Wise, P. M. Nonhuman primate models of menopause workshop. Biol Reprod, *68*(1) (2003): 10-18.

Beral, V., & Million Women Study, C. Breast cancer and hormone-replacement therapy

in the Million Women Study. Lancet, *362*(9382) (2003): 419-427.

Bord, S., Horner, A., Beavan, S., & Compston, J. Estrogen receptors alpha and beta are differentially expressed in developing human bone. J Clin Endocrinol Metab, *86*(5) (2001): 2309-2314.

Boskey, A. L. Matrix proteins and mineralization: an overview. Connect Tissue Res, *35*(1-4) (1996): 357-363.

Boskey, A. L., & Coleman, R. Aging and bone. J Dent Res, *89*(12) (2010): 1333-1348.

Bouxsein, M. L., & Karasik, D. Bone geometry and skeletal fragility. Curr Osteoporos Rep, *4*(2) (2006): 49-56.

Brzezinski, A., & Debi, A. Phytoestrogens: the "natural" selective estrogen receptor modulators? Eur J Obstet Gynecol Reprod Biol, *85*(1) (1999): 47-51.

Burger, H. The menopausal transition--endocrinology. J Sex Med, *5*(10) (2008): 2266-2273.

Burgess, T. L., Qian, Y., Kaufman, S., Ring, B. D., Van, G., Capparelli, C., et al. The ligand for osteoprotegerin (OPGL) directly activates mature osteoclasts. J Cell Biol, *145*(3) (1999): 527-538.

Burr, D. Estimated intracortical bone turnover in the femur of growing macaques: implications for their use as models in skeletal pathology. Anat Rec, *232*(2) (1992): 180-189.

Burr, D., &Akkus, O. Bone morphology and organization. In Burr, D., & Allen M. (Eds), *Basic and Applied Biology* (pp. 3-25). London: Academic press.

Cao, X. Targeting osteoclast-osteoblast communication. Nat Med, *17*(11) (2011): 1344-1346.

Cauley, J. A. Estrogen and bone health in men and women. Steroids, *99*(Pt A) (2015): 11-15.

Cenci, S., Toraldo, G., Weitzmann, M. N., Roggia, C., Gao, Y., Qian, W. P., et al. Estrogen deficiency induces bone loss by increasing T cell proliferation and lifespan through IFN-gamma-induced class II transactivator. Proc Natl Acad Sci U S A, *100*(18) (2003): 10405-10410.

Chang, J., Wang, Z., Tang, E., Fan, Z., McCauley, L., Franceschi, R., et al. Inhibition of osteoblastic bone formation by nuclear factor-kappaB. Nat Med, *15*(6) (2009): 682-689.

Chen, G., Sircar, K., Aprikian, A., Potti, A., Goltzman, D., & Rabbani, S. A. Expression of RANKL/RANK/OPG in primary and metastatic human prostate cancer as markers of disease stage and functional regulation. Cancer, *107*(2) (2006): 289-298.

Chen, H., Senda, T., & Kubo, K. Y. The osteocyte plays multiple roles in bone remodeling and mineral homeostasis. Med Mol Morphol, *48*(2) (2015): 61-68.

Chen, H., Zhou, X., Fujita, H., Onozuka, M., & Kubo, K. Y. Age-related changes in trabecular and cortical bone microstructure. Int J Endocrinol, *2013* (2013): 213234.

Chlebowski, R. T., Hendrix, S. L., Langer, R. D., Stefanick, M. L., Gass, M., Lane, D., et al. Influence of estrogen plus progestin on breast cancer and mammography in healthy postmenopausal women: the Women's Health Initiative Randomized Trial. JAMA, *289*(24) (2003): 3243-3253.

Cho, S. W. Role of osteal macrophages in bone metabolism. J Pathol Transl Med, *49*(2) (2015): 102-104.

Christensen, K., Doblhammer, G., Rau, R., & Vaupel, J. W. Ageing populations: the challenges ahead. Lancet, *374*(9696) (2009): 1196-1208.

Clarke, B. Normal bone anatomy and physiology. Clin J Am Soc Nephrol, *3 Suppl 3* (2008): S131-139.

Clarke, B. L., & Khosla, S. Female reproductive system and bone. Arch Biochem Biophys, *503*(1) (2010): 118-128.

Cooper, C., Campion, G., & Melton, L. J., 3rd. Hip fractures in the elderly: a world-wide projection. Osteoporos Int, *2*(6) (1992): 285-289.

Cummings, S. R., & Melton, L. J. Epidemiology and outcomes of osteoporotic fractures. Lancet, *359*(9319) (2002): 1761-1767.

Delmas, P. D., Eastell, R., Garnero, P., Seibel, M. J., Stepan, J., & Committee of Scientific Advisors of the International Osteoporosis, F. The use of biochemical markers of bone turnover in osteoporosis. Committee of Scientific Advisors of the International Osteoporosis Foundation. Osteoporos Int, *11 Suppl 6* (2000): S2-17.

DiGirolamo, D. J., Clemens, T. L., & Kousteni, S. The skeleton as an endocrine organ. Nat Rev Rheumatol, *8*(11) (2012): 674-683.

Dorr, L. D., Arnala, I., Faugere, M. C., & Malluche, H. H. Five-year postoperative results of cemented femoral arthroplasty in patients with systemic bone disease. Clin Orthop Relat Res(259) (1990): 114-121.

Dorr, L. D., Faugere, M. C., Mackel, A. M., Gruen, T. A., Bognar, B., & Malluche, H. H. Structural and cellular assessment of bone quality of proximal femur. Bone, *14*(3) (1993): 231-242.

Douketis, J. Hormone replacement therapy and risk for venous thromboembolism: what's new and how do these findings influence clinical practice? Curr Opin Hematol, *12*(5) (2005): 395-400.

Eastell, R., O'Neill, T. W., Hofbauer, L. C., Langdahl, B., Reid, I. R., Gold, D. T., et al. Postmenopausal osteoporosis. Nat Rev Dis Primers, *2* (2016): 16069.

Egermann, M., Goldhahn, J., & Schneider, E. Animal models for fracture treatment in osteoporosis. Osteoporos Int, *16 Suppl 2* (2005): S129-138.

Ehrlich, P. J., & Lanyon, L. E. Mechanical strain and bone cell function: a review. Osteoporos Int, *13*(9) (2002): 688-700.

Ettinger, M. P. Aging bone and osteoporosis: strategies for preventing fractures in the elderly. Arch Intern Med, *163*(18) (2003): 2237-2246.

Falahati-Nini, A., Riggs, B. L., Atkinson, E. J., O'Fallon, W. M., Eastell, R., & Khosla, S. Relative contributions of testosterone and estrogen in regulating bone resorption and formation in normal elderly men. J Clin Invest, *106*(12) (2000): 1553-1560.

Fata, J. E., Kong, Y. Y., Li, J., Sasaki, T., Irie-Sasaki, J., Moorehead, R. A., et al. The osteoclast differentiation factor osteoprotegerin-ligand is essential for mammary gland development. Cell, *103*(1) (2000): 41-50.

Fazzalari, N. L., Kuliwaba, J. S., Atkins, G. J., Forwood, M. R., & Findlay, D. M. The ratio of messenger RNA levels of receptor activator of nuclear factor kappaB ligand to osteoprotegerin correlates with bone remodeling indices in normal human cancellous bone but not in osteoarthritis. J Bone Miner Res, *16*(6) (2001): 1015-1027.

Feng, J. Q., Ward, L. M., Liu, S., Lu, Y., Xie, Y., Yuan, B., et al. Loss of DMP1 causes rickets and osteomalacia and identifies a role for osteocytes in mineral metabolism. Nat Genet, *38*(11) (2006): 1310-1315.

Florencio-Silva, R., Sasso, G. R., Sasso-Cerri, E., Simoes, M. J., & Cerri, P. S. Biology of Bone tissue: structure, function, and factors that influence bone cells. Biomed Res Int, *2015* (2015): 421746.

Fortman, J., Heweet, T., & Halliday, L. (2002). *The laboratory nonhuman primate*. USA: CRC Press LLC.

Froberg, M. K., Garg, U. C., Stroncek, D. F., Geis, M., McCullough, J., & Brown, D. M. Changes in serum osteocalcin and bone-specific alkaline phosphatase are associated with bone pain in donors receiving granulocyte-colony-stimulating factor for peripheral blood stem and progenitor cell collection. Transfusion, *39*(4) (1999): 410-414.

Frost, H. M. The role of changes in mechanical usage set points in the pathogenesis of osteoporosis. J Bone Miner Res, *7*(3) (1992): 253-261.

Gambacciani, M., Monteleone, P., Sacco, A., & Genazzani, A. R. Hormone replacement therapy and endometrial, ovarian and colorectal cancer. Best Pract Res Clin Endocrinol Metab, *17*(1) (2003): 139-147.

Giannoudis, P., Tzioupis, C., Almalki, T., & Buckley, R. Fracture healing in osteoporotic fractures: is it really different? A basic science perspective. Injury, *38 Suppl 1* (2007): S90-99.

Gibon, E., Lu, L., & Goodman, S. B. Aging, inflammation, stem cells, and bone healing. Stem Cell Res Ther, *7* (2016): 44.

Goodenough, D. A., Goliger, J. A., & Paul, D. L. Connexins, connexons, and intercellular communication. Annu Rev Biochem, *65* (1996): 475-502.

Goodman, A. L., Descalzi, C. D., Johnson, D. K., & Hodgen, G. D. Composite pattern of circulating LH, FSH, estradiol, and progesterone during the menstrual cycle in cynomolgus monkeys. Proc Soc Exp Biol Med, *155*(4) (1977): 479-481.

Grady, D., Gebretsadik, T., Kerlikowske, K., Ernster, V., & Petitti, D. Hormone replacement therapy and endometrial cancer risk: a meta-analysis. Obstet Gynecol, *85*(2) (1995): 304-313.

Grimaud, E., Soubigou, L., Couillaud, S., Coipeau, P., Moreau, A., Passuti, N., et al. Receptor activator of nuclear factor kappaB ligand (RANKL)/osteoprotegerin (OPG) ratio is increased in severe osteolysis. Am J Pathol, *163*(5) (2003): 2021-2031.

Hamada, Y., Watanabe, T., Chatani, K., Hayasawa, S., & Iwamoto, M. Morphometrical comparison between Indian- and Chinese-derived rhesus macaques (*Macaca mulatta*). Anthropol Sci, *113* (2005): 183-188.

Harvey, N., Dennison, E., & Cooper, C. Osteoporosis: impact on health and economics. Nat Rev Rheumatol, *6*(2) (2010): 99-105.

Hatano, H., Siegel, H. J., Yamagiwa, H., Bronk, J. T., Turner, R. T., Bolander, M. E., et al. Identification of estrogen-regulated genes during fracture healing, using DNA microarray. J Bone Miner Metab, *22*(3) (2004): 224-235.

Havill, L. M., Hale, L. G., Newman, D. E., Witte, S. M., & Mahaney, M. C. Bone ALP and OC reference standards in adult baboons (*Papio hamadryas*) by sex and age. J Med Primatol, *35*(2) (2006): 97-105.

Heim, M., Frank, O., Kampmann, G., Sochocky, N., Pennimpede, T., Fuchs, P., et al. The phytoestrogen genistein enhances osteogenesis and represses adipogenic differentiation of human primary bone marrow stromal cells. Endocrinology, *145*(2) (2004): 848-859.

Hodgson, S. F., Johnson, K. A., Muhs, J. M., Lufkin, E. G., & McCarthy, J. T. Outpatient percutaneous biopsy of the iliac crest: methods, morbidity, and patient acceptance. Mayo Clin Proc, *61*(1) (1986): 28-33.

Hughes, A., Stewart, TL., &Mann, V. (2012). Extraction of Nucleic Acids from Bone. In Helfrich, MH., & Ralston, SH. (Eds.), *Bone Research Protocols*. (pp. 249-259). Totowa, NJ: Humana Press

Ikeda, T., Utsuyama, M., & Hirokawa, K. Expression profiles of receptor activator of nuclear factor kappaB ligand, receptor activator of nuclear factor kappaB, and osteoprotegerin messenger RNA in aged and ovariectomized rat bones. J Bone Miner Res, *16*(8) (2001): 1416-1425.

Itoh, F., Kojima, M., Furihata-Komatsu, H., Aoyagi, S., Kusama, H., Komatsu, H., et al. Reductions in bone mass, structure, and strength in axial and appendicular skeletons associated with increased turnover after ovariectomy in mature cynomolgus monkeys and preventive effects of clodronate. J Bone Miner Res, *17*(3) (2002): 534-543.

Jayo, M. J., Jerome, C. P., Lees, C. J., Rankin, S. E., & Weaver, D. S. Bone mass in female cynomolgus macaques: a cross-sectional and longitudinal study by age.

Calcif Tissue Int, *54*(3) (1994): 231-236.

Jee, W. S., & Yao, W. Overview: animal models of osteopenia and osteoporosis. J Musculoskelet Neuronal Interact, *1*(3) (2001): 193-207.

Jerome, C. P., & Peterson, P. E. Nonhuman primate models in skeletal research. Bone, *29*(1) (2001): 1-6.

Ji, J., Amzaleg, Y., Kittivanichkul, D., Borjesson, A., Windahl, S., Ma, D., et al. Estrogens and selective estrogen receptor modulators differentially antagonize Runx2 in mesenchymal progenitor cells. Unpublished manuscript (2017).

Johnell, O., & Kanis, J. A. An estimate of the worldwide prevalence and disability associated with osteoporotic fractures. Osteoporos Int, *17*(12) (2006): 1726-1733.

Jones, S. J., & Boyde, A. Experimental study of changes in osteoblastic shape induced by calcitonin and parathyroid extract in an organ culture system. Cell Tissue Res, *169*(4) (1976): 499-465.

Justesen, J., Stenderup, K., Ebbesen, E. N., Mosekilde, L., Steiniche, T., & Kassem, M. Adipocyte tissue volume in bone marrow is increased with aging and in patients with osteoporosis. Biogerontology, *2*(3) (2001): 165-171.

Kanis, J. A. (2007). *WHO Technical Report*. UK: University of Sheffield

Kanis, J. A., Johnell, O., Oden, A., Dawson, A., De Laet, C., & Jonsson, B. Ten year probabilities of osteoporotic fractures according to BMD and diagnostic thresholds. Osteoporos Int, *12*(12) (2001): 989-995.

Kanis, J. A., McCloskey, E. V., Johansson, H., Cooper, C., Rizzoli, R., Reginster, J. Y., et al. European guidance for the diagnosis and management of osteoporosis in postmenopausal women. Osteoporos Int, *24*(1) (2013): 23-57.

Kates, S. L., & Ackert-Bicknell, C. L. How do bisphosphonates affect fracture healing? Injury, *47 Suppl 1* (2016): S65-68.

Kavanagh, K., Koudy Williams, J., & Wagner, J. D. Naturally occurring menopause in cynomolgus monkeys: changes in hormone, lipid, and carbohydrate measures with hormonal status. J Med Primatol, *34*(4) (2005): 171-177.

Khosla, S., Melton, L. J., 3rd, & Riggs, B. L. The unitary model for estrogen deficiency and the pathogenesis of osteoporosis: is a revision needed? J Bone Miner Res, *26*(3) (2011): 441-451.

Khosla, S., Oursler, M. J., & Monroe, D. G. Estrogen and the skeleton. Trends Endocrinol Metab, *23*(11) (2012): 576-581.

Khosla, S., & Riggs, B. L. Pathophysiology of age-related bone loss and osteoporosis. Endocrinol Metab Clin North Am, *34*(4) (2005): 1015-1030.

Kim, J. N., Lee, J. Y., Shin, K. J., Gil, Y. C., Koh, K. S., & Song, W. C. Haversian system of compact bone and comparison between endosteal and periosteal sides using three-dimensional reconstruction in rat. Anat Cell Biol, *48*(4) (2015): 258-261.

Kim, N. S., Kim, H. J., Koo, B. K., Kwon, M. C., Kim, Y. W., Cho, Y., et al. Receptor activator of NF-kappaB ligand regulates the proliferation of mammary epithelial cells via Id2. Mol Cell Biol, *26*(3) (2006): 1002-1013.

Kittivanichkul, D., Charoenphandhu, N., Khemawoot, P., & Malaivijitnond, S. *Pueraria mirifica* alleviates cortical bone loss in naturally menopausal monkeys. J Endocrinol, *231*(2) (2016a): 121-133.

Kittivanichkul, D., Watanabe, G., Nagaoka, K., & Malaivijitnond, S. Changes in bone mass during the perimenopausal transition in naturally menopausal cynomolgus monkeys. Menopause, *23*(1) (2016b): 87-99.

Klein-Nulend, J., Bakker, A. D., Bacabac, R. G., Vatsa, A., & Weinbaum, S. Mechanosensation and transduction in osteocytes. Bone, *54*(2) (2013): 182-190.

Kohrt, W. M., Snead, D. B., Slatopolsky, E., & Birge, S. J., Jr. Additive effects of weight-bearing exercise and estrogen on bone mineral density in older women. J Bone Miner Res, *10*(9) (1995): 1303-1311.

Komori, T. Regulation of osteoblast differentiation by transcription factors. J Cell Biochem, *99*(5) (2006): 1233-1239.

Kostenuik, P. J., Nguyen, H. Q., McCabe, J., Warmington, K. S., Kurahara, C., Sun, N., et al. Denosumab, a fully human monoclonal antibody to RANKL, inhibits bone resorption and increases BMD in knock-in mice that express chimeric (murine/human) RANKL. J Bone Miner Res, *24*(2) (2009): 182-195.

Kousteni, S., Bellido, T., Plotkin, L. I., O'Brien, C. A., Bodenner, D. L., Han, L., et al. Nongenotropic, sex-nonspecific signaling through the estrogen or androgen receptors: dissociation from transcriptional activity. Cell, *104*(5) (2001): 719-730.

Kress, B. C. Bone alkaline phosphatase: methods of quantitation and clinical utility. J Clin Ligand Assay, *21* (1998): 139-148.

Lacey, D. L., Tan, H. L., Lu, J., Kaufman, S., Van, G., Qiu, W., et al. Osteoprotegerin ligand modulates murine osteoclast survival *in vitro* and *in vivo*. Am J Pathol, *157*(2) (2000): 435-448.

Lee, C. C., Fletcher, M. D., & Tarantal, A. F. Effect of age on the frequency, cell cycle, and lineage maturation of rhesus monkey (*Macaca mulatta*) CD34+ and hematopoietic progenitor cells. Pediatr Res, *58*(2) (2005): 315-322.

Lee, H. R., Kim, T. H., & Choi, K. C. Functions and physiological roles of two types of estrogen receptors, ERalpha and ERbeta, identified by estrogen receptor knockout mouse. Lab Anim Res, *28*(2) (2012): 71-76.

Lee, N. K. Molecular understanding of osteoclast differentiation and physiology. Endocrinol Metab, *25* (2010): 264-269.

Legrand, J. J., Fisch, C., Guillaumat, P. O., Pavard, J. M., Attia, M., De Jouffrey, S., et al. Use of biochemical markers to monitor changes in bone turnover in cynomolgus monkeys. Biomarkers, *8*(1) (2003): 63-77.

Lelovas, P. P., Xanthos, T. T., Thoma, S. E., Lyritis, G. P., & Dontas, I. A. The laboratory rat as an animal model for osteoporosis research. Comp Med, *58*(5) (2008): 424-430.

Li, M., Shen, Y., Qi, H., & Wronski, T. J. Comparative study of skeletal response to estrogen depletion at red and yellow marrow sites in rats. Anat Rec, *245*(3) (1996): 472-480.

Li, S., Abdel-Wahab, A., & Silberschmidt, V. V. Analysis of fracture processes in cortical bone tissue. Engineering Fracture Mechanics, *110* (2013): 448-458.

Li, X. J., & Jee, W. S. Adaptation of diaphyseal structure to aging and decreased mechanical loading in the adult rat: a densitometric and histomorphometric study. Anat Rec, *229*(3) (1991): 291-297.

Lill, C. A., Hesseln, J., Schlegel, U., Eckhardt, C., Goldhahn, J., & Schneider, E. Biomechanical evaluation of healing in a non-critical defect in a large animal model of osteoporosis. J Orthop Res, *21*(5) (2003): 836-842.

Liu, J. M., Zhao, H. Y., Ning, G., Zhao, Y. J., Chen, Y., Zhang, Z., et al. Relationships between the changes of serum levels of OPG and RANKL with age, menopause,

bone biochemical markers and bone mineral density in Chinese women aged 20-75. Calcif Tissue Int, *76*(1) (2005): 1-6.

Lu, C., Hansen, E., Sapozhnikova, A., Hu, D., Miclau, T., & Marcucio, R. S. Effect of age on vascularization during fracture repair. J Orthop Res, *26*(10) (2008): 1384-1389.

Macdonald, H. M., Nishiyama, K. K., Kang, J., Hanley, D. A., & Boyd, S. K. Age-related patterns of trabecular and cortical bone loss differ between sexes and skeletal sites: a population-based HR-pQCT study. J Bone Miner Res, *26*(1) (2011): 50-62.

Mackie, E. J., Ahmed, Y. A., Tatarczuch, L., Chen, K. S., & Mirams, M. Endochondral ossification: how cartilage is converted into bone in the developing skeleton. Int J Biochem Cell Biol, *40*(1) (2008): 46-62.

Malaivijitnond, S. Medical applications of phytoestrogens from the Thai herb *Pueraria mirifica*. Front Med, *6*(1) (2012): 8-21.

Malaivijitnond, S., Kiatthaipipat, P., Cherdshewasart, W., Watanabe, G., & Taya, K. Different effects of *Pueraria mirifica*, a herb containing phytoestrogens, on LH and FSH secretion in gonadectomized female and male rats. J Pharmacol Sci, *96*(4) (2004): 428-435.

Malluche, H. H., Mawad, H., & Monier-Faugere, M. C. Bone biopsy in patients with osteoporosis. Curr Osteoporos Rep, *5*(4) (2007): 146-152.

Manolagas, S. C. Birth and death of bone cells: basic regulatory mechanisms and implications for the pathogenesis and treatment of osteoporosis. Endocr Rev, *21*(2) (2000): 115-137.

Marks, S. C., Jr., & Walker, D. G. The hematogenous origin of osteoclasts: experimental evidence from osteopetrotic (microphthalmic) mice treated with spleen cells from beige mouse donors. Am J Anat, *161*(1) (1981): 1-10.

Marsell, R., & Einhorn, T. A. The biology of fracture healing. Injury, *42*(6) (2011): 551-555.

Martin-Millan, M., Almeida, M., Ambrogini, E., Han, L., Zhao, H., Weinstein, R. S., et al. The estrogen receptor-alpha in osteoclasts mediates the protective effects of estrogens on cancellous but not cortical bone. Mol Endocrinol, *24*(2) (2010): 323-334.

Matsuo, K., & Otaki, N. Bone cell interactions through Eph/ephrin: bone modeling, remodeling and associated diseases. Cell Adh Migr, *6*(2) (2012): 148-156.

McCalden, R. W., McGeough, J. A., Barker, M. B., & Court-Brown, C. M. Age-related changes in the tensile properties of cortical bone. The relative importance of changes in porosity, mineralization, and microstructure. J Bone Joint Surg Am, *75*(8) (1993): 1193-1205.

Melton, L. J., 3rd, Atkinson, E. J., O'Connor, M. K., O'Fallon, W. M., & Riggs, B. L. Bone density and fracture risk in men. J Bone Miner Res, *13*(12) (1998): 1915-1923.

Melton, L. J., 3rd, Chrischilles, E. A., Cooper, C., Lane, A. W., & Riggs, B. L. Perspective. How many women have osteoporosis? J Bone Miner Res, *7*(9) (1992): 1005-1010.

Menaa, C., Kurihara, N., & Roodman, G. D. CFU-GM-derived cells form osteoclasts at a very high efficiency. Biochem Biophys Res Commun, *267*(3) (2000): 943-946.

Meunier, P., Courpron, P., Edouard, C., Bernard, J., Bringuier, J., & Vignon, G. Physiological senile involution and pathological rarefaction of bone. Quantitative and comparative histological data. Clin Endocrinol Metab, *2*(2) (1973): 239-256.

Miyakoshi, N., Sato, K., Abe, T., Tsuchida, T., Tamura, Y., & Kudo, T. Histomorphometric evaluation of the effects of ovariectomy on bone turnover in rat caudal vertebrae. Calcif Tissue Int, *64*(4) (1999): 318-324.

Modder, U. I., Clowes, J. A., Hoey, K., Peterson, J. M., McCready, L., Oursler, M. J., et al. Regulation of circulating sclerostin levels by sex steroids in women and in men. J Bone Miner Res, *26*(1) (2011): 27-34.

Moustafa, A., Sugiyama, T., Prasad, J., Zaman, G., Gross, T. S., Lanyon, L. E., et al. Mechanical loading-related changes in osteocyte sclerostin expression in mice are more closely associated with the subsequent osteogenic response than the peak strains engendered. Osteoporos Int, *23*(4) (2012): 1225-1234.

Mucowski, S. J., Mack, W. J., Shoupe, D., Kono, N., Paulson, R., & Hodis, H. N. Effect of prior oophorectomy on changes in bone mineral density and carotid artery intima-media thickness in postmenopausal women. Fertil Steril, *101*(4) (2014):

1117-1122.

Muschler, G. F., Nitto, H., Boehm, C. A., & Easley, K. A. Age- and gender-related changes in the cellularity of human bone marrow and the prevalence of osteoblastic progenitors. J Orthop Res, *19*(1) (2001): 117-125.

Nelson, H. D., Humphrey, L. L., Nygren, P., Teutsch, S. M., & Allan, J. D. Postmenopausal hormone replacement therapy: scientific review. JAMA, *288*(7) (2002): 872-881.

Nih Consensus Development Panel on Osteoporosis Prevention, D., & Therapy. Osteoporosis prevention, diagnosis, and therapy. JAMA, *285*(6) (2001): 785-795.

O'Brien, E. A., Williams, J. H., & Marshall, M. J. Osteoprotegerin ligand regulates osteoclast adherence to the bone surface in mouse calvaria. Biochem Biophys Res Commun, *274*(2) (2000): 281-290.

Odvina, C. V., Zerwekh, J. E., Rao, D. S., Maalouf, N., Gottschalk, F. A., & Pak, C. Y. Severely suppressed bone turnover: a potential complication of alendronate therapy. J Clin Endocrinol Metab, *90*(3) (2005): 1294-1301.

Onal, M., Xiong, J., Chen, X., Thostenson, J. D., Almeida, M., Manolagas, S. C., et al. Receptor activator of nuclear factor kappaB ligand (RANKL) protein expression by B lymphocytes contributes to ovariectomy-induced bone loss. J Biol Chem, *287*(35) (2012): 29851-29860.

Oryan, A., Alidadi, S., & Moshiri, A. Current concerns regarding healing of bone defects. Hard Tissue, *26* (2013): 1-12.

Oursler, M. J. Direct and indirect effects of estrogen on osteoclasts. J Musculoskelet Neuronal Interact, *3*(4) (2003): 363-366.

Parfitt, A. M. The cellular basis of bone turnover and bone loss: a rebuttal of the osteocytic resorption--bone flow theory. Clin Orthop Relat Res(127) (1977): 236-247.

Parfitt, A. M. Bone remodeling. Henry Ford Hosp Med J, *36*(3) (1988): 143-144.

Pecina, M., Smoljanovic, T., Cicvara-Pecina, T., & Tomek-Roksandic, S. Osteoporotic fractures in the elderly. Arh Hig Rada Toksikol, *58*(1) (2007): 41-47.

Pisani, P., Renna, M. D., Conversano, F., Casciaro, E., Di Paola, M., Quarta, E., et al. Major osteoporotic fragility fractures: Risk factor updates and societal impact.

World J Orthop, *7*(3) (2016): 171-181.

Quarto, R., Thomas, D., & Liang, C. T. Bone progenitor cell deficits and the age-associated decline in bone repair capacity. Calcif Tissue Int, *56*(2) (1995): 123-129.

R Core Team. R: A language and environment for statistical computing. R Foundation for Statistical Computing, Vienna, Austria (2015).

Reid, M. (2011). *Handbook of osteoporosis* (pp.13-19).London: Springer Healthcare.

Riggs, B. L., & Hartmann, L. C. Selective estrogen-receptor modulators -- mechanisms of action and application to clinical practice. N Engl J Med, *348*(7) (2003): 618-629.

Riggs, B. L., Khosla, S., & Melton, L. J., 3rd. A unitary model for involutional osteoporosis: estrogen deficiency causes both type I and type II osteoporosis in postmenopausal women and contributes to bone loss in aging men. J Bone Miner Res, *13*(5) (1998): 763-773.

Riggs, B. L., Melton, L. J., 3rd, Robb, R. A., Camp, J. J., Atkinson, E. J., Peterson, J. M., et al. Population-based study of age and sex differences in bone volumetric density, size, geometry, and structure at different skeletal sites. J Bone Miner Res, *19*(12) (2004): 1945-1954.

Riggs, B. L., Melton, L. J., Robb, R. A., Camp, J. J., Atkinson, E. J., McDaniel, L., et al. A population-based assessment of rates of bone loss at multiple skeletal sites: evidence for substantial trabecular bone loss in young adult women and men. J Bone Miner Res, *23*(2) (2008): 205-214.

Riggs, B. L., Wahner, H. W., Dunn, W. L., Mazess, R. B., Offord, K. P., & Melton, L. J., 3rd. Differential changes in bone mineral density of the appendicular and axial skeleton with aging: relationship to spinal osteoporosis. J Clin Invest, *67*(2) (1981): 328-335.

Robinson, L. J., Yaroslavskiy, B. B., Griswold, R. D., Zadorozny, E. V., Guo, L., Tourkova, I. L., et al. Estrogen inhibits RANKL-stimulated osteoclastic differentiation of human monocytes through estrogen and RANKL-regulated interaction of estrogen receptor-alpha with BCAR1 and Traf6. Exp Cell Res, *315*(7) (2009): 1287-1301.

Roggia, C., Gao, Y., Cenci, S., Weitzmann, M. N., Toraldo, G., Isaia, G., et al. Up-

regulation of TNF-producing T cells in the bone marrow: a key mechanism by which estrogen deficiency induces bone loss in vivo. Proc Natl Acad Sci U S A, *98*(24) (2001): 13960-13965.

Roodman, G. D. Regulation of osteoclast differentiation. Ann N Y Acad Sci, *1068* (2006): 100-109.

Rossouw, J. E., Anderson, G. L., Prentice, R. L., LaCroix, A. Z., Kooperberg, C., Stefanick, M. L., et al. Risks and benefits of estrogen plus progestin in healthy postmenopausal women: principal results From the Women's Health Initiative randomized controlled trial. JAMA, *288*(3) (2002): 321-333.

Schaffler, M. B., & Burr, D. B. Primate cortical bone microstructure: relationship to locomotion. Am J Phys Anthropol, *65*(2) (1984): 191-197.

Schilling, T., Ebert, R., Raaijmakers, N., Schutze, N., & Jakob, F. Effects of phytoestrogens and other plant-derived compounds on mesenchymal stem cells, bone maintenance and regeneration. J Steroid Biochem Mol Biol, *139* (2014): 252-261.

Setchell, K. D. Phytoestrogens: the biochemistry, physiology, and implications for human health of soy isoflavones. Am J Clin Nutr, *68*(6 Suppl) (1998): 1333S-1346S.

Sims, N. A., & Martin, T. J. Coupling the activities of bone formation and resorption: a multitude of signals within the basic multicellular unit. Bonekey Rep, *3* (2014): 481.

Sinha, K. M., & Zhou, X. Genetic and molecular control of osterix in skeletal formation. J Cell Biochem, *114*(5) (2013): 975-984.

Smith, Y. S., Varela, A., & Jolette, J. (2011). Nonhuman primate models of osteoporosis. In Duque, G.,& Watanabe, K. (Eds.), *Osteoporosis Research* (pp. 135-157). London: Springer.

Srivastava, S., Toraldo, G., Weitzmann, M. N., Cenci, S., Ross, F. P., & Pacifici, R. Estrogen decreases osteoclast formation by down-regulating receptor activator of NF-kappa B ligand (RANKL)-induced JNK activation. J Biol Chem, *276*(12) (2001): 8836-8840.

Stein, G. S., Lian, J. B., van Wijnen, A. J., Stein, J. L., Montecino, M., Javed, A., et al. Runx2 control of organization, assembly and activity of the regulatory

machinery for skeletal gene expression. Oncogene, *23*(24) (2004): 4315-4329.

Strong, A. L., Ohlstein, J. F., Jiang, Q., Zhang, Q., Zheng, S., Boue, S. M., et al. Novel daidzein analogs enhance osteogenic activity of bone marrow-derived mesenchymal stem cells and adipose-derived stromal/stem cells through estrogen receptor dependent and independent mechanisms. Stem Cell Res Ther, *5*(4) (2014): 105.

Sun, L., Peng, Y., Sharrow, A. C., Iqbal, J., Zhang, Z., Papachristou, D. J., et al. FSH directly regulates bone mass. Cell, *125*(2) (2006): 247-260.

Suthon, S., Jaroenporn, S., Charoenphandhu, N., Suntornsaratoon, P., & Malaivijitnond, S. Anti-osteoporotic effects of *Pueraria candollei* var. *mirifica* on bone mineral density and histomorphometry in estrogen-deficient rats. J Nat Med, *70*(2) (2016a): 225-233.

Suthon, S., Matsuo, K., & Malaivijitnond, S.. (2016b, June 10-11). *Pueraria mirifica* phytoestrogens interrupt RANKL/OPG/RANK signaling in osteoblast precursor ST2 cells, but not in osteoblast-osteoclast coculture. Paper presented at the Proceedings of the 11th conference on science and technology for youths, Bangkok International Trade and Exhibition Center, Thailand.

Svedbom, A., Hernlund, E., Ivergard, M., Compston, J., Cooper, C., Stenmark, J., et al. Osteoporosis in the European Union: a compendium of country-specific reports. Arch Osteoporos, *8* (2013): 137.

Sweet, M. G., Sweet, J. M., Jeremiah, M. P., & Galazka, S. S. Diagnosis and treatment of osteoporosis. Am Fam Physician, *79*(3) (2009): 193-200.

Syed, F. A., Modder, U. I., Roforth, M., Hensen, I., Fraser, D. G., Peterson, J. M., et al. Effects of chronic estrogen treatment on modulating age-related bone loss in female mice. J Bone Miner Res, *25*(11) (2010): 2438-2446.

Szulc, P., & Seeman, E. Thinking inside and outside the envelopes of bone: dedicated to PDD. Osteoporos Int, *20*(8) (2009): 1281-1288.

Szulc, P., Seeman, E., Duboeuf, F., Sornay-Rendu, E., & Delmas, P. D. Bone fragility: failure of periosteal apposition to compensate for increased endocortical resorption in postmenopausal women. J Bone Miner Res, *21*(12) (2006): 1856-1863.

Teitelbaum, S. L., & Ross, F. P. Genetic regulation of osteoclast development and

function. Nat Rev Genet, *4*(8) (2003): 638-649.

Tella, S. H., & Gallagher, J. C. Prevention and treatment of postmenopausal osteoporosis. J Steroid Biochem Mol Biol, *142* (2014): 155-170.

Thompson, D. D., Simmons, H. A., Pirie, C. M., & Ke, H. Z. FDA Guidelines and animal models for osteoporosis. Bone, *17*(4 Suppl) (1995): 125S-133S.

Tiyasatkulkovit, W., Charoenphandhu, N., Wongdee, K., Thongbunchoo, J., Krishnamra, N., & Malaivijitnond, S. Upregulation of osteoblastic differentiation marker mRNA expression in osteoblast-like UMR106 cells by puerarin and phytoestrogens from *Pueraria mirifica*. Phytomedicine, *19*(13) (2012): 1147-1155.

Tiyasatkulkovit, W., Malaivijitnond, S., Charoenphandhu, N., Havill, L. M., Ford, A. L., & VandeBerg, J. L. *Pueraria mirifica* extract and puerarin enhance proliferation and expression of alkaline phosphatase and type I collagen in primary baboon osteoblasts. Phytomedicine, *21*(12) (2014): 1498-1503.

Tomkinson, A., Gevers, E. F., Wit, J. M., Reeve, J., & Noble, B. S. The role of estrogen in the control of rat osteocyte apoptosis. J Bone Miner Res, *13*(8) (1998): 1243-1250.

Trisomboon, H., Malaivijitnond, S., Suzuki, J., Hamada, Y., Watanabe, G., & Taya, K. Long-term treatment effects of *Pueraria mirifica* phytoestrogens on parathyroid hormone and calcium levels in aged menopausal cynomolgus monkeys. J Reprod Dev, *50*(6) (2004a): 639-645.

Trisomboon, H., Malaivijitnond, S., Watanabe, G., & Taya, K. Estrogenic effects of *Pueraria mirifica* on the menstrual cycle and hormone-related ovarian functions in cyclic female cynomolgus monkeys. J Pharmacol Sci, *94*(1) (2004b): 51-59.

Trisomboon, H., Malaivijitnond, S., Watanabe, G., & Taya, K. Ovulation block by *Pueraria mirifica*: a study of its endocrinological effect in female monkeys. Endocrine, *26*(1) (2005): 33-39.

Turner, A. S. Animal models of osteoporosis--necessity and limitations. Eur Cell Mater, *1* (2001): 66-81.

Ucer, S., Iyer, S., Kim, H. N., Han, L., Rutlen, C., Allison, K., et al. The effects of aging and sex steroid deficiency on the murine skeleton are independent and mechanistically distinct. J Bone Miner Res, *32*(3) (2017): 560-574.

Urasopon, N., Hamada, Y., Asaoka, K., Cherdshewasart, W., & Malaivijitnond, S. *Pueraria mirifica*, a phytoestrogen-rich herb, prevents bone loss in orchidectomized rats. Maturitas, *56*(3) (2007): 322-331.

Urasopon, N., Hamada, Y., Cherdshewasart, W., & Malaivijitnond, S. Preventive effects of *Pueraria mirifica* on bone loss in ovariectomized rats. Maturitas, *59*(2) (2008): 137-148.

Vaananen, H. K., Zhao, H., Mulari, M., & Halleen, J. M. The cell biology of osteoclast function. J Cell Sci, *113 (Pt 3)* (2000): 377-381.

Vanderschueren, D., Venken, K., Ophoff, J., Bouillon, R., & Boonen, S. Clinical Review: Sex steroids and the periosteum--reconsidering the roles of androgens and estrogens in periosteal expansion. J Clin Endocrinol Metab, *91*(2) (2006): 378-382.

Vaninetti, S., Baccarelli, A., Romoli, R., Fanelli, M., Faglia, G., & Spada, A. Effect of aging on serum gonadotropin levels in healthy subjects and patients with nonfunctioning pituitary adenomas. Eur J Endocrinol, *142*(2) (2000): 144-149.

Vimalraj, S., Arumugam, B., Miranda, P. J., & Selvamurugan, N. Runx2: Structure, function, and phosphorylation in osteoblast differentiation. Int J Biol Macromol, *78* (2015): 202-208.

Wada, T., Nakashima, T., Hiroshi, N., & Penninger, J. M. RANKL-RANK signaling in osteoclastogenesis and bone disease. Trends Mol Med, *12*(1) (2006): 17-25.

Weinbauer, G. F., Niehoff, M., Niehaus, M., Srivastav, S., Fuchs, A., Van Esch, E., et al. Physiology and Endocrinology of the Ovarian Cycle in Macaques. Toxicol Pathol, *36*(7S) (2008): 7S-23S.

Weitzmann, M. N., & Pacifici, R. Estrogen deficiency and bone loss: an inflammatory tale. J Clin Invest, *116*(5) (2006): 1186-1194.

Wong, R., & Rabie, B. Effect of puerarin on bone formation. Osteoarthritis Cartilage, *15*(8) (2007): 894-899.

Wong, R. W., & Rabie, A. B. Effect of daidzein on bone formation. Front Biosci (Landmark Ed), *14* (2009): 3673-3679.

Wong, R. W., & Rabie, A. B. Effect of genistin on bone formation. Front Biosci (Elite Ed), *2* (2010): 764-770.

Woolf, A. D. The global perspective of osteoporosis : the ILAR lecture, June 2004,

Berlin. Clin Rheumatol, *25*(5) (2006): 613-618.

World Health Organization. Prevention and management of osteoporosis. World Health Organ Tech Rep Ser, *921* (2003): 1-164, back cover.

Wronski, T. J., Cintron, M., & Dann, L. M. Temporal relationship between bone loss and increased bone turnover in ovariectomized rats. Calcif Tissue Int, *43*(3) (1988): 179-183.

Zebaze, R. M., Ghasem-Zadeh, A., Bohte, A., Iuliano-Burns, S., Mirams, M., Price, R. I., et al. Intracortical remodelling and porosity in the distal radius and post-mortem femurs of women: a cross-sectional study. Lancet, *375*(9727) (2010): 1729-1736.

Zhang, C. Molecular mechanisms of osteoblast-specific transcription factor Osterix effect on bone formation. Beijing Da Xue Xue Bao, *44*(5) (2012): 659-665.

Zheng, W., Jimenez-Linan, M., Rubin, B. S., & Halvorson, L. M. Anterior pituitary gene expression with reproductive aging in the female rat. Biol Reprod, *76*(6) (2007): 1091-1102.

Zhu, L. L., Blair, H., Cao, J., Yuen, T., Latif, R., Guo, L., et al. Blocking antibody to the beta-subunit of FSH prevents bone loss by inhibiting bone resorption and stimulating bone synthesis. Proc Natl Acad Sci U S A, *109*(36) (2012): 14574-14579.

VITA

Miss Donlaporn Kittivanichkul was born on April 23rd, 1990 in Bangkok, Thailand. She graduated a Bachelor of Science (B.Sc. in Veterinary Science) from Faculty of Veterinary Technology, Kasetsart University, Bangkok, Thailand with the first class honor in 2011. In 2012, she started her study in Doctor of Philosophy Program in Zoology at Department of Biology, Faculty of Science, Chulalongkorn University. She was fully supported by Thailand Research Fund through the Royal Golden Jubilee PhD for her study. She also got the research funding from the 90th Anniversary of Chulalongkorn University Fund, Chulalongkorn University.

She was supported from Japan Student Services Organization (JASSO), Ministry of Education, Culture, Sports, Science and Technology, Japan to carry two-month research under the supervision of Professor Gen Watanabe at the Veterinary Physiology Laboratory, Department of Veterinary Medicine, Faculty of Agriculture, Tokyo University of Agriculture and Technology (TUAT), Japan (2004 and 2005). During her Ph.D. study she did a poster presentation (February 27th, 2014) at the 1st Seminar of the Indulging in Science Research, TUAT. She also orally presented her work at (i) The 7th Intercongress Symposium of the Asia and Oceania Society of Comparative Endocrinology (AOSCE) (March 18th, 2014), National Taiwan Ocean University, Keelung, Taiwan and received a travel grant award, (ii) the 8th Federation of the Asian and Oceanian Physiological Societies (FAOPS) (November 25th, 2015), Centara Grand & Bangkok Convention Centre at Centralworld, Bangkok, Thailand and received the Young Scientist Award, (iii) The 8th Congress of AOSCE (June 24th, 2016), Korea University College of Medicine, Seoul, Korea and was awarded the Excellent Presentation Award and (iv) The 18th RGJ-Ph.D. Congress (June 10th, 2017), Richmond stylish convention hall, Nonthaburi, Thailand and received the Popular vote for poster presentation. She has published her research work in the international scientific journal, entitled “Changes in bone mass during the perimenopausal transition in naturally menopausal cynomolgus monkeys”, in Menopause (IF= 3.172) in 2016. In the same year she has published another paper, entitled “Pueraria mirifica alleviates cortical bone loss in naturally menopausal monkeys”, in Journal of Endrocrinology (IF=4.498). Last year of her Ph.D. study, she experienced a six-month bone research under the supervision of Professor Baruch Frenkel at the Department of Orthopaedic Surgery and of Biochemistry & Molecular Biology, Institute for Genetic Medicine, Keck School of Medicine, University of Southern California, USA.